2020

Focal Augmentation of Somatostatin Interneuron Function and Subsequent Circuit Effects in Developmentally Malformed, Epileptogenic Cortex

Nicole Ekanem
Virginia Commonwealth University

Focal Augmentation of Somatostatin Interneuron Function and Subsequent Circuit Effects in Developmentally Malformed, Epileptogenic Cortex

A dissertation submitted in partial fulfillment of the requirements for the degree of Doctor of Philosophy in Neuroscience at Virginia Commonwealth University

by

Nicole Ekanem
M.S. Virginia Commonwealth University, 2015

Advisor: Kimberle Jacobs, Ph.D.
Associate Professor
Department of Anatomy and Neurobiology

Virginia Commonwealth University
Richmond, Virginia
June, 2020

This is wholly dedicated to my Partner, every space and every letter.

Every tap of this worn keyboard.

Every exasperated defeated and then triumphant breath.

I cannot imagine being able to complete this without your kindness and your care.

Thank you. I'm definitely not crying.

Acknowledgements

Special thanks to Amanda Furman, M.S. – THANK YOU for your help with all the animal surgeries. I will forever be in awe of the artful consistency the freeze lesion model took in your skilled and patient hands.

Thanks to Jarrett Wann for assistance with data analyses.

And finally, abundant thanks to Martina Hernandez, Laura Reed, M.D., Purrkinje Jones, Esq., my GSPB staff, and Crossmodal collaborators for your gracious friendship through these tumultuous years 😊. It has become abundantly clear that a support system is critical to avoid the worst as a BPOC in the labyrinthian silos of academia. I am very lucky to have met you all.

Unknown Disorder
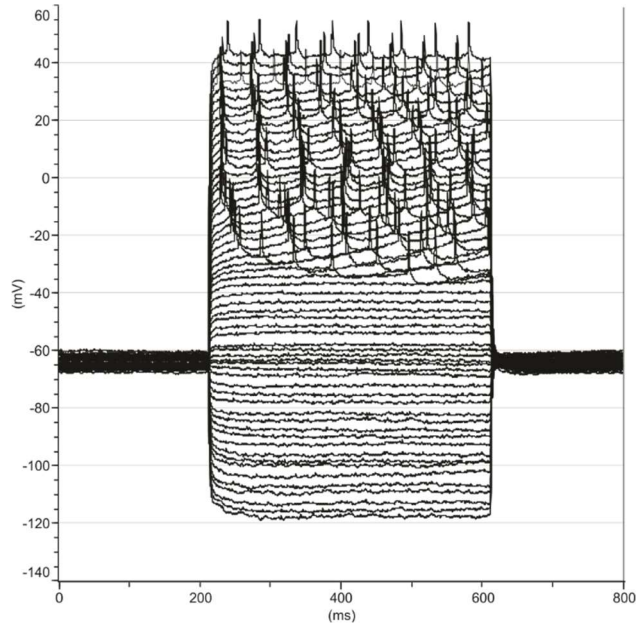
2018

Table of Contents

List of Figures and Tables

List of Abbreviations and Definitions

˚C   degrees Celsius

aCSF   artificial cerebrospinal fluid

AED   antiepileptic drugs

AMPA(R)   glutamate receptor

Arch   archaerhodopsin

APV   NMDA receptor antagonist

CAMKII Ca^{2+}/calmodulin-dependent protein kinase II

CNS   central nervous system

ChR   channelrhodopsin

Cre   Cre recombinase; **enzyme**

Cre-*lox*   Cre-*lox* recombination; **site-specific genetic recombination technique**

DIC   Differential interference contrast; **optical microscopy illumination technique**

DNQX   AMPA receptor antagonist

E/I   excitation/inhibition; **ratio**

EPSC   excitatory postsynaptic current

eEPSC   evoked EPSC

mEPSC   miniature EPSC; **postsynaptic response to neurotransmitter released by single**

presynaptic vesicle

sEPSC   spontaneous EPSC

FS   fast spiking

GABA   γ-aminobutyric acid

GFP   green fluorescent protein

IPSC   inhibitory postsynaptic current

eIPSC   evoked IPSC

mIPSC   miniature IPSC; **postsynaptic response to neurotransmitter released by single**

presynaptic vesicle

sIPSC   spontaneous IPSC

IPSP   inhibitory postsynaptic potential

LTS   low threshold spiking

mGluR   metabotropic glutamate receptor

mM   milli-Molar

mOsm   milli-Osmole

NMDA(R)   glutamate receptor

NR2B   NMDAR subunit

P   postnatal day

PMR   paramicrogyral region

PV   parvalbumin

SST   somatostatin

μm   micrometer

μM   micro-Molar

VB   ventrobasal complex of thalamus

VIP   vasoactive intestinal peptide

YFP   yellow fluorescent protein
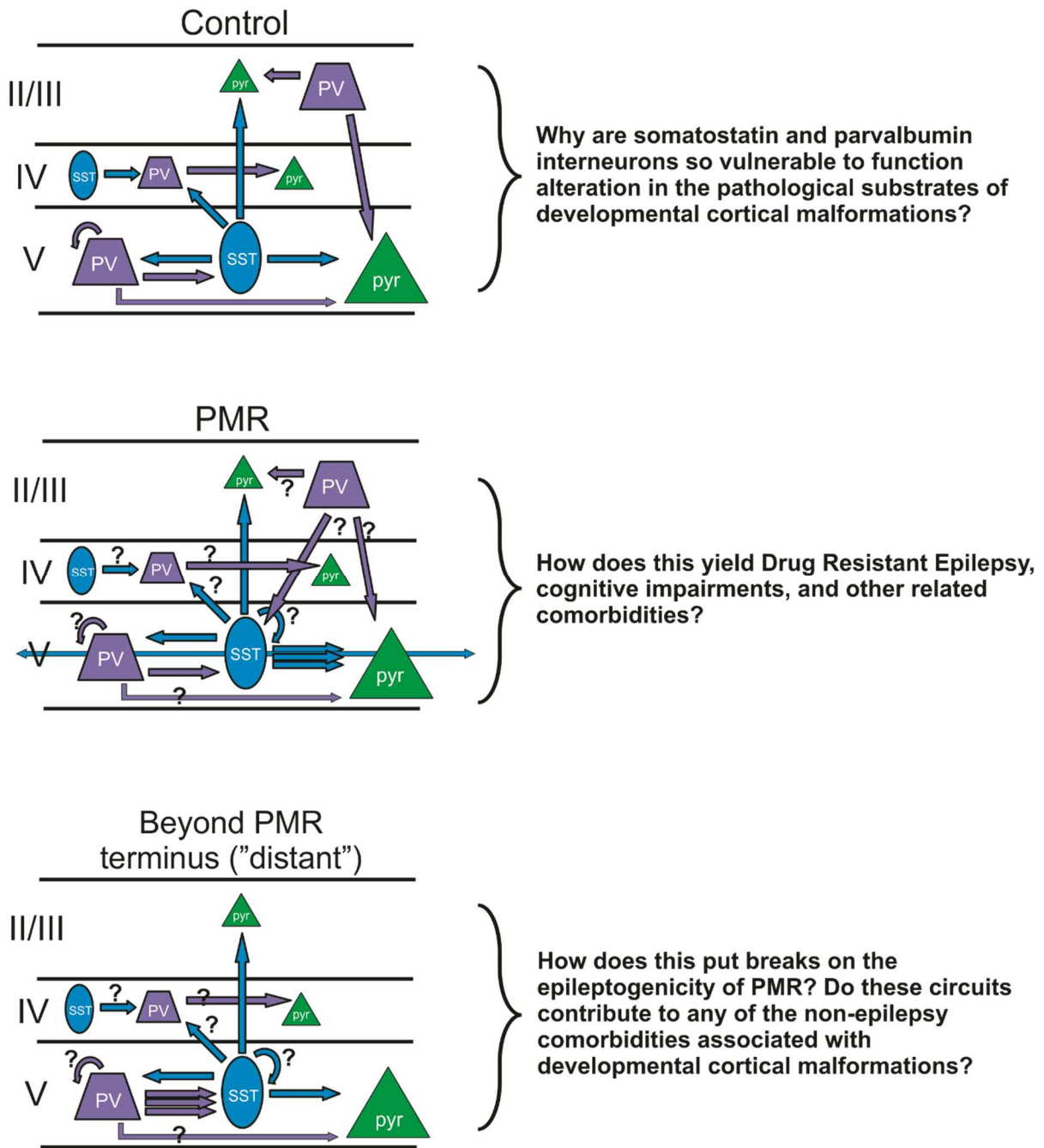
Figure 1.1 There are innumerable questions regarding the state of inhibitory circuit alterations within developmentally malformed and epileptogenic neocortex. As well, how these changes may prime the cortex for, incite initiation of, or promote propagation of epileptiform network-level phenomena remains unknown. The work in this correspondence will address some of these questions and through several novel discoveries, we move ever closer to uncovering means for viable treatment strategies.

Chapter 1

Introduction to Drug Resistant Epilepsy, Interneuron circuitry, and Optogenetic interrogation of pathological neocortical substrates.

1.1 *Epilambanein* – to seize; to be taken hold

> *"... [If at] the time of his fit he clenches his hands [tightly as] though rigor has seized him, and, with legs extended, greatly convulsed...; [if] he loses consciousness and foam comes from his mouth...; [if] he cries "u'āyi!" or utters a sound (like an animal)...[while] saliva flows from his mouth and his neck is pressed down to the left... [then] it is* miqtu."
>
> *"…If at the time of the possession his mind is consciously aware, [the demon] can be driven out…, [but if] his mind is not so aware, [the demon] cannot..."*
> *The Saikikku*

What we now call *epilepsy* pervades history, both religious and medical. Termed *antašubba* (Sumerian) or *miqtu* (Akkadian), *the falling disease* is thought to have been first noted in the *Saikikku (*All Diseases), a Babylonian cuneiform medical text completed in 1046 BC (Wilson and Reynolds 1990, Eadie and Bladin 2001). Records from antiquity across a sundry of cultures contain harrowing, sharp illustrations of sudden paroxysmal loss of motor control, of animalistic cries of pain and confusion…of demonic possession (Eadie and Bladin 2001). *Epilambanein*, the Greek word from which epilepsy is derived, was to be feared as sacred. Naturally though with time, this perspective shifted as slow discovery steadily revealed epilepsy's root as a physical disease; a stance posited quite early on in the Hippocratic writings '*On the Sacred Disease',* dated from around 400 BC (Temkin 1933, Eadie and Bladin 2001). Approaching modernity, the International League against Epilepsy (ILAE) defined this disease as the chronic predisposition to recurrent, unprovoked seizures; a definition to which a 2014 revision added some operational

specificity in the form of three criteria that an individual must meet to warrant a diagnosis (Fisher et al. 2014, Rao and Lowenstein 2015).

1.1.1 Regional and worldwide prevalence and incidence of epilepsy

Now defined, additional challenges arise when trying to determine epilepsy's worldwide prevalence and incidence given the inevitability of variation across geographical populations based on socioeconomic differences, age of onset, case ascertainment methodologies, lack of door-to-door studies, disparities in definitions, and other such factors (Fiest et al. 2017, Janmohamed et al. 2019, Lee et al. 2019, Naimo et al. 2019). Still much epidemiological work has been done in spite of these discrepancies. For high income communities, it is reported that there is an estimated prevalence ranging from 2.7 to 7.1 out of 1000 while in low and low-middle income economies, the range is estimated to be quite a bit larger: 2.2 to 22.2 out of 1000 (Banerjee et al. 2009, Janmohamed et al. 2019). Cumulative global incidence appears to be 50 to 67.7 out of 100,000 per year (Hauser and Hersdorffer 1990, Stafstrom and Carmant 2015, Fiest et al. 2017). Meta-analyses also revealed that globally, there is a higher proportion of individuals with epilepsy in developed countries and in urban areas of resource-limited countries than elsewhere (Bell et al. 2014). Nevertheless and all together, about 0.5 to 1% of the global population now suffers from epilepsy (Stafstrom and Carmant 2015) which of course involves the endurance of spontaneous epileptic seizures in their many forms and modalities plus the neurobiological and somatic morbidities; high risk of serious psychocognitive and psychosocial deficits; great personal and societal financial burden; increased risk of bodily injury; reduced quality of life; and increased mortality associated with this condition (Skjei and Dlugos 2011, Fisher et al. 2014, Rao and Lowenstein 2015, Naimo et al. 2019). With these staggering numbers in mind, research and development in the field has led to the identification and explication of

epilepsy's pathophysiology, which informs methodology for a clinician's diagnostic workup and eventually their therapeutic approach (Fitsiori et al. 2019). Experts know now that there are myriad brain pathologies from which this disease can emerge, which continues to motivate the field to uncover epilepsy's glacial unknowns.

1.1.2 Epileptic Seizures: Definition, Screening, and Treatments

Before delving into presently used approaches to ameliorate seizures - the major, chameleonic symptom of this disease - we must first define what epileptic seizures are and how they are screened for. Through that information we may explore their expansive range of etiologies and treatments.

Epileptic seizures are phenomena comprising symptoms fundamentally related to dysfunctional electrical activity in the brain such that may occur with disturbances to the balance between network excitation and inhibition. Single or concomitant pathologies may occur at any stage from genes all the way up to network level circuitry, leading to the Gestalt emergence of seizures and seizure-related electrical events (Rao and Lowenstein 2015, Stafstrom and Carmant 2015). Due to how these emergent events can arise from any part of an individual's cerebral cortex and involve any cortical modality, among other factors, such as whether the inciting pathology is genetic or acquired and presents focally or in a widespread manner, seizure presentation can vary wildly between individuals. The following criteria are therefore used by clinicians to assist with identification of seizure origination and type: focal; generalized; combined generalized and focal; and unknown. Each criterion contains several subgroupings. Focal seizure subgroupings are as follows: with either preservation of (focal aware) or loss of (focal impaired) consciousness during epileptic events, manifestations may be termed tonic, clonic, or atonic if there is motor involvement. "Non-motor" events will feature cognitive,

autonomic, and/or emotional characteristics. The focal classification and all associated subgroups pertain to epileptic seizures which arise from one hemisphere, although it is possible for certain types of focal seizures to propagate to both hemispheres. Generalized seizure subgroupings differ slightly; seizures under this umbrella may also exhibit motor involvement - termed tonic, clonic, tonic-clonic, myoclonic tonic-clonic, atonic, or myoclonic atonic. Non-motor generalized seizures are also referred to as absence and can be "typical, atypical, myoclonic, and absence with eyelid myoclonia" (Stafstrom and Carmant 2015, Scheffer et al. 2017, Falco-Waltera et al. 2018, Naimo et al. 2019).

Epilepsies associated with congenital or acquired lesions used to be referred to as "symptomatic localization-related" meaning seizure presentation would depend on the part of the brain that has become epileptogenic. Categorically these events initiate focally then spread and exhibit a more generalized phenotype (Stafstrom and Carmant 2015). It is unknown however how these events arise.

These recurrent and unprovoked (or reflex) seizures, often heavily multifactorial and idiopathic in nature, arise in around 50 million individuals worldwide (World Health Organization website, www.who.int/en), inviting great complexity as the etiologies underlying these are immensely vast, widely varied, and typically poorly understood (Bladin et al. 2000, Hayashi et al. 2002, Frey 2003, Sedel et al. 2007, Schuele and Luders 2008, Stafstrom and Carmant 2015). Advancements with multidisciplinary screening tools are therefore of critical importance as tailored methodologies are required to thoroughly and accurately investigate an individual's syndromic and etiologic circumstances to guide treatment decisions and dispel some of the difficulties inherent to this disease (Skjei and Dlugos 2011, Fitsiori et al. 2019, Naimo et al. 2019).

One ubiquitously used screening tool is the electroencephalogram (EEG) or electrocorticography (intracranial EEG, ECoG) to screen for spontaneous, high-amplitude voltage changes, sharp waves, focal spikes, or slowing in readouts of an individual's brain activity, such that would occur during a seizure or in between seizures during interictal periods (Rao and Lowenstein 2015). EEG and ECoG thereby allows clinicians to determine the type or types of seizures an individual has (Glauser et al. 2016). Clinicians also make use of laboratory techniques to identify possible genetic, metabolic, infectious, inflammatory, or autoimmune causes (Hussain and Sankar 2011, Yuan et al. 2014, Chen et al. 2017, Almoguera et al. 2019, Dahlin and Prast-Nielsen 2019, Lee et al. 2019, Marchi et al. 2019, Naimo et al. 2019) and neuroimaging techniques including magnetic resonance imaging (Fitsiori et al. 2019), to detect possible structural irregularities from which epilepsies can arise, such as from developmental cortical malformations (Skjei and Dlugos 2011, Naimo et al. 2019). With this multidisciplinary toolbox, experts may investigate the underlying etiology of an individual's epilepsy which can initiate or be acquired at any age (Skjei and Dlugos 2011, Glauser et al. 2016). It is of note that infant or child-onset epilepsies are more commonly associated with developmental cortical malformations, genetic conditions, or metabolic disorders compared to adult-onset epilepsies which tend to arise from acquired pathologies such as brain tumor, stroke, immune-mediated disorder, or CNS infection (Lee et al. 2019, Marchi et al. 2019). Traumatic brain injury accounts for a large number of epilepsy-emergent cases across all ages, with 20 to over 40% of cases exhibiting post-traumatic seizures and epilepsy (Lee et al. 2019).

Few viable treatment strategies for some individuals with epilepsy have been identified and explicated. Most individuals living with epilepsy (around 70%) find relief with anti-epileptic drugs (AEDs) of which there are just over 20 (Rao and Lowenstein 2015, Stafstrom and Carmant

2015). These therapies arose from the field's now disputed stance that seizures result from unbridled propagation of excessively synchronous firing between large neuron ensembles; a phenomenon caused by imbalances between circuit excitation and inhibition. Thusly AEDs act to decrease the brain's electrical activity via various, generalized excitation dampening or inhibition enhancing mechanisms relevant to one's specific type of epilepsy (Bui et al. 2015, Rao and Lowenstein 2015, Naimo et al. 2019). An AED's ultimate function is therefore to singularly constrain seizures, rather than to amend the disease itself; modification of underlying epileptogenesis by any AED has not yet been demonstrated (Devinsky et al. 2013).

The remaining 30-40% of global populations experiencing AED-resistant epileptic seizures require alternative treatment strategies including those who experience seizure relief from AED usage, but suffer from serious side effects (Kwan and Brodie 2006, Rao and Lowenstein 2015). Certain candidates among this cohort may be receptive to seizure relief with specific anti-inflammatory or immunosuppressive treatments (Li et al. 2012, Devinsky et al. 2013). Others must look elsewhere such as to responsive deep brain stimulation, vagus nerve stimulation, a ketogenic diet, or even probiotic treatment (Rao and Lowenstein 2015, Dahlin and Prast-Nielsen 2019).

Surgical resection is another treatment alternative clinicians may utilize, were the patient to possess focal epileptogenic loci, identifiable by use of EEG and ECoG (Glauser et al. 2016). Some words to address biomarker identification for epileptogenic foci: it is of traditional thinking, such that underlies AED development, that hypersynchronous neuronal firing underlies seizure-related spontaneous, high-amplitude voltage changes in EEG readouts, however, groups have begun to challenge blanket hypersynchrony as the root of all epilepsy and propose this to be too oversimplified (Jiruska et al. 2012). In its place, new rationale has been introduced that

describes seizures to emerge from complicated interactions between neuron subpopulations wherein synchrony is dynamic in nature, undergoing changes on "multiple spatial and temporal scales" (Rao and Lowenstein 2015). This new perspective was born from studies involving the use of microelectrode arrays to record the activity of single neurons during seizures. Not susceptible to information muddling inherent to macroscopic EEG-based recordings that comprise the activities of thousands of neurons, these studies have revealed finer-scale patterns that may assist with surgical planning. From studies using such techniques a center-surround schematic has been proposed to underlie epileptogenesis from the observation that seizure-originating regions can be subdivided into a central 'core', exhibiting intense, synchronous, high frequency oscillations (80 Hz and higher, rates may depend on the nature of the underlying epileptogenic lesion) and a surrounding 'penumbra', wherefrom readings will show lower frequency, desynchronized neuronal firing. It is thought that inhibitory projections from the core out to the penumbra creates a strong limiter and acts as an endogenous restraint on seizure propagation, which suggests that, the epileptogenic site is much smaller than total brain area affected by the onset of a seizure. A clinician might perhaps ascertain epileptogenic regions based on the "phase-locking" of high frequencies in the gamma range (80-150 Hz, core) to lower frequency ictal rhythms (penumbra). It is of note though that the mechanisms driving the start and termination of a seizure are largely unknown.

Despite this biomarker being potentially robust, symptoms return in around 40% of epileptic patients who receive surgery (Sisodiya 2000, Blumcke et al. 2009, Rao and Lowenstein 2015). So, many individuals remain spate with epilepsies that are wholly resistant to treatment and must endure unmanageable recurrent and spontaneous seizures

1.1.3 Medical Intractability of Epilepsy

As for what causes treatment resistance, we must first settle on a definition of medically intractable, pharmaco-, treatment-, or drug-resistant epilepsy (DRE), which the ILAE in 2010 proposed, should be "the failure of adequate trials of two tolerated, appropriately chosen and used antiepileptic drug (AED) schedules (whether as monotherapies or in combination) to achieve sustained seizure freedom" (Kwan et al. 2010). Reviews of medical records in Southern Finland, Singapore, Southern France, and the Al-Kharga district of Egypt reveals that DRE as defined above is prevalent in a range of 0.7 – 1.36 out of 1000 individuals with epilepsy (Eriksson and Koivikko 1997, Kun et al. 1999, Picot et al. 2008, Farghaly et al. 2013, Janmohamed et al. 2019). Incidence on the other hand exhibits some discrepancies between studies and age groups. In children, incidence proportions range at 6.9-40%, while in adults 30-51% has been reported (Oskoui et al. 2005, Skjei and Dlugos 2011, Gilioli et al. 2012, Chen et al. 2018, Kalilani et al. 2018, Janmohamed et al. 2019). Discrepancies aside, drug-resistance is clearly common and the mechanisms underlying it still remain hypothetical.

Certain theories have been developed in attempts to address drug resistance. One such theory is the drug transporter hypothesis, which suggests that overexpression of multidrug efflux transporters is central to drug-resistance by way of reducing the concentrations of AEDs at their intended targets (Tishler et al. 1995). The group who initially proposed this found evidence of one such transporter, P-glycoprotein (P-gp, encoded by the multidrug resistance-1 gene, MDR1), to be increased in capillary endothelium and astrocytes in 19 patients with intractable epilepsy undergoing surgery. P-gp transports various AEDs from the brain to the blood so its overexpression could limit access of AEDs to the brain, thereby reducing possible therapeutic efficacy (Löscher and Potschka 2005a, Devinsky et al. 2013). Further evidence has been supplied

by studies wherein P-gp expression was demonstrated to be overexpressed at the luminal side of endothelial cells, in astrocytic endfeet, and in dysplastic neurons of developmental glioneuronal lesions, and lesions involved with hippocampal sclerosis, cortical dysplasia, and dysembryoplastic neuroepithelial tumor (DNET); conditions beholden to intractable epilepsy (Sisodiya et al. 2002, Aronica et al. 2003). It has also been proposed that over-expression of P-gp and other similar drug transporters might act as a biomarker of a "drug-resistance zone" (Zhang and Kwan 2019). Despite this, clinical administration of selective P-gp inhibitors remains largely ineffective in human subjects in the 20+ years since the theory was introduced (Devinsky et al. 2013).

Another popular hypothesis of DRE is target theory, citing drug resistance to be caused by alteration of a drug's molecular target site (Janmohamed et al. 2019). Various studies have shown wide-ranging alterations in receptor subunit expressions in $GABA_A$ receptors (Bethmann et al. 2008), as well as in voltage-dependent ion channels (Ragsdale and Avoli 1998, Remy et al. 2003) in epileptic, drug-resistant animal subjects and human patients (Remy and Beck 2006). The target hypothesis however requires more work to understand the precise molecular and physiological changes causing altered sensitivity which could affect the pharmacokinetic (absorption, distribution and metabolism) and pharmacodynamics processes involved with resistance to antiepileptic drugs. These are often widely varied, which is reflected by the diverse clinical response of patients with the same prognostic profile to the treatment with anticonvulsant (Remy et al. 2003, Löscher 2005b, Naimo et al. 2019). Additionally, currently available drugs have widely varied mechanisms of action; making concurrent alterations of targets for most to be somewhat unlikely (Tang et al. 2017, Janmohamed et al. 2019).

Other theories exist, including the intrinsic severity hypothesis (Rogawski 2013) which suggests drug-resistance to be an "acquired and self-perpetuating phenomenon" (Kwan and Brodie 2002) by way of the epileptic discharges structurally and functionally modifying certain neural receptors (Kwan and Brodie 2002), but individuals with DRE are a highly heterogeneous group and no theory in isolation can explain failure of multiple drugs in every patient (Janmohamed et al. 2019). A holistic approach that integrates information from multiple systems and multiple hypothetical frameworks could possibly provide answers to these complex questions (Naimo et al. 2019).

1.2 Developmental Cortical Malformations are commonly associated with DRE

> *"...Patterns may be very illuminating and important, but the underlying causal agencies must be separately specified (though often they are not)."*
> *Peter A. Corning, Ph.D.*

1.2.1 Developmental Cortical Malformations

Whatever the molecular mechanism, DRE is a very common sequelae to developmental cortical malformations (DCMs), especially in infants and children (Flint and Kriegstein 1997, Wyllie 2000, Guerrini and Carrozzo 2002, Berg and Kelly 2006, Skjei and Dlugos 2011, Borggraefe et al. 2019, Fitsiori et al. 2019, Naimo et al. 2019) with 40% of DREs diagnosed as associated with congenital or acquired DCM (Guerrini et al. 2003). To investigate, it may suit the purposes of some to frame DRE in this context as Gestalt, a property or "pattern" emergent from an amassing of "underlying causal agencies" unspecified and unknown.

DCMs including cortical dysplasia, tumor, sclerosis (scarring), vascular malformation, and a multitude more (Stafstrom and Carmant 2015) stem from a variety of etiologies that cause

aberrations of central development; the timing of which will determine the type or types of resulting structural abnormalities (Squier and Jansen 2014). During incipience, congenital circumstances or an acquired insult (ischemic, mechanical, etc.) could inhibit the generation of cells, while disruptions at later stages could result in improper migration and/or eradicate cells already present (Barkovich and Kjos 1992, Guerrini et al. 2003). These are a few examples in a sundry of different varieties, spanning a vast array of severities and inducing factors. This writing will focus on polymicrogyria, a complex spectrum of cortical malformations (Stutterd and Leventer 2014) representing 20% of all DCMs (Leventer et al. 2010), and its pathology promoting characteristics.

1.2.2 Polymicrogyria

Polymicrogyria (PMG) is commonly associated with a wide range of syndromic symptoms with very limited potential for amelioration with pharmacological intervention or surgical resection such as intellectual disability, global developmental delay, spasticity, psychiatric illnesses, and more, with the most common being DRE – 75 to 87%; 65% intractable (Kuzniecky et al. 1993, Sisodiya 2004, Guerrini and Filippi 2005, Leventer et al. 2008, Leventer et al. 2010, Shain et al. 2013, Rao and Lowenstein 2015, Donkelaar 2016, Maillard and Ramantani 2018). There remains no standardized classification system for PMG, yet this grouping of focal, diffuse, unilateral, or bilateral disorders is commonly categorized by widely heterogeneous imaging patterns; as well as by the timing of the inciting congenital or injurious disruption of cortical development (Friede 1989, Leventer et al. 2010, Barkovich 2010a, Barkovich 2010b, Squier and Jansen 2014, Donkelaar 2016). PMG-inciting events typically occur towards the end of and after the neuronal migratory period, through the earliest aspects of cortical organization (Judkins et al. 2011, Barkovich et al. 2012, Donkelaar 2016). Etiologies can be acquired and destructive in utero via perinatal ischemic or infectious insult such as with fetal

cerebral ischemia or intrauterine cytomegalovirus (Dvorak and Feit 1977, Montenegro et al. 2002, Gaytant et al. 2003, Barkovich 2010a, Donkelaar 2016) comprise genetic mutations and copy number variations (Lee et al. 1997, Stutterd and Leventer 2014), or metabolic disorders (van der Knaap and Valk 1991). Congenital circumstances have been suggested to yield DCM by way of "disturbances in cell proliferation, neuronal migration, and/or programmed cell death (Stutterd and Leventer 2014). As these insults, congenital or otherwise, often result in the emergence of PMG in association with other CNS disorders, rather than alone. These can include periventricular nodular heterotopia, excessive scattered neurons in the underlying white matter, agenesis of the corpus callosum and brainstem or cerebellar abnormalities (Squier and Jansen 2014, Stutterd and Leventer 2014, Maillard and Ramantani 2018).

First described in 1916 (Bielschowsky 1916), PMG features cortical over-folding; common indications include an irregular, bumpy cortical surface made up of excessive and abnormally small gyrations (Sisodiya 2004, Barkovich 2010b, Squier and Jansen 2014, Stutterd and Leventer 2014, Donkelaar 2016). At a smaller scale, iterations of PMG exhibit heterogeneous irregularities of cortical structure and lamination (Squier and Jansen 2014), while still retaining some function despite micro- and macroscopic aberrance (Araujo et al. 2006).

As extent and location of malformed brain area will influence the types of resultant symptoms, so will etiological timing. For instance, PMG can exhibit an unlayered phenotype if inciting factors occur at $16^{th} – 24^{th}$ weeks of gestation, but a four-layered phenotype with insult at later stages, $18^{th} – 24^{th}$ weeks (Barth 1987, Friede 1989, Guerrini and Carrozzo 2002). Occasionally though, both may be found in the same patient and can even overlap (Judkins et al. 2011, Squier and Jansen 2014). In any case, both circumstances are bordered by an immediate transition to typical appearing cortex (Kuzniecky et al. 1993), which was originally dismissed as

functionally eloquent when it is in fact part of the pathogenic substrate inherent to PMG's many clinical manifestations. In human patients, it has been observed that regions extending beyond visibly (MRI-detectable) malformed tissue exhibit epileptogenesis (Araujo et al. 2006, Chassoux et al. 2008, Ramantani et al. 2013, Maillard and Ramantani 2018), which can be accurately delineated to success with the use of EEG or ECoG.

Pinpointing an alternative treatment target for individuals with PMG or other related malformations is essential as so many lives are ensnared by its many clinical manifestations. Work in this work will utilize an animal model of human polymicrogyria to study poorly understood epilepsy-promoting cellular mechanisms therein. It is also to be considered that some or all additional clinical manifestations may arise from the same undetermined pathological substrates, therefore this work may be applicable across multiple contexts.

1.3 Animal model of resistant epilepsy associated PMG; the transcranial freeze lesion

1.3.1 Background and freeze-lesion methodology

To examine how these medically retractable pathologies emerge, many make use of the transcranial freeze lesion model that produces histopathology similar to human four-layered PMG (Dvorak et al. 1978). By placing a freezing probe onto the uncovered leptomeninges (Squier and Jansen 2014) of a neonatal rodent pup for some seconds, a transcranial ischemic lesion will be created (Dvorak and Feit 1977, Dvorak et al. 1978). Contact freezing during this period will thrombose blood vessels, and cause the necrosis of neurons present on the cortical plate (Barth 1987, Squier and Jansen 2014), which at this period of cortical development, comprise layers IV, V, and VIa (Dvorak et al. 1978). To generate an appropriate histopathological correlate to four-layered human PMG, the injurious freeze lesion was

implemented on postnatal day one (P1) in rodents as previously performed (Dvorak and Feit 1977, Humphreys et al. 1991), as this time point corresponds with the 18th to 24th gestational week in humans when cortical neuroblast migration is taking place

Following the injury, superficially-intended neuroblasts and capillaries will continue to migrate to the cortical plate, leading to the development of a focal microgyric region of dyslaminated cortex containing four layers, instead of the typical six (Dvorak and Feit 1977). The superficial aspect of the microgyrus, denoted with Arabic numerals (Jacobs et al. 1999b) as layers 1 and 2 are anatomically similar and continuous to adjacent neocortical layers I and II/III (Dvorak and Feit 1977, Dvorak et al. 1978, Jacobs et al. 1996, Rosen et al. 1996), with layer 2 being relatively cell dense compared to layer 1 (Rosen et al. 1996), similar to the pattern observed in normal appearing neocortical layers II/III versus layer I. Layer 3, containing a small population of small somata, glia-resembling cells (Dvorak and Feit 1977), is relatively thin and terminates abruptly where the microgyrus meets adjacent six-layered cortex (Crome 1952, de Leon 1972). Layer 4 is similar to and often contiguous with layer VIb of adjoined normal appearing cortex. This all aligns with what is seen clinically (Crome 1952, de Leon 1972). The normal appearing expanse of cortex adjoining the microgyrus is the hyperexcitable substrate from which epileptiform activity can be generated; represented experimentally via electrical evocation in ex vivo slices. Termed the paramicrogyral region, or PMR (Jacobs et al. 1996), this hyperexcitable area offers researchers a unique lens, allowing for suitable evaluation of the proclivity for epileptogenic circumstances to emerge from a hyperexcitable brain. Hyperexcitability, a prominent characteristic observed in human PMG and critical component to epileptogenesis, is observed in the PMR of rats lesioned on postnatal day (P) 1 at survival ages up to P90, while rats lesioned on P0 display a decreased incidence in epileptiform responses

following survival age of P40 (Jacobs et al. 1999a). Similarly, Kellinghaus et al. found no difference in the amount of cortical excitability in adult (P60) rats that were lesioned at P0 compared to non-lesioned rats of that same age (Kellinghaus et al. 2007). Further, Dvorak et al. demonstrated that this same lesion performed on rats at P4 would not induce a microgyric malformation, once again adding credence to the time-specificity, or critical period, required for an inciting error to result in anomalous layering; the possible development of hyperexcitability however was not tested at this time point (Dvorak et al. 1978).

Human PMG-associated seizures may begin in newborns at birth or be delayed for years (Pascual-Castroviejo et al. 2001, Fasulo et al. 2012, Fitsiori et al. 2019). Rats freeze-lesioned singularly at P1 do not exhibit spontaneous seizure behaviors, however they are prone to exhibit epileptiform activity in slices associated with the induced microgyrus consistently and reproducibly at P12 (Jacobs et al. 1996, Jacobs et al. 1999a, Scantlebury et al. 2004) a timepoint correlated with humans at birth (Sengupta 2013). It is of note though that spontaneous seizure behaviors have been demonstrated to occur in rats with multiple freeze lesions induced prenatally, 18 days post-conception (Kamada et al. 2013), and in mice with single freeze lesions induced on P0 – P1 (spontaneous non-convulsive seizure events primarily during slow wave sleep, Sun et al. 2016). As will be discussed in more detail below, the onset timings of hyperexcitability and epileptogenicity within this region are delayed and staggered. Researchers can study the PMR to reveal particular alterations that might distinctly occur before the area becomes hyperexcitable, after it becomes excitable, and those that may contribute to epileptogenesis. This animal model, wherein rodents are freeze lesioned at P1 is therefore an accepted and robust method for the study of the epileptogenic mechanisms inherent to human polymicrogyria.

Studies reported in this communication will take place within epileptogenic PMR, since this area, being sensitive to the generation of epileptiform activity, is an advantageous place to look for epileptogenic mechanisms. Cellular and subcellular characteristics of the model, as they pertain to the induction of epileptiform activity, will be delineated in the following sections. Despite the cited breadth in observations in alterations within the microgyrus, PMR, and other related areas, it is still under investigation how epilepsy, cognitive impairment, and other such sequelae emerge from the abundance of altered cellular and subcellular phenomena.

1.3.2 Cellular and sub-cellular disturbances in the freeze-lesion model of DCM

Much work has been done to identify the manner of disturbance that the freeze lesion imparts on neocortex and interconnected areas, however, there are still many unanswered questions. Provided in the following section is a survey of human PMG cellular and subcellular characteristics recapitulated in the animal model. If there are any gaps, information from other specimens will be provided.

To start, neurons within the associated visibly malformed cortical area, the microgyrus, are not generated in response to the lesion, but instead, are prenatally generated and migrate through or around the damaged area to reach their final station (Rosen et al. 1996). It was demonstrated that cell-dense layer 2 within the microgyrus contains neurons generated between embryonic days 17 through 20 (Rosen et al. 1996), which would normally occupy layers III and IV in non-developmentally malformed neocortex (Rosen et al. 1996). Neurons formed earlier at embryonic day 15 were not found in the microgyrus (Rosen et al. 1996); a significant find, since these neurons would have inhabited the deep neocortical layers, consistent with the FL model's mechanism of ischemia-induced cell death selective to deep-layer neurons due to the timing of the applied insult. These local, prenatally generated neurons within the microgyrus exhibit

widespread disorganization of laminar architecture as conveyed by glial fibrillary acidic protein and glutamate staining (Humphreys et al. 1991) and are delayed developmentally (along with neurons inhabited within PMR), as indicated by the persistence of elements typically eliminated early in non-injured cortex (Cepeda et al. 2006). One cellular example of this is the presence of normally transitory Cajal-Retzius cells in P12 rat PMR cortex; these cells, which possess a role in normal corticogenesis (Frotscher 1998) are typically absent in control tissue by this postnatal age (Super et al. 1997, Eriksson et al. 2001).

Subcellularly within PMR, certain membrane receptors comprise prematurely expressed subunits. One report revealed a decrease in all GABA$_A$ subunits with the exception of α3 (Redecker et al. 2000), classically known to decrease in expression and be replaced in the second postnatal week with mature subunits, α1 or α4 (Laurie et al. 1992). Another demonstrated similarly that the expression of α3 and α2, another immature subunit, persists within PMR, at the expense of mature α1 (Defazio and Hablitz 1999). As all GABA$_A$ receptor binding sites occur at the interfaces of the receptor class' typical two alpha subunits and a beta subunit or a gamma subunit (Richter et al. 2012), the persistence of a premature phenotype may be a contributing factor to another observation of decreased binding to GABA$_A$ receptors in PMR, with binding levels reaching normalcy outside of this range (Zilles et al. 1998). Taken together, these findings suggest not only that there is altered expression and persistent immaturity of inhibitory GABA$_A$ receptor within freeze-lesion induced PMR, but that there may also be reduced receptor density. Excitatory glutamate receptors also exhibit changes. For instance, increases in AMPA and kainite receptor binding have been demonstrated (Zilles et al. 1998) and persistence and enhanced functioning of the immature NR2B embryonic subunit containing NMDA receptors has been demonstrated (Defazio and Hablitz 2000, Cepeda et al. 2006).

Glia are also affected in numerous ways, which undoubtedly, however undefinedly occupy a significant part of PMG related pathogeneses. Fibers resembling radial glia have been observed within lesioned cortex up to the fifth postnatal week, an immature element typically absent in non-injured cortex by this point in development (Rosen et al. 1992). Also in the malformed area, reactive gliosis (glial scarring) occurs (Wetherington et al. 2008, Devinsky et al. 2013) wherein already-present astrocytes exhibit hypertrophy, increased complexity, and increased arborization of their cellular processes. Upregulated expression of various proteins such as glial fibrillary protein (GFAP, common marker for reactive astrocytosis) is well documented to take place within the microgyral region of young freeze lesioned rodents (Hanson et al. 2016). Importantly, it has been observed in humans that various forms of epilepsy initiate within or adjacent to glial scar tissue (Mckhann et al. 2000). Clinicians even consider gliosis to be a predictor of developing post-traumatic epilepsy (Guerreiro et al. 2003). Continued study in the field has revealed many ways through which epileptogenicity can arise from astrocyte dysfunction.

Metabotropic glutamatergic receptors (mGluR) 3, 5, and 8 have been documented to exhibit increased expression in reactive astrocytes; with mGluR5 being of particular interest since expression of this protein typically decreases with maturity (Panatier and Robitaille 2016). Adding nuance to the persistent, dysmature expression of elevated mGluR5 into adulthood, it is possible for astrocytes to induce neuronal synchrony though the induction of NR_{2B} subunit containing extrasynaptic NMDAR-mediated slow inward currents (also known as slow transient currents). These are proposed to be induced by astrocytic glutamate released in response to strong mGluR5-activation or by direct uncaging of calcium within astrocytes (Pasti et al. 1997, Angulo et al. 2004, Fellin et al. 2004, Tian et al. 2005). With this we are introduced to one

possible contributor to observed high levels of extracellular glutamate present within PMR (Campbell and Hablitz 2008) and perhaps even an epileptogenic mechanism. Interestingly, it has been demonstrated that within reactive astrocytes, there is crosstalk between mGluR5 and excitatory amino acid transporters (EAAT), wherein mGluR5 dynamically controls their functionality (Vermeiren et al. 2005). EAAT1 (GLAST) and EAAT2 (GLT-1), expressed by astrocytes, are responsible for a great proportion of glutamate regulation (Tanaka et al. 1997), and themselves display peculiar alterations within the malformation proper and PMR. It has been reported in adult humans that with increased dysplastic severity, there is larger decrement as well as increased diffusivity of both GLT-1 and GLAST expression in astrocytes, which may also occur in rodents, as it has been reported that in mature PMR, the domain an astrocyte executes glutamate transport within, is larger than what is observed within controls (Armbruster et al. 2014). This can be indicative of a loss of typically non-overlapping "astrocytic domain organization" (Panatier and Robitaille 2016), a phenomenon associated with the ferrous chloride rodent model of post-traumatic epilepsy (Oberheim et al. 2008). Another report provides more temporal and spatial specificity with observations that expression of GLT-1 is higher in PMR than controls of young lesioned rats (pre-epileptogenesis), but following epileptogenesis, GLT-1 expression drops lower than controls (Armbruster et al. 2014). Curiously, this appeared true for astrocytes exhibiting high or low GFAP profiles, presuming astrocytic reactivity or quiescence respectively. Expression of GLAST on the other hand is high in pre-epileptogenic microgyrus and is correlated with high GFAP expressing (presumed reactive) astrocytes. Post-epi, GLAST expression remains high in the microgyrus with an increase also spreading into proximal aspects of the adjoined PMR. At this time point though, GLAST expression is the same between high and low GFAP expressing astrocytes. It is believed that immature astrocytes express a higher

GLAST to GLT-1 ratio; this immature characteristic persists in PMR of the mature FL brain (Armbruster et al. 2014). This is important as low to no GLT-1 expression is associated with "lethal spontaneous seizures" (Tanaka et al. 1997). There is conflicting data regarding whether glutamate transport by way of astrocytic GLT-1 and GLAST remains unchanged in PMR compared to sham (Hanson et al. 2016) or is sharply reduced in PMR (Campbell and Hablitz 2008).

Astrocytic EAAT function depends on Kir4.1 channels which have been documented to exhibit reduced expression in reactive astrocytes (Dossi et al. 2018). These inwardly rectifying potassium channels "establish a negative resting potential that drives the electrogenic uptake of glutamate" (Robel and Sontheimer 2015), therefore impairments in Kir4.1 function would serve to exacerbate EAAT dysfunction. While this has not been directly assessed in the freeze lesion model, lowered Kir4.1 expression and consequent reduction in potassium buffering is a noted feature other rodent models of epileptogenesis (David et al. 2009) and in human cases of mesial temporal sclerosis, a common cause of intractable temporal lobe epilepsy in humans (Steinhäuser et al. 2012). Also documented to be impaired in reactive astrocytes of epileptogenic tissue (Robel and Sontheimer 2015), astrocytic water channels (aquaporin-4, AQP4), which mediate bidirectional flow of water between extracellular space and the blood (blood brain barrier) are critical here as impairments with water regulation "decreases extracellular space volume which may promote seizures by increasing extracellular K concentrations and possibly enhancing non-synaptic neuronal interactions" (Devinsky et al. 2013).

Associated with both Kir4.1 downregulation and AQP4 dysfunction is disruption of the blood brain barrier which has been demonstrated to be localized to epileptogenic regions (Sweeney et al. 2019) and involve increased expression of multidrug transport proteins in

perivascular astrocytes, another subcellular hallmark of DCM. This is hypothesized to be a "'second line of defense' mechanism to protect the brain from toxins that may enter due to BBB breakdown" (Löscher and Friedman 2020). Overexpression of these efflux transporters, multidrug resistance protein 1 (MDR1, or p-glycoprein, P-gp) and multidrug resistance-associated protein 1, MRP1 (Ak et al. 2007), can also lead to decreased expression of AEDs in brain thereby reducing possible therapeutic efficacy (Löscher and Potschka 2005a, Devinsky et al. 2013). This is the premise of the drug transporter hypothesis of drug-resistance introduced in section *1.3 medical retractability of epilepsy*. The group who initially proposed this theory found P-gp to be increased in astrocytes and capillary endothelium in humans with intractable epilepsy undergoing surgery (Löscher and Potschka 2005a), while in a non-DCM brain, MDR1/P-gp expression is typically absent and MRP1 expression is very weak in astrocytes (Ak et al. 2007). This has been corroborated in other studies wherein P-gp expression was demonstrated to be overexpressed in astrocytic endfeet (as well as at the luminal side of endothelial cells and in dysplastic neurons) of developmental glioneuronal lesions and lesions associated with cortical dysplasia (Sisodiya et al. 2002, Aronica et al. 2003). While this astrocytic phenomenon has not yet been showcased in the freeze lesion model, it has in other rodent models for intractable epilepsy (Löscher and Potschka 2005a) and may be important to keep in consideration while hypothesizing about the emergent nature of epilepsy in DCM.

In regard to other glia, an assessment of oligodendrocyte dysfunction has not been performed in rodents, but it has been assessed in a polymicrogyric model induced in gyrencephalic ferrets that oligodendrocytic markers APC, pH3, and Olig2 (also a marker for astrocyte precursors in rodent brains) were not changed between normal and malformed brains (Masuda et al. 2015). It should be noted however that oligodendrocytes and astrocytes exhibit

gap junction coupling which each other (Magnotti et al. 2011), so oligodendrocytes' true contribution to pathogenesis may not yet be fully understood.

Little is known about macrophage and microglia alterations in DCM, however limited assessment has been performed in human focal cortical dysplasia (caused by DCM) wherein microglia cells and macrophages were observed in high numbers within developmentally malformed areas of cortex. Activated microglia in particular were found clustered around dysplastic neuronal cells and around blood vessels, with increased density correlating with seizure frequency (Boer et al. 2006). Correspondingly, microglia-derived inflammatory factors are often found in malformed regions (Devinsky et al. 2013), and remarkably certain anti-inflammatory treatments do work for seizure relief in retractable patients (Li et al. 2012, Devinsky et al. 2013).

1.3.3 Anatomical and functional connectivity disturbances in the freeze-lesion model of DCM

Various methodologies have revealed the transformed nature of the anatomical connections to, within, and from malformed regions of cortex and adjacent PMR. To start, local pyramidal cell afferents and commissural fibers are organized abnormally within microgyrus and around it in PMR as disclosed by neuronal tracers injected into the microgyrus proper, PMR, and contralateral 'homotopic' cortex disclose (Giannetti et al. 1999, Giannetti et al. 2000). Thalamocortical fibers and the thalamic nuclei from which they derive are also transformed. The ventrobasal complex (VB) for instance, normally conveying direct connections to the somatosensory cortex, has fewer neurons in animals with a developmental lesion in this cortical area (Rosen et al. 2006). Thalamocortical efferents leaving VB appear to hyperinnervate PMR (Rosen et al. 2000); a premise supported with observed scarcities of cytochrome oxidase and neurofilament staining within the microgyrus proper, but an overabundance of staining within

PMR, compared to controls (Humphreys et al. 1991, Jacobs et al. 1999c). Importantly, this suggests that with the loss of their intended destination, presumed excitatory projections originally aimed for the microgyrus were redirected rather than eliminated (Humphreys et al. 1991, Jacobs et al. 1999c). This hyperinnervation of PMR by excitatory thalamocortical and cortico-cortical afferents is followed by varied consequences that suggest an onset of hyperexcitability. There is a general increased level of miniature excitatory postsynaptic current (mEPSC, current evoked by quanta of presynaptically released vesicular glutamate) activity in pyramidal neurons within layer V of PMR, as compared to the same within layer V of homologous control cortex (Jacobs and Prince 2005) indicating that excitatory afferents are not only structurally increased, but functionally increased as well. Spontaneous excitatory postsynaptic current (sEPSC, current evoked by spontaneous synaptic activity) and mEPSC frequencies have also been shown to rise incrementally in rats, from pre-epileptogenic ages P7 to P11 (Zsombok and Jacobs 2007), on top of the already high mEPSC in PMR (Jacobs and Prince 2005). This young age group precedes the age (P12) at which epileptiform activity can be evoked (Jacobs et al. 1999a), suggesting that this incremental s/mEPSC increase may contribute in some way to the onset of epileptogenesis. The mEPSC increase in this age group supports not only the premise that an increased number of excitatory afferents may exist in the PMR, but also brings up the possibility of an increased release probability from these neurons (Zsombok and Jacobs 2005). A third type of EPSC, electrically evoked (eEPSC, currents that are experimentally evoked by electrical stimulation), are multipeaked, have larger amplitudes, and greater area in PMR, further evidencing the presence of increased excitatory input to the PMR. All of this together implies that functional excitability is increased within the PMR. This hyperexcitability was demonstrated to exist all the way up to P118; animals older than P118 were not assessed

(Jacobs et al. 1996). Hyperexcitability is an epileptogenic mechanism, and thusly, it was uncovered that stimulation of cortex to generate local field potentials at a distance of 0.5 mm to 2 mm away from the microgyrus resulted in evoked epileptiform activity (Jacobs et al. 1999a). PMR can be functionally delineated in this way. Resection of the microgyrus is not necessary for PMR to be epileptogenic, in fact, resection of the malformed area has not been shown to ameliorate the ability to evoke epileptiform activity from PMR (Jacobs et al. 1999a). This is a key feature of human DCM that the rodent freeze lesion model is able to recapitulate.

In addition to alterations with excitatory circuitry, functional changes as induced by thalamocortical and corticocortical hyperinnervation of PMR also involve inhibitory circuitry. Electrically evoked inhibitory postsynaptic currents (eIPSCs) appear enhanced for a subset of pyramidal cells in layer V of lesioned cortex. This enhancement is diminished to control values following bath application of APV and DNQX, respective NMDA and AMPA receptor antagonists (Jacobs and Prince 2005), indicating that the excitatory hyperinnervation is conveyed to inhibitory cells as well as excitatory ones. Miniature (m)IPSC frequency was not shown to be altered in PMR, which suggests a maintained number of inhibitory synapses, assuming release probability is preserved at these terminals (Jacobs and Prince 2005). Another study alternatively demonstrated a decrease in inhibitory post synaptic potential (IPSP) within layer II/III pyramidal neurons in PMR (Luhmann et al. 1998), however, due to these measured responses being multi-synaptic, the reduced may actually be an observation of disinhibition. Nevertheless, a reduction in the number of immunoreactive cells of a certain inhibitory GABAergic interneuron subpopulation has been demonstrated (Jacobs and Prince 2005). What these contradictions potentially mean for the inhibitory network, as impaired in the lesioned brain, will be discussed at length in subsequent sections.

1.3.4 Involvement of inhibitory interneurons in epilepsy-promoting characteristics of microgyria

Intuitively, epilepsy, as induced by hyperexcitable PMR cortex in this model, should be causally linked to the increased excitatory afferentation and enhanced glutamatergic receptor binding and functioning (Jacobs et al. 1999c, Jacobs and Prince 2005, Zsombok and Jacobs 2007). This has been demonstrated consistently and reproducibly over the years. However, and as introduced above, there is further evidence implicating both excitatory and inhibitory networks (Jacobs et al. 1999b). Lines of evidence submit that increased excitation alone cannot account for PMR hyperexcitability, including the demonstrated delay that occurs between the increase in excitatory input to PMR pyramidal cells and the later onset of epileptogenesis (Jacobs et al. 1999a, Zsombok and Jacobs 2007). Further, increased excitatory input to at least some inhibitory targets has been established and implied (Jacobs and Prince 2005), which supports the possibility that enhanced and not diminished inhibitory function, may play a critical role in the pathophysiology of epileptogenesis (Prince and Jacobs 1998, Klaassen et al. 2006, Mann and Mody 2008). The experiments described in this communication focus on two neocortical interneuron subtypes that have been implicated mechanistically in such a way by previous studies for the purpose of confirming whether or not it imparts a grander epileptiform activity-promoting influence in PMR cortex, as compared to its influence in control cortex. The grand intention is to uncover possible avenues for DRE treatment strategy development and the key may lie with the neocortical interneurons.

1.4 Interneurons: categorization and comprehensive survey

"It is claimed that at least 3 of the 7 deadly sins are mediated by neuropeptides…
[our] regulators of physiological processes."

Fleur L. Strand

For many decades, interneurons as we know them now, maintained elusive indefinability. This term, which since the discovery of neuronal inhibition we now use as a categorical name for local circuit inhibitory neurons that share space with, but exist in structural and functional contrast to excitatory principal neurons, was shadowed by a behemoth point of contention: the lack of universally accepted classification criteria.

Interneuronal research has been ongoing since the 19th century when the father of modern neuroscience, Santiago Ramon y Cajal described a varied assortment of 'short-axon' neurons intermingled within hippocampal circuitry (Ramón y Cajal 1893). The century of research that followed deemed interneurons to be the "epitome of cellular diversity in the CNS" (Maccaferri and Lacaille 2003), exhibiting immense variation in every phenotypic aspect (Ascoli et al. 2008) and contribution to local circuitry, particularly among those that provide neurotransmission via the production and release of GABA, γ-aminobutyric acid (Maccaferri and Lacaille 2003). Of course, with great diversity comes great complexity (Allen and Monyer 2015) and while research carried on robustly through history, there was no standardization of criteria employed by groups to describe studied cells, yielding difficulties commonly experienced when attempts were made to usefully compare extrapolations between different manuscripts. To resolve this hindrance, attempts at categorical standardization have been attempted in recent years. It has resultantly been suggested to concurrently apply certain criteria to build extricable descriptions of

interneurons—these include morphological, neurochemical, physiological, and circuitry considerations (Ascoli et al. 2008).

Now, interneuronal classification is progressing past inciting sentiments likened to Babel (Maccaferri and Lacaille 2003); we enter a period wherein neuronal research is teeming with myriad information about these incredibly diverse cells and their enormously varied characteristics. It is now known that the CNS houses extensive, specialized subpopulations of projecting and local circuit inhibitory interneurons, with common subtypes shared between differing locations. Through the application of aforementioned criteria, successful comparisons can and have been attempted *for decades* (McBain and Fisahn 2001, Maccaferri and Lacaille 2003, Markram et al. 2004, Fishell and Rudy 2011).

1.4.1 Creating context: morphological, neurochemical, electrophysiological, and network interconnectivity criteria in the neocortex versus hippocampus

Depending on the region within mammalian cerebral cortex, GABAergic interneurons occupy 10-25% of total neuronal populace, wherein they function to entrain the activities of diverse neuron ensembles (Le Magueresse and Monyer 2013). More specifically, at least 20 distinct interneuron subtypes have been identified in neocortex (Fishell and Rudy 2011) and at least 21 in hippocampus (Klausberger and Somogyi 2008, Krook-Magnuson et al. 2012). These specific and distinct interneuron subtypes, in conjunction with other cellular bodies, form invariably complex, entwined networks within the central nervous system which ultimately underlie complex cognitive phenomena such as insight, or annoyance. To attempt to understand such computational intricacies, cell-level identification and characterization of the involved bodies is essential; made possible in recent decades due to the advancement of probing

neuroscientific techniques. Extrapolation from procedures such as infrared visualization of cells in slices, single-cell anatomical reconstruction, intracellular and patch clamp electrophysiological recordings, immunocytochemical detection, single cell rtPCR, animal transgenics, and other molecular biological methods like optogenetics (Maccaferri and Lacaille 2003), has revealed a wealth of information about the morphological, neurochemical, electrophysiological, and network interconnected identities of many interneuronal subtypes. Using these criteria, it becomes possible to comparatively navigate through disparate regions of the CNS at the cellular level, wherein we may observe GABAergic interneurons as they reside, function, and contribute to their respective network circuitries. The following is a survey of categorization methods and how they have been used to classify well studied interneuron subtypes, as well as discussion about certain well-categorized types as they may concurrently exist within different parts of the brain.

Morphological criteria

With the development of labeling techniques came more sophisticated examinations of interneuron morphology, which possesses multiple domains that can vary between subtypes (Buhl et al. 1994). Somata, for instance, can differ in shape, width, and orientation of their main axes relative to the pial surface in neocortex or, in hippocampus, relative to the cellular layer (Ascoli et al. 2008). Branches from somata, or dendritic and axonal arborizations, can also be described. Dendrites, typically aspiny (without spines - small dendritic protrusions that received input from a single axon) in mature interneurons (Douglas and Martin 1998), tend to exhibit unipolar, bipolar, or multipolar branching polarities. Bitufted is often used as an elaboration on the bipolar dendritic arrangement, describing neurons that give rise to two clusters of primary dendrite branches originating from ovoid-shaped somata, which extend radially or tangentially in

opposing directions (Porter et al. 1998, Zilberter et al. 1999, Markram et al. 2004, Ascoli et al.

2008). Further, dendrites of numerous polarity types can be confined within specific cortical

laminae or columns. It is important, however, to note that the extreme variability of dendritic

morphology, within interneuron types with similar somata, precludes this category from reliably

serving to define types of interneurons alone (Markram et al. 2004). This leads to axon structure

as a third morphological category, which, in conjunction with dendritic information, can

differentiate interneurons as these aspects are specialized to project through cortical functional

columns and/or cortical or hippocampal lamina in particular ways, and terminate at discrete

domains of target neurons (Markram et al. 2004). Interneuron axons can target discretely target

the axons, somata and perisomatic domains, as well as proximal dendrites, dendrites alone, or

dendrites and dendritic tufts (Miles et al. 1996, Defelipe 1997, Somogyi et al. 1998, Markram et

al. 2004) of target neurons - this particular premise will be discussed further in subsequent

sections.

Early categorization criteria heavily relied on morphology since many interneurons carry

particularly complex dendritic and/or axonal architectures and as such, were given seemingly

straightforward descriptive designations accorded by these striking patterns (Maccaferri and

Lacaille 2003). Many of these designations are still in use today including, but not limited to,

two broadly used classes, chandelier and basket cells; and less broadly used, bitufted and double

bouquet. Chandelier cells, found in both neocortex and hippocampus, possess vertically directed

dendrites with or without scant spines and an axon with terminal portions that form short,

vertical rows of boutons (cartridges) which resemble eponymous chandeliers, terminating on the

axon initial segments of target pyramidal neurons (Somogyi et al. 1982, Wang et al. 2002).

Basket cells show a basket-like appearance and terminate around the somata or perisomatic

regions of postsynaptic cells. These interneurons are very abundant, making up about 50% of all inhibitory neurons (Markram et al. 2004), and come in three main forms: large, small, and nest. Large basket cells possess multipolar, apiny dendrites and expansive axonal arborizations that extend beyond originating layers into those above and below, as well as into neighboring columns. Large basket cells, found in both neocortex and hippocampus, also exhibit bitufted or bipolar dendritic architecture, and can even possess triangular-shaped somata (Jones and Peters 1984, Wang et al. 2002, Markram et al. 2004). Small basket cells are found mainly within neocortex, and depending the originating layer, they can possess multipolar (layer IV) and bitufted or bipolar (layer II/III) dendrites with spines plus locally oriented thick and highly varicose axonal arborizations that do not typically extend beyond a single cortical layer or column (Kisvárday et al. 1985, Markram et al. 2004). Nest basket cells are described as exhibiting architecture similar to small basket cells but with relatively simpler dendritic spread and axonal architecture (Wang et al. 2002). Finally, double bouquet cells possess bitufted dendrites and a uniquely arranged axon that bundles into a tight fascicular cylinder otherwise termed a 'horse-tail' (Somogyi and Cowey 1981).

It is of common practice to alternatively refer to hippocampal interneurons based on the layers that contain the interneuron's soma and axonal processes. For example, oriens-lacunosum moleculare (O-LM) interneurons, who's cell body originates in the staratum oriens and projects through the stratum lacunosum (Freund and Buzsaki 1996). Long projecting interneurons are also referred to via this scheme (Gulyás et al. 2003). Furthermore, investigators have used morphological nomenclature to emphasize interneuron projections that overlap with specific pyramidal cells afferents, one example being lacunosum-moleculare/perforant pathway (LM-PP) -associated cells (Vida et al. 1998). Given all of these possibilities for morphological

31

nomenclature, it is not unusual for different investigators to presumably describe the same interneuron using different descriptors (Maccaferri and Lacaille 2003), one example being horizontal-cells (Mcbain et al. 1994) and O-LM cells (Vida et al. 1998) to describe the same neuron.

While Ramon y Cajal was remarkably able to distinguish around 20 types of interneurons in the hippocampus through his study of Golgi impregnations (Ramón y Cajal 1893, de Lorente 1934), it is not typical anymore for characterizations to rely solely on morphology and omit additional criteria (Maccaferri and Lacaille 2003) when attempting to ascertain an interneuron's role within a circuit. Nevertheless, valuable information about cell subtype-specific contributions to a network can be extrapolated from its morphological architecture.

Neurochemical criteria

In addition to morphological criteria, and due to the advancement of immunohistochemical tools, investigators began to notice distinguishing characteristics in the innate neurochemical signatures of interneurons that can differentiate them from other types of neurons within the CNS.

Early on, it was observed that many of these morphologically distinct cells uniquely contain γ-aminobutyric acid (GABA, Storm-Mathisen et al. 1983) and GABA-synthesizing enzymes GAD65 and GAD67 (Ribak 1978, Freund and Buzsaki 1996) alongside a sundry of additional neurochemical expression patterns that could be used to differentiate between presumably separate, non-overlapping subpopulations of GABAergic interneurons (Markram et al. 2004). It is of note that neurochemical expression patterns are subject to change during development and due to plasticity, conferring an added level of specificity to this criterion (McBain and Fisahn 2001). Commonly probed molecular markers in both the neocortex and

hippocampus include calcium-binding proteins calbindin (CB), calretinin (CR), and parvalbumin (PV); bioactive neuropeptides somatostatin (SST), vasointestinal peptide (VIP), cholecystokinin (CCK), and neuropeptide Y; neurotransmitter synthesizing enzyme, neuronal nitric oxide synthase (nNOS); extracellular glycoprotein, reelin (Freund and Buzsaki 1996, McBain and Fisahn 2001, Ascoli et al. 2008, Krook-Magnuson et al. 2012); and voltage gated ion channels (Du et al. 1996, Martina et al. 1998). These neurochemicals can be co-expressed within the same cells. Calcium-binding proteins CB, CR, and PV, have been found to express singly (Demeulemeester et al. 1989, Rogers and Resibois 1992), or pairs as observed between PV and CB or CB and CR to a lesser extent (Kawaguchi and Kubota 1997). Co-expression has been observed between neurochemicals and specific voltage gated ion channels as well. For example, channels Kv3.1b and Kv3.2 are expressed in all PV containing interneurons. Kv3.2 is also expressed in about 40% of SST containing interneurons (Du et al. 1996, Martina et al. 1998). Calcium-binding protein and neuropeptide co-expression has been observed between SST and NPY (Kawaguchi and Kubota 1997), VIP and CCK (Kubota and Kawaguchi 1993), VIP and CR (Porter et al. 1998), CR and CCK (Kawaguchi and Kubota 1997), and SST with PV (Katona et al. 1999, Maccaferri et al. 2000, Losonczy et al. 2002). Nonetheless and despite all of these combinations, interneurons with identical neurochemical screens can possess different functional properties (McBain and Fisahn 2001), so this categorization is not typically used exclusively.

There are observed correlations between neurochemical markers and cellular morphology; however, and to elaborate on the preceding statement, marker expression can be dissimilarly expressed in morphologically similar interneurons with different functional properties (Freund 2003). Chandelier cells, for example, have been described to contain PV with or without CB or SST (Defelipe et al. 1989), but never CR, CCK, VIP, or NPY (Defelipe 1999).

Large basket cells express a more broad screen of markers including CB, PV, NPY, CCK, and occasionally also SST; furthermore, they reportedly never express VIP (Markram et al. 2004). Small basket cells express VIP (Kisvárday et al. 1985, Markram et al. 2004) and nest basket cells have been reported to atypically express CR, but never VIP (Markram et al. 2004). Bitufted cells express CB, CR, NPY, VIP, SST, and CCK; and never PV (Markram et al. 2004). Finally, double bouquet cells express CB and possibly also co-express CB with CR and VIP with CCK; but never PV or NPY (Defelipe et al. 1990, Markram et al. 2004). Some more correlations: PV is always expressed with O-LM and bistratified cells (Maccaferri et al. 2000), SST is always expressed within Martinotti cells (Wahle 1993, described in subsequent sections) and VIP is always expressed in small basket cells, some double bouquet cells (Kawaguchi and Kubota 1997), and some bipolar cells (Kawaguchi and Kubota 1984).

Electrophysiological criteria

To allow for the characterization of electrophysiological and synaptic properties of interneurons, intracellular recordings in brain slices can help researchers determine what role an interneuron plays in microcircuit activity and macrocircuit computation (Maccaferri and Lacaille 2003). Investigation of this nature has revealed subtype-distinguishing passive, subthreshold electrical properties which include, but are not limited to membrane potential, time constant, input resistance, or rheobase, as well as suprathreshold electrical properties such as the fingerprint pattern of discharged action potentials fired in response to experimental current step injections (Markram et al. 2004). Definable and comparable characteristics of such action potential trains include: threshold voltage, spike amplitude, spike half width, and spike afterhyperpolarizations.

Born from the observation of spike trains exhibiting high frequencies (> 50 Hz) and short durations with deep, fast afterhyperpolarizations, and lacked frequency adaptation (Schwartzkroin and Mathers 1978, Kawaguchi and Hama 1987), the 'fast-spiking' designation was established (Jonas et al. 2004) and is the most prominent electrophysiological subtype within neocortex, occupying 40% of all interneuron populace across all layers (Fishell and Rudy 2011). Fast spiking interneurons also exist within the hippocampus (Fishell and Rudy 2011). Further investigations of intrinsic excitability later identified other interneuron types with voltage-dependent burst-firing, such as low threshold spiking interneurons that fire bursts of action potentials at lower, or relatively hyperpolarized potential thresholds (Lacaille and Schwartzkroin 1988) compared to their fast-spiking counterparts. Further pattern designations like regular- or irregular-spiking, among others, have been observed between assumed morphologically and neurochemically distinct interneuron subtypes (Lacaille et al. 1987, Kawaguchi and Hama 1988, Kawaguchi and Kubota 1993, Porter et al. 1998, Markram et al. 2004, Toledo-Rodriguez et al. 2004, Ascoli et al. 2008). Certain suprathreshold designations correlate with neurochemical expression patterns. For instance, accommodating or irregular spiking interneurons tend to express CR (Porter et al. 1998); bursting interneurons, CB; and fast spiking, PV (Kawaguchi 1993, Toledo-Rodriguez et al. 2004). Also stereotyped across certain interneuron subtypes are rectification and rebound behaviors that occur in the response to the injection of hyperpolarizing current steps (Ascoli et al. 2008). Finally, within the hippocampus certain interneuron cell types exhibit phase-specific firing during network oscillations (Krook-Magnuson et al. 2012) and in fact, there is a diverse repertoire of interneuron firing behaviors observed in relation to hippocampal rhythmic oscillatory activity (Bland et al. 2002), briefly discussed in subsequent sections.

While these electrophysiological responses are distinguishing within standardized experimental conditions using brain slices perfused in artificial cerebral spinal fluid, *in vivo*, neurons are subject to synaptic bombardment at a much grander scale. This along with the potential for neuromodulatory control, observed discharge properties could be profoundly altered from what is observed experimentally (Steriade 2000, Markram et al. 2004). Regardless these response patterns under experimental conditions are undeniably valuable markers that build on our understanding of the relationships between electrical behavior, and morphology, neurochemical, and synaptic properties of the microcircuit (Markram et al. 2004).

Network interconnectivity criteria

Finally, to assess how interneurons of certain morphologies, neurochemical signatures, and electrophysiological properties may variably function within their circuits, it is imperative to delineate the network interconnectivity of interneuron subtypes. This categorization criteria is multifaceted and involves determinations of the innervations interneurons receive (Markram et al. 2004), the types of postsynaptic neurons they target (excitatory neurons, inhibitory neurons, or both (Freund and Gulys 1997)), which cellular subdomain they selectively target on specific postsynaptic neurons (Defelipe 1997, Somogyi et al. 1998, Markram et al. 2004, Mittmann et al. 2004), and whether connectivity is confined within or between particular structures (Klausberger and Somogyi 2008).

Afferentation

Interneurons can receive both excitatory and inhibitory synapses onto their somata or dendrites (Douglas and Martin 1998). Such inputs can be designated asymmetric or type I if they are glutamatergic and excitatory or symmetric (type II), if GABAergic and inhibitory (Peters 1991). Within the hippocampus and neocortex, interneurons can receive excitatory afferents

from several intrinsic, in-structure sources and extrinsic, out-of-structure sources; while inhibitory afferents will likely come from intrinsic sources(Lacaille et al. 1987, Miles et al. 1996, McBain and Fisahn 2001). The quantitative nature of excitatory and inhibitory input to three neurochemically defined interneuronal populations has been quantified in the hippocampus. The total number of excitatory and inhibitory synapses is several fold higher on PV containing cells than they are onto CB or CR containing (16,000:4,000/2,200), while the ratio of inhibitory GABA inputs is higher onto CB+ (30%) and CR+ interneurons (20%), than onto PV+ (6%, Gulyás et al. 1999). Furthermore, PV+ and CR+ interneurons receive synapses within all layers of the hippocampus, while CB receives highly specific input largely from Schaffer-collateral afferents in the stratum radiatum. Such high input specificity purportedly indicates that CB+ interneurons may be activated in a feed-forward manner from Schaffer-collaterals, while PV+ and CR+ cells are activated in both a feedforward manner from Schaffer-collaterals, entorhinal fibers, and thalamic afferents, but are also activated in a feedback manner by local CA1 recurrent collaterals (Gulyás et al. 1999).

Potentially related to influence by specific afferent pathways, interneurons also express glutamatergic receptors AMPA and NMDA differentially between GABAergic subtypes and other neuron types (Mcbain and Dingledine 1993). To compare interneurons to excitatory principal cells using this metric, it was determined that the time course of excitatory transmission through AMPA receptors onto interneurons is more rapid and of greater amplitude than transmission by equivalent afferent pathways onto principal neurons (Geiger et al. 1999, McBain and Fisahn 2001). Multiple properties may be responsible for this difference, namely differential electrotonic properties, proximity of excitatory synaptic inputs to the cell's soma, and AMPA receptor composition. Next, between cell types, synaptic activation of NMDA receptors can lead

to excitatory postsynaptic potentials (EPSPs) of markedly different kinetics, which affect spike timing and synaptic integration (Maccaferri and Dingledine 2002). This likely because of the variable nature of cell-type specific expression levels (Nyíri et al. 2003). These cell-type specific, but heterogeneous (Losonczy et al. 2002) differences in the response to glutamatergic transmission can play an important roles in the regulation of synaptic integration and long-term potentiation forming EPSP-spike coupling (Taube and Schwartzkroin 1988). Synapses can also exhibit facilitation or depression, the progressive increase or decrease, respectively, of synaptic event amplitudes (McBain and Fisahn 2001). Although many connections from pyramidal cells onto interneurons show frequency dependent facilitation (Thomson and Deuchars 1997, Markram et al. 1998, Wang et al. 1999), some interneurons receive depressing synapses instead (Thomson and Deuchars 1997, Wang et al. 1999). Demonstrated via simultaneous paired-recordings between a presynaptic pyramidal neuron and different types of postsynaptic interneurons, accommodating, dendritically bitufted interneurons exhibited mostly facilitating synapses with presynaptic pyramidal neurons, while, and conversely, as mostly depressed synapses in non-accommodating multipolar (likely basket cells, Wang et al. 1999, Markram et al. 2004). In other words, presynaptic neurons of the same type (pyramidal neurons in this case) can demonstrate differential glutamatergic transmission patterns onto morphologically-distinct interneurons. Recruitment of interneuron subtypes thusly with different integrative and spike timing properties has a profound impact on GABA release (Maccaferri and Dingledine 2002) from interneurons onto their postsynaptic targets.

As a result of the hippocampal CA1 region's relatively simple cellular architecture, limited afferentation, and extensive examination by numerous groups, the interconnectivity of interneuron subtypes within this area has been characterized extensively (Fishell and Rudy

2011). Early anatomical work indicates that different types of hippocampal interneurons can be distinguished on the basis of specific afferents they received, particularly those that originate in CA1 (Freund and Buzsaki 1996). A hurried digression: there is a heavy reliance on using connectivity as a subtype's main identifier in hippocampal research, making extrapolations of cell types difficult to compare with those from other brain regions. Despite this, many well-studied interneuron subtypes within CA1 seem to share functional and lineage relationships to those found in neocortex (Tricoire et al. 2010).

Efferentation

Interneuronal axons possess the ability to arborize vertically within functional columns and across lamina, or horizontally across columns and within lamina (Markram et al. 2004, Ascoli et al. 2008), for example certain interneuron subtypes within layer V of neocortex can project their axons to targets specifically within a column or specifically within lamina (Otsuka and Kawaguchi 2009). Interneurons can also send projections into white matter and contact distant brain regions as has been demonstrated to occur with certain hippocampal interneuron subpopulations (Gulyás et al. 2003). This was once considered uncommon in neocortical interneurons, so neocortical interneurons are often referred to as 'local circuit' to typify this regional limitation in works from previous decades (Letinic et al. 2002).

Reports posit that inhibitory interneurons may form as many as 30 synapses per target with an average of 15; far more than the synapses formed by their excitatory counterparts (Somogyi et al. 1998, Gupta et al. 2000, Markram et al. 2004). Interneurons can selectively innervate cells from populations of both excitatory or other inhibitory cells (Acsády et al. 1996, Gulyás et al. 1996) even in areas where diverse cell types are physically intermingled (Krook-Magnuson et al. 2012). The specificity of interneuronal target specialization is subtype-

dependent and influenced by the connectivity between neighboring pyramidal-inhibitory pairs (Yoshimura and Edward 2005, Krook-Magnuson et al. 2012). It has been proposed that there are three principles governing this target-selecting capability. Firstly, each interneuron subtype undergoes 'synapse mapping' whereby it forms synapses onto a target with specific temporal dynamics. Secondly, the 'interaction principle' conveys that the presynaptic and postsynaptic neurons must interact to determine the type of potential synapse formed. Lastly, the inhibitory post synaptic potential (IPSP), a postsynaptic event evoked by the inhibitory action of GABA, may vary from a single interneuron onto its numerous targets; however, since the GABA release probability from an interneuron and degree of IPSP depression or facilitation onto groups of different target neurons are identical there will be 'synaptic homogeneity' (Gupta et al. 2000, McBain and Fisahn 2001).

Synapses formed from interneurons onto specific cellular subdomains conceptually link the function of an interneuron with the spatial characteristics of its axon (Maccaferri and Lacaille 2003). Spatially, an axon can target a post-synaptic cell in a distributed, gradient, or clustered pattern (Ascoli et al. 2008). Alluded to previously, different types of interneurons seem especially capable of targeting distinct subdomains along the axo-somatic-dendritic axes of principal neurons, as well as other inhibitory interneurons (Defelipe 1997, Somogyi et al. 1998, Markram et al. 2004). While the dynamics of GABAergic release are, as discussed previously, dependent on interneuron afferentation as well as on the interneuron's intrinsic firing capabilities, the ultimate function of interneuronal inhibition is highly dependent on the particular subdomain it selectively forms synapses with. Inhibition received on one part of a neuron will not necessarily impart the same network effect to inhibition received elsewhere.

To begin, axon initial segment-targeting interneurons are uniquely positioned to edit a neuron's output by affecting the generation and timing of action potential firing (Markram et al. 2004). Interneurons that target somatic or perisomatic subdomains function to regulate the local generation of Na^+-dependent action potentials thereby controlling the gain or amplification of summated potentials and resultantly, the eventual action potential discharge of the target cell (Miles et al. 1996, McBain and Fisahn 2001, Freund 2003). This action involves these cells with the phasing and synchronization of neuronal activity (Cobb et al. 1995), as is reflected by one recognized role of interneurons, the synchronization of pyramidal cells during rhythmic activity (McBain and Fisahn 2001). Next, extremely diverse subpopulations of interneurons are dendritically-targeting (Klausberger 2009). Inhibition provided at dendritic locations influences dendritic processing and the integration of synaptic inputs (Segev and London 1999) by modifying dendritic voltage-gated currents, shunting excitatory inputs at sites distal to the soma (Callaway and Ross 1995, Hoffman et al. 1997), and regulating dendritic Ca^{2+}-dependent action potentials (Miles et al. 1996). These interneurons can also influence synaptic plasticity locally by interacting with back-propagating action potentials (Magee and Johnston 1997), and by affecting the generation and propagation of dendritic Ca^{2+} spikes (McBain and Fisahn 2001). Lastly, interneurons that target distal dendrites or tufts impact local dendritic integration (Markram et al. 2004). Cortical interneurons can also be coupled electrically through gap junctions in the membranes of somata, dendrites, and axons (McBain and Fisahn 2001). Just like afferents, the dynamics of GABAergic connections from inhibitory interneurons onto their targets can have facilitating, depressing, or a combination of both (Markram et al. 1998, Gupta et al. 2000) effects; this varies across layers (Wang et al. 1999).

At least some interneurons in certain brain areas are capable of selectively innervating specific subsets of glutamatergic cells from the total available population, targeting those only with specific long distance projection targets; this is a unique kind of microcircuit specialization unique to the hippocampus allows interneurons to regulate specific subnetworks and information-processing channels (Krook-Magnuson et al. 2012). Mentioned under *Electrophysiological criteria*, another hippocampus-specific criterion employed for the classification of interneuronal populations is *in vivo* temporal dynamics. Specific interneuron subtypes fire at particular phases of specific network oscillations; in other words, they show selectivity at which preferred temporal window they release GABA during hippocampal oscillations (Klausberger 2009). Observations of this phenomenon provides evidence that hippocampal functional networks are not hardwired, but are context-specific and recruited dynamically by these oscillations (Cobb et al. 1995, Klausberger et al. 2003, Somogyi and Klausberger 2005, Kwag and Paulsen 2009, Ellender and Paulsen 2010, Fishell and Rudy 2011).

In summary, based on incoming and outgoing network connectivity plus intrinsic properties, interneurons can generate rhythmicity and control the output of large populations of principal cells and other interneurons (Buzsáki and Chrobak 1995). This role in controlling network activity depends on multiple properties, including inhibitory inputs (Whittington et al. 1995, Hájos and Mody 1997, Bartos et al. 2002), electrical coupling between interneurons (Fukuda and Kosaka 2000, Traub et al. 2003), their oscillatory properties (Chapman and Lacaille 1999), and the synaptic inhibition they generate in pyramidal cells (Cobb et al. 1995).

1.4.2 Comparative survey of interneuron subtypes

Using the criteria summarized above, many cohorts of GABAergic interneurons have been described as observed to exist concurrently or distinctly within cerebral neocortex and/or the hippocampus.

1.4.2.1 Neocortex: Parvalbumin+, fast spiking interneurons

One of the most common subtypes of GABAergic interneuron within neocortex are PV+ fast spiking cells (Fishell and Rudy 2011), an action potential firing phenotype attributable to their prominent expression of Kv3.1b and Kv3.2, ion channels that feature markedly rapid activation and deactivation kinetics (Du et al. 1996, Martina et al. 1998, Rudy and McBain 2001). Two well-studied configurations within this group are chandelier cells and basket cells, both derived embryonically from the medial ganglionic eminence (MGE, Fishell and Rudy 2011).

PV+ chandelier cells, found in cortical layers II-VI, with a bias for superficial layers, target the axon initial segments of 20-50% local pyramidal neurons, each one innervated by an average of 4 chandelier cells (Defelipe et al. 1989, Defelipe 1997, Woodruff et al. 2009, Inan et al. 2013, Blazquez-Lorca et al. 2014, Sultan et al. 2018). Functionally, axon targeting in such a way places these interneurons in a powerful position to override the complex dendritic integration and somatic gain by editing action potential output (Somogyi et al. 1982, Markram et al. 2004). It has been suggested that through GABA-release, chandelier cells can elicit a depolarizing postsynaptic response at axon initial segments (Fishell and Rudy 2011), a phenomenon first demonstrated in layers II/III of human and rat neocortex (Szabadics et al. 2006) and attributed to the relative absence of the chloride extruding transporter, KCC2, within these specialized axonal compartments. A lack of this transporter and no compensatory means

otherwise to extrude chloride causes concentrations of the ion to be elevated inside of the subcellular compartment, thereby causing the release of GABA by chandelier cells to depolarize the membrane and elicit action potentials (Szabadics et al. 2006, Woodruff et al. 2009, Fishell and Rudy 2011). Similar axon-targeting interneurons have been described in the hippocampus (Ganter et al. 2004), however, their function is so far reported to be inhibitory.

PV+ basket cells typically populate cortical layers II-VI and target the somatic and perisomatic domains of both excitatory and inhibitory neurons (Wang et al. 2002, Fishell and Rudy 2011). As the most abundant GABAergic interneuron subtype, they are thought to be the strongest provider of inhibition within the neocortex and thusly exhibit high connectivity rates. In fact, it has been demonstrated within mouse visual cortex that PV+ basket cells exhibit a greater than 75% connection rate with targets within 200 μm of the interneuron's site of origination (Holmgren et al. 2003), a high rate that is possibly indicative of blanket or non-specific inhibition (Packer and Yuste 2011). PV+ basket neurons that originate from superficial layers II/III connect to same-layer commissural and associative projecting pyramidal neurons, and to outside layer (V) cortico-cortical projecting pyramidal neurons (Fishell and Rudy 2011, Atallah et al. 2012). There is a tendency for these connections to be reciprocal (Yoshimura and Edward 2005). Populations that originate from granular layer IV uniquely receive facilitating excitatory synapses and are thought to mediate feed-forward inhibition through connections with stellate cell populations therein in addition to pyramidal neurons (Galarreta and Hestrin 1998, Gibson et al. 1999, Gibson et al. 2005, Scott et al. 2007). PV+ fast-spiking cells can form autapses with themselves and other PV+ fast-spiking interneurons (Fishell and Rudy 2011), which PV+ neurons that originate from layer V do to a relatively high extent wherein about 40% of a PV+ basket cell's received perisomatic inhibitory inputs arise from self (Deleuze et al.

2019). PV+ neurons that originate from layer VI exhibit some heterogeneity in terms of size of somata, range of dendritic arbor, and location of axonal targeting (Perrenoud et al. 2013).

It has been suggested that the circuitry of these interneurons remains largely plastic into young adulthood, as observed *in vivo* using optogenetics in post-adolescent cortex of mice. PV+ basket cells demonstrated the potential to structurally rewire, with rates of axonal bouton dynamism (additions and subtractions) of 10.10% and 9.47%, respectively, for over seven days post-adolescence (Kuhlman and Huang 2008). Through dynamic targeting of somatic and perisomatic subdomains of their various post-synaptic partners, PV+ basket cells are involved with the phasing and synchronization of neuronal activity (Cobb et al. 1995) as they can control the gain of summated potentials and resultantly, the action potential discharge of a target cell (Miles et al. 1996, McBain and Fisahn 2001, Freund 2003, Atallah et al. 2012). One example of this lies with the generation of certain oscillatory patterns including attention-predicting gamma oscillations (20-80 Hz). A causal relationship between the synchronous activity of PV+ FS interneurons and the generation of said oscillation array has been directly observed *in vivo* within barrel cortex (Cardin et al. 2009).

Parvalbumin expression emerges relatively late in post natal development, so identification of these neuronal subtypes may rely on electrophysiolocal characterization depending on the developmental stage experimentation takes place during (del Río et al. 1994, Gonchar et al. 2007)

1.4.2.2 Neocortex: Somatostatin+ interneurons

Another grouping of GABAergic interneurons is the starkly heterogenous populations of somatostatin positive (SST+) neurons. These also originate from embryonic MGE and are distinguishable by differential intrinsic firing properties, neurochemical marker expression, and

respective network interconnectivity (Butt et al. 2005, Xu et al. 2006, Gonchar et al. 2007, Miyoshi et al. 2007, McGarry et al. 2010).

Martinotti cells make up a sizeable majority (80%) of SST+ cells within neocortex (McGarry et al. 2010). Classically this term described neurons with somata originating in infragranular layers V and VI with axons that project superficially to layer I. Martinotti cells are now known to originate in all layers II-VI (Fishell and Rudy 2011). They often have markedly elaborate bitufted dendritic morphologies that form very high densities of spiny boutons (though not as high as those on pyramidal neurons, Markram et al. 2004, Kawaguchi et al. 2006, Kubota et al. 2011), branch locally or descend into deeper layers (Wang et al. 2004), and receive strongly facilitating excitatory synapses (Oviedo and Reyes 2002, Kapfer et al. 2007, Silberberg and Markram 2007, Fanselow et al. 2008, Hull et al. 2009). Like in PV+ fast spiking cells, kinetically rapid Kv3.2 is also expressed in about 40% of SST containing interneurons, which may include the Martinotti subtype. An important distinction from PV+ fast spiking cells though is that SST+ Martinotti cells exhibit a relatively low threshold for action potential initiation, low enough to fire spikes in response to single axon inputs (Yavorska and Wehr 2016). Electrophysiologically referred to as such (low threshold spiking, LTS, Fishell and Rudy 2011), LTS neurons also possess the unique capacity to fire so-called rebound-spikes, or action potential spikes or burst following relief of hyperpolarization due to their expression of T-type calcium channels (Yavorska and Wehr 2016).

Contrary to the comparatively non-specific targeting of PV+ basket cells, SST+ LTS interneurons have been observed to show synapse selectivity. Typically, Martinotti cells target the distal dendrites of pyramidal neurons and fast-spiking interneurons, but rarely will they target other LTS interneurons (Gibson et al. 1999). Layer IV SST+ interneurons target the dendrites of

PV+ neurons primarily. Demonstrating this specific instance of disinhibition, experimental silencing of SST+ cells exclusively within layer IV of barrel cortex resulted in a markedly observed increase in PV+ neuron firing and consequent decrease in the firing of pyramidal neurons (Xu et al. 2013).

An additional SST+ LTS subtype, morphologically dissimilar to Martinotti cells (Markram et al. 2004), are dendritically-targeting bitufted cells (or double bouquet) that originate within layers II through VI. These cells receive facilitating excitatory synapses from pyramidal neurons and possess wide, horizontally spanning axonal architecture (Markram et al. 2004).

An approximate third of all SST+ neurons in mouse frontal, somatosensory, and visual cortices co-express calretinin (CR). SST+/CR+ cells are described to be concentrated in superficial layers II/III, with differing connectivity arrangements to their CR- counterparts. For instance, SST+/CR- cells receive strong excitatory input from layers II/III and IV while SST+/CR+ receive mainly from layers II/III (Xu and Callaway 2009). There are suggestions that these two subtypes are derived from separate embryonic locations (113-115). SST+/CR+ neurons share similar features with SST+/CR- Martinotti cells, although they differ electrophysiologically as their action potential firing pattern is fast spiking-like and comprises narrower spikes with faster afterhyperpolarization periods. They also differ in the horizontal extension of their dendritic fields and lastly in their number of primary processes (Markram et al. 2004, Xu et al. 2006).

There are populations of SST+ cells that are also strongly positive for neuronal nitric oxide synthase (nNOS+) and these have been demonstrated to receive local inputs, but project long distance to other cortical areas (Tomioka et al. 2005, Kubota et al. 2011). These cortico-

cortical interneuron populations are akin in various ways to certain projection neurons seen in the hippocampus (Higo et al. 2009, Jinno 2009).

In addition to the LTS and fast spiking-like electropysiological phenotypes cited above, SST+ interneurons may exhibit other spiking patterns including regular spiking, bursting, or stuttering. Some 90% of SST+ neurons show strong accommodation in these trains (Yavorska and Wehr 2016). SST+ neurons that do not exhibit strong accommodation tend to be fast spiking-like.

To understand the computational contributions from each interneuron type, it is of use to functionally compare them. SST+ neurons which as stated receive facilitating excitatory afferents, target dendrites, and exhibit strongly accommodating firing patterns are of course functionally distinct to PV+ neurons which target somatic and perisomatic subdomains of neurons, receive and send depressing connections, and exhibit a non-accommodating and 'fast' spiking pattern. In the visual cortex, superficial layer SST+ interneurons have been implicated to be involved with surround suppression, a phenomenon describing a neuron's tendency to fire less when a stimulus exists outside of its receptive field (Adesnik et al. 2012). Comparing the functional contributions by SST+ and PV+ cells within visual cortex, dendrite-targeting SST+ have been reported to subtract information from excitatory responses to the effect of sharpening stimulus selectivity, while soma-targeting PV+ divide responses and preserve stimulus selectivity. Subtractive activity by SST+ interneurons therefore shifts response levels while PV+ interneurons alter response gain (Wilson et al. 2012).

Somatostatin itself is a bioactive inhibitory neuropeptide adding additional nuance to the complex role an SST+ cell can carry within its circuit (Yavorska and Wehr 2016). SST, distributed throughout the whole cell, can be released from dense-core vesicles from axons as

well as from dendrites (Ludwig and Pittman 2003) under conditions that differ from those that precede GABA release, such as repetitive high-frequency firing (Kits and Mansvelder 2000). Cellular and synaptic functions of SST release have been fairly studied in hippocampus: some observations of SST-mediated function include inhibiting presynaptic glutamate release (Tallent and Siggins 1997), reduction of dendritic spines and excitatory synapses with repeated release (Hou and Yu 2013), reduction of GABA-mediated inhibitory post-synaptic potentials (IPSPs, Leresche et al. 2000), and production of non-GABA mediated IPSPs (Yavorska and Wehr 2016) via multiple mechanisms including reducing voltage-gated calcium currents and increasing potassium currents (Viana and Hille 1996, Schweitzer et al. 1998). Network level phenomena that directly pertain to SST-release have been studied more extensively in the neocortex providing the field with suggestions that SST plays important roles in learning and retention may be able to prevent the generation of epileptic activity (Yavorska and Wehr 2016).

1.4.2.3 Neocortex: VIP+, reelin+, CR+, CB+, and nNOS+ interneurons

Most of the remaining interneuron populations within the cortex are embryonically derived from the caudal ganglionic eminence (CGE) and concentrated more in superficial lamina I through III, wherein 60% of the total cortical interneuronal populace resides. Further, CGE-derived interneurons occupy 30% of total cortical interneurons (Lee et al. 2010, Miyoshi et al. 2010, Fishell and Rudy 2011). Within this population is a subgroup of interneurons that exclusively and highly express ionotropic serotonin receptor, 5HT3aR. It is of note that PV-/SST-/5HT3aR+ cells account for nearly 100% of all GAD-67 expressing neurons in somatosensory cortex (Lee et al. 2010).

Certain CGE-derived interneurons are vasointestinal peptide positive (VIP+). These interneurons, possessing bipolar, bitufted, or multipolar dendritic architectures, are enormously

heterogeneous and occupy about 40% of the CGE-derived population (Fishell and Rudy 2011).

Two main subtypes include a subpopulation that co-expresses CR: VIP+/CR+ interneurons

originate from layers II/III and V (Cauli et al. 1997, Porter et al. 1998, Markram et al. 2004) can

be bitufted or bipolar with small spindle or ovoid somata and narrow bipolar dendrites that

extend vertically within columns, towards layers I or VI (Peters and Harriman 1988, Peters

1990). They receive depressing synapses from pyramidal neurons (Porter et al. 1998). Following

injections of depolarizing current, the bitufted configuration exhibits irregular spiking or an

initial burst of action potentials followed by irregularly spaced action potentials. Another

subtype that are VIP+/CR-, have bitufted or multipolar dendrites and are referred to as fast-

adapting cells due to their strongly adapting firing pattern (Fishell and Rudy 2011). Functionally,

different populations of VIP+ cells preferentially target other interneurons (Acsády et al. 1996,

Hájos et al. 1996, Staiger et al. 2004, Dávid et al. 2007, Caputi et al. 2008, Pi et al. 2013).

Reelin is another neuropeptide expressed in 40-50% of the CGE-derived interneuron

population. Reelin+ interneurons are heterogeneous, but two major subtypes exist within layers

II/III and V (Markram et al. 2004). One are GABAergic neurogliaform cells (Kawaguchi and

Kubota 1996), which are suggested to mediate tonic inhibition via nonsynaptic release or,

volume transmission, of GABA (Oláh et al. 2009, Fishell and Rudy 2011). Other poorly defined

VIP- and reelin- interneurons have been observed (Batista-Brito and Fishell 2009, Lee et al.

2010, Rudy et al. 2011).

At least two types of CCK+ interneurons have been described in neocortex; some co-

express VIP while the rest do not (Wang et al. 2002, Gonchar et al. 2007, Xu et al. 2010).

CCK+/VIP- interneurons in neocortex resemble the morphology and functional properties of

better studied CCK+ basket cells in hippocampus, to be introduced in subsequent sections (Freund and Katona 2007, Fishell and Rudy 2011).

CB+ double bouquet cells originate within layers II-IV and are known to inhibit basal dendrites of pyramidal neurons (Somogyi and Cowey 1981, Defelipe et al. 1990, Markram et al. 2004). Depressing synapses have been observed for connections from pyramidal neurons onto layers II/III CB+ double bouquet cells (Buhl et al. 1997, Wang et al. 1999).

There are two types of nNOS+ cells in neocortex; some across the two types express other markers like SST+ (mentioned in previous section) and PV+, and present with differing morphologies and laminar distributions (Kubota et al. 2011).

1.4.2.4 Hippocampus: PV+ and SST+ interneurons and their cortical correlates

PV+ basket cells and chandelier cells also exist within the hippocampus and are closely homologous to the aforementioned neocortical versions in many attributes. Firstly, the locations of their output synapses, peri/somata and axon initial segments respectively, are conserved between structures. Next, their intrinsic electrophysiological properties (fast-spiking firing phenotype), properties of input and output synapses, expression of PV, as well as site of embryonic derivation (MGE) additionally suggest that these subtypes are highly comparable (Fishell and Rudy 2011). Some functional differences do exist, namely with PV+ basket cells. The hippocampal iteration is context-dependent, meaning firing rates can change depending on the behavioral state of the animal (movement, sleep, quiet wakefulness) as revealed by juxtacellular recordings (Lapray et al. 2012).

Neocortical SST+ Martinotti cells have a hippocampal correlate as well in oriens-lacunosum (O-LM) cells. O-LM cells, named for their layers of origination and termination, co-express SST with PV, but possess the electrophysical properties and long distal dendrite-

targeting axons of their cortical SST+ counterparts (Forro et al. 2015). Hippocampal O-LM cells also have uncommonly facilitating excitatory postsynaptic potentials (EPSPs, Ali and Thomson 1998, Losonczy et al. 2002) which indicates that they receive input from facilitating synapses similar to cortical layer II/III SST+ bitufted cells (Reyes et al. 1998). Excitatory connections to most other interneurons, such as PV+ basket cells are depressing EPSPs (Ali and Thomson 1998, Reyes et al. 1998).

1.4.2.5 Hippocampus: nNOS+, CCK+, VIP+, CR+, projection interneurons and cortical correlates

GABAergic neurogliaform cells appear to exist in both hippocampus and neocortex in morphologically similar configurations with some unique properties in common (Fuentealba et al. 2008, Tricoire et al. 2010). There are disparate populations of neurogliaform cells in the hippocampus. Some arise from CGE, like neocortical neurogliaform cells (Fishell and Rudy 2011), but the majority arise from MGE and express nNOS (Fuentealba et al. 2008, Tricoire et al. 2010). These cell bodies originate within the layers, strata lacunosum-moleculare (Fishell and Rudy 2011). nNOS+ neurogliaform cells strongly resemble ivy cells, the largest interneuron population within the hippocampus. Ivy cells are also nNOS+ (Fuentealba et al. 2008, Szabadics and Soltesz 2009, Tricoire et al. 2010), but originate within the stratum pyramidale, and send branches to dendrites of pyramidal cells within stratum radiatum and stratum oriens (Allen and Monyer 2015). It is so far unknown if there are any MGE-derived neurogliaform homologs in neocortex.

CCK+ interneurons have been relatively well studied within the hippocampus. At least five classes have been identified in CA1 (Klausberger et al. 2003), including CCK+/VIP+ basket cells, CCK+/VIP- basket cells (Somogyi et al. 2004), Schaffer collateral-associated cells (Vida et

al. 1998), lacunosum-moleculare/perforant pathway-associated cells, and lacunosum-molecular/radiatum/perforant pathway-associated cells (Cossart et al. 1998, Vida et al. 1998). It is of note that CCK+ basket cells are sharply distinct from both neocortical and hippocampal PV+ basket cells (Freund 2003) in that PV+ baskets receive more excitatory input (Gulyás et al. 1999, Mátyás et al. 2004). Hippocampal populations of VIP+ interneurons (some co-express CR), may co-express CCK (Fishell and Rudy 2011), and preferentially target other interneurons as is observed in certain VIP+ populations within the neocortex (Acsády et al. 1996, Fishell and Rudy 2011). Just like in neocortex, it is suggested that VIP+ hippocampal cells are derived from CGE (Somogyi et al. 2004, Lee et al. 2010, Vucurovic et al. 2010).

CR+ interneurons (some co-express VIP) in the hippocampus also preferentially target other interneurons (Gulyás et al. 1996). These aspiny cells have a unique feature of being located in all layers of the hippocampus and frequently form dendro-dendritic and axo-dendritic contacts with each other (Fishell and Rudy 2011).

Some examples of projection GABAergic neurons within the hippocampus are subiculum-projecting trilaminar cells that originate in CA1. These cells are also known as 'back-projecting' since they provide widespread innervation to CA1, CA3, and the dentate hilus (Sik et al. 1994, Sik et al. 1995). There are also hippocampal-septal cells (Freund and Buzsaki 1996) which express SST and CB. Their somata, which possess markedly long dendrites, originate throughout the all parts of the hippocampus. Axon collaterals from these cells can project over very long distances (Gulyás et al. 2003).

1.4.2.6 Hippocampal: bistratified interneurons, subtype with no cortical correlate

Bistratified cells are a designation for a commonly studied subtype of GABAergic interneuron first described within the CA1 area of the hippocampus (Buhl et al. 1994, Pawelzik

et al. 1999, Maccaferri et al. 2000). These PV+ fast spiking (Pawelzik et al. 2002, Fujiwara-Tsukamoto et al. 2010) cells possess 'bistratified' axons that target the dendrites of CA1 pyramidal cells in stratum oriens and stratum radiatum and receive input from schaffer collaterals and CA1 pyramidal neurons. Bistratified cells make synapses with small dendritic shafts of pyramidal cells. There are also SST+ bistratified cells (Allen and Monyer 2015). Functionally, they fire at the trough of theta oscillations, a property somewhat similar to O-LM cells, however, while O-LM cells are silenced during this events, bistratified cells fire strongly (Klausberger et al. 2003). The firing properties of bistratified cells has been further compared to O-LM during movement and sleep as these two subtypes comparably co-release SST and GABA on distinct dendritic domains of pyramidal neurons. Bistratified cells fired at higher rates during sleep than O-LM cells. Like hippocampal PV+ basket cells, mean firing rates appeared to be associated with changes in the behavioral state of the animal (Katona et al. 2014).

1.4.3 With all of this context, we study interneuron circuit alterations using optogenetics and electrophysiology

Illustrated in Figure 1.1, we have quite the puzzle on our hands, or perhaps on our benches, assimilating all of the above context into the developmental story of microgyria induced intractable pathologies. Nevertheless, using optogenetics in combination with electrophysiology, we aim to focus on two select interneuron subtypes, somatostatin-immunostaining neurons and parvalbumin-immunostaining neurons, and how they contribute to intractable consequences of DCM.

Work we have done using these techniques, to be discussed in subsequent chapters, has revealed even more information about interneuronal functioning, tied as inextricably to their

identities as their determined morphologies, intrinsic capabilities, and molecular patterns. We follow in the footsteps of pioneers who paved the way and established now dogmatic approaches to circuit interrogation through the use of opsins (Prince 1985, Kuhlman and Huang 2008, Cardin et al. 2009, Adesnik et al. 2012, Atallah et al. 2012, Royer et al. 2012, Wilson et al. 2012, Hu et al. 2013, Osawa et al. 2013, Sukhotinsky et al. 2013, Szydlowski et al. 2013, Xu et al. 2013, Ledri et al. 2014).

Chapter 2
Increased output and extended laminar spread of layer V somatostatin interneurons in developmentally malformed epileptogenic cortex

Figure 2.1 Graphical abstract representing results presented in Chapter 2. We demonstrate primarily herein that output from SST neurons onto layer V pyramidal neurons recovers to control levels beyond the terminus of epileptogenic PMR (≥ 2 mm "distant" to the microgyrus). Additionally, we demonstrate that SST neurons exhibit extended arbors within layer V. This functionally correlates to greater IPSC amplitudes recorded from layer V pyramidal neurons in response to distant, same-layer activation of SST neurons.

We demonstrated in our previous report that enhanced output from SST neurons is restricted to within layer SST neuron to pyramidal neuron connections. Output to layer V pyramidal neurons from external layers II/III SST neurons are statistically similar in PMR versus controls (Ekanem, et al. 2019). It is presently unknown whether this remains the case in lesioned tissue beyond the terminus of PMR.

Chapter 2

Increased output and extended laminar spread of layer V somatostatin interneurons in developmentally malformed epileptogenic cortex
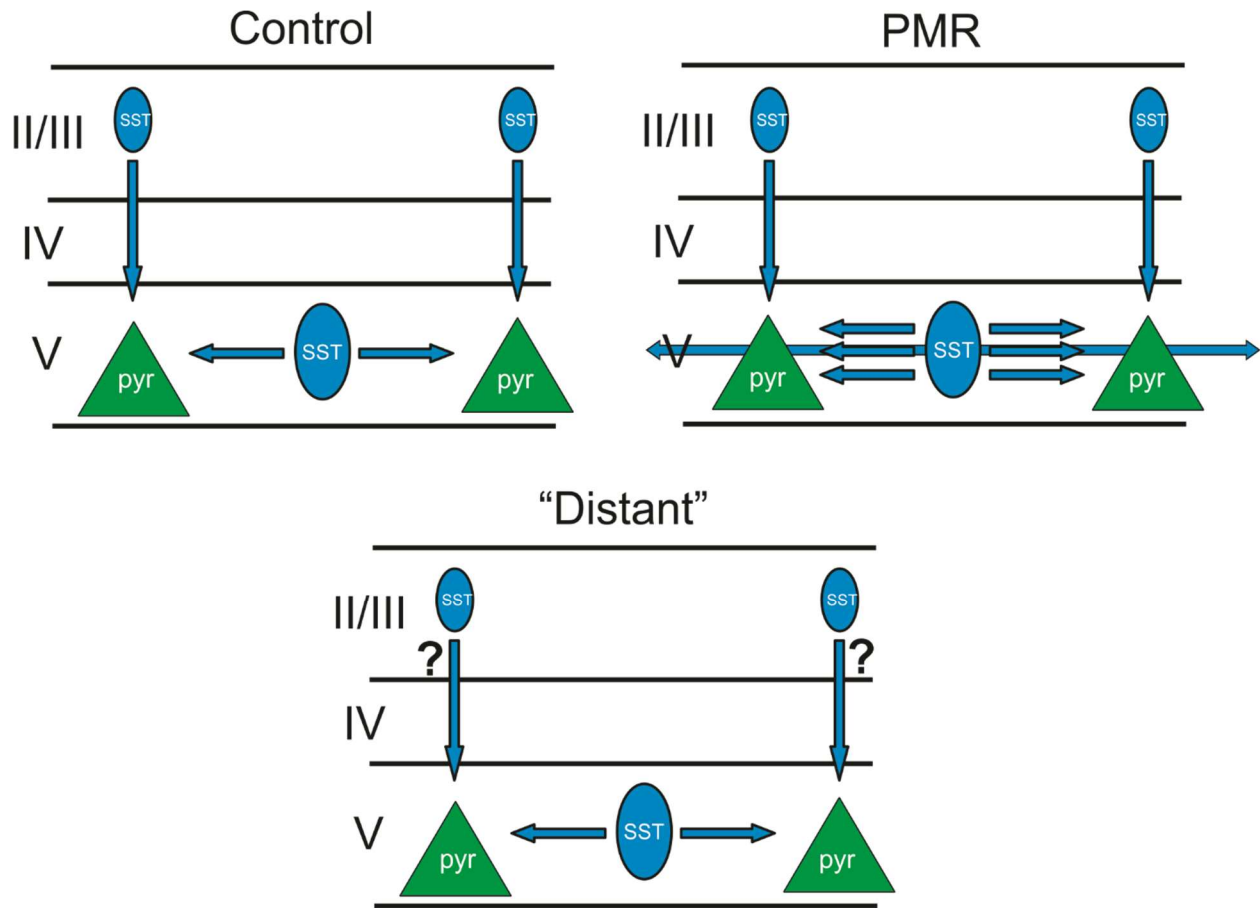
2.1: Abstract

Drug-resistant epilepsy is a common clinical sequela of developmental cortical malformations, however much remains unknown about what aberrant circuit alterations underlie its onset and persistence. To address this gap in knowledge, we utilized the transcranial freeze lesion model in optogenetic mice to dissect pathological changes to circuit function associated with developmental microgyria. We demonstrated previously that layer V pyramidal neurons receive larger amplitudes of inhibitory post synaptic currents (IPSCs) from somatostatin-positive (SST+) neurons within the epileptogenic paramicrogyral region (PMR) compared to control. This effect was shown to exclude SST+ neurons from layers II/III, suggesting sequestered involvement from the layer V SST+ population. Here, we searched for effect focality and mechanism using the same optogenetic mouse line (SST-Cre x floxed channelrhodopsin-2). Voltage clamp recordings from layer V pyramidal neurons beyond the terminus of PMR showed control level IPSCs with the activation of SST+ cells. Furthermore, current clamp recordings from SST+ neurons within PMR demonstrated a novel structural schematic for within-layer arborization of these interneurons: results suggest SST+ neurons within PMR exhibit arbors spread to physically occupy wider domains within layer V. These extended arbors include axons as layer V pyramidal neurons show greater percentages of IPSC amplitudes with distant SST+ neuron activation, suggesting a viable mechanism for the observed SST+ neuron mediated output enhancement. These novel discoveries will provide the field with more context as to the role SST+ neurons potentially play in the modulation of epileptogenesis.

2.2: Introduction

Pharmacoresistance, pestilent to 30-50% of individuals of all ages with epilepsy or other type of seizure disorders (Kun et al. 1999, Oskoui et al. 2005, Picot et al. 2008, Skjei and Dlugos 2011, Farghaly et al. 2013, Janmohamed et al. 2019), is particularly prevalent amongst individuals with developmental cortical malformations (DCM). This is especially true of infants and children within this population (Flint and Kriegstein 1997, Wyllie 2000, Guerrini and Carrozzo 2002, Guerrini et al. 2003, Berg and Kelly 2006, Skjei and Dlugos 2011, Borggraefe et al. 2019, Fitsiori et al. 2019, Naimo et al. 2019). Successful identification or application of viable treatment alternatives is limited as very little is known about the cellular mechanisms underlying this phenomenon. One such alternative for example, surgical resection, is unfortunately associated with a return of symptoms in about 40% of individuals with DCMs (Sisodiya 2000, Blumcke et al. 2009, Rao and Lowenstein 2015).

To address this gap in knowledge, we model the DCM class polymicrogyria with the transcranial freeze lesion technique, to investigate and uncover novel, pathological circuit paradigms corresponding with the generation of epileptiform activity and possibly other disease-associated sequelae. These can include spastic paresis, severe encephalopathy, as well as cognitive impairments like deficits in learning and memory (Guerrini and Carrozzo 2002, Araujo et al. 2006, McClure et al. 2006). In fact, the freeze-lesion model we utilize has been shown to mar the speed of auditory processing in rodents, a phenomenon associated with higher incidence of developmental dyslexia in humans (McClure et al. 2006). The development of such pathologies is often considered to be born from neocortical imbalances of excitation and inhibition and many other groups have focused their investigations thusly (Patrick et al. 2006, Takano 2012, Jin et al. 2014, Wang et al. 2014, Takano and Matsui 2015). Along these lines, we

uncovered possibly pathological dysfunction by somatostatin (SST) interneurons within layer V, possessing specific anatomical, molecular, and electrophysiological characteristics, making them discernable from other neuron types.

The present study functions to elaborate on the extent to which this population of neurons, typically weak in influence (Xiang et al. 2002), seem to exhibit a functionally enhanced phenotype within layer V of the paramicrogyral region (PMR), an expanse of cortex adjoining the malformation from which epileptiform activity is easily evocable. We find that layer V SST functional enhancement is limited to epileptogenic PMR, outside of which it presents at control levels. Further, we find that SST+ neuron arbors within PMR may exhibit an extended within-layer reach, suggesting a pathological circuit paradigm wherein SST+ neurons impart this functionally enhanced effect by way of increased presynaptic afference. These findings have important implications as continued elucidation of SST dysfunction is required in order to fully understand this enigmatic and potentially pathological circuit paradigm.

2.2: Materials and Methods

All animal and experimental protocols were conducted in accordance with the Virginia Commonwealth University Institutional Animal Care and Use Committee, which adhere to regulations including, but not limited to those set forth in the Guide for the Care and Use of Laboratory Animals, 8th Edition (National Research Council).

Animals

To achieve expression of the light-sensitive channelrhodopsin2 (ChR2) in SST-expressing interneurons, SST-Cre mice (Jackson Laboratory, Farmington, CT; strain 013044) were bred with floxed ChR2 mice (Ai32; Jackson Laboratory, strain 012569). Mice were housed with dam

and litter siblings on a 12/12 hour light/dark cycle at 72°F, with continuous access to water and standard rodent chow. <mark>Approximately 150 mice were used across all experiments.</mark>

Animal surgery

Transcranial freeze lesion surgery was used to induce bilateral microgyria over the somatosensory cortices of post natal day 1 (P1) female and male mouse pups. Mice were anesthetized through hypothermia and sustained in that state for the duration of the surgery via submersion in an ice-water slurry. Upon confirmed unresponsiveness via toe and tail pinch, skin overlying the skull was incised coronally from right to left temporal ridge at the midpoint between bregma and lambda to expose the skull above the somatosensory cortex. A rectangular probe ~2 mm in length cooled to −60° C was placed at the midpoints between the sagittal suture and temporal ridge on both hemispheres for 5 seconds. Sham mice had skin overlying the skull incised and skull exposed without placement of probe within time frames identical to the surgery cohort. Afterwards, the skin was sutured and the pup was rewarmed and returned to the dam. As this is survival surgery, the procedure was performed under sterile conditions. To further ensure survival, sham or freeze-lesion surgery was only performed on P1 mice weighing 1.3 mg or higher.

Ex Vivo Slice Preparation

Acute brain slices from female and male mice aged between P12 and P21 were prepared from freeze-lesioned mice and sibling controls, consisting of 50% unoperated naïve and 50% sham mice. At all measures used in this work, sham and naïve cells were not significantly different and were therefore both included in the control cohort. Mice were rapidly anesthetized with an overdose of isoflurane until unresponsive to tail and toe pinches and decapitated after transcardial perfusion with cold (4° C) standard sucrose slicing solution containing (in mmol/L)

2.5 KCl, 1.25 NaH2PO4, 10 MgCl2, 0.5 CaCl2, 26 NaHCO3, 11 glucose and 234 sucrose

(George and Jacobs 2011). In some cases, mice younger than P15 were not perfused prior to

decapitation; no differences in slice health were observed between these and perfused cohorts. In

the same standard sucrose slicing solution, 300 μm slices were obtained with a Leica VT1200S

vibratome (Leica Biosystems; Wetzlar, Germany) and immediately stored in artificial

cerebrospinal fluid (aCSF) containing (in mmol/L): 126 NaCl, 3.5 KCl, 1.25 NaH2PO4, 1.2

CaCl2, 1 MgSO4, and 26 NaHCO3, maintained at pH 7.3 with continuous infusion of 95%

oxygen, 5% CO_2. Slices were maintained at 34° C for 1 hour and then allowed to cool to room

temperature and maintained thusly until time of recording.

Electrophysiological Recordings

Prior to recording, prepared slices were moved to a recording chamber and continuously

perfused with 34° C aCSF infused with 95% oxygen, 5% CO_2.

Whole cell patch clamp cellular recordings were obtained from pyramidal and SST+

neurons within layer V of somatosensory cortex, 0.5-1.0 mm from the induced sulcus (PMR), ≥

2 mm from the induced sulcus (distant), and homotopic control cortex (*Figure 2.2*). Neuronal

subtype was determined prior to recording based on neuronal morphology under differential

interference contrast (DIC) optics, wherein confirmation of an apical dendrite was used to

identify pyramidal neurons and fluorescence of green fluorescent protein (GFP) reporter

associated with ChR2 was used to identity SST+ neurons. For this reason, SST+ neurons will be

referred to as SST-GFP. Extracellular solution comprised aCSF with DL-2-amino-5-

phosphonopentanoic acid (APV, NMDA receptor antagonist, 50 μmol/L) and 6,7-

dinitroquinoxaline-2,3-dione (DNQX, AMPA receptor antagonist, 20 μmol/L). Some

experiments additionally included gabazine (SR-95531, GABA receptor antagonist, 20 μmol/L)

with the above. Recordings were obtained using glass micropipettes (3-4.8 MΩ) containing one of three intracellular solutions. One, designated "high chloride" (E_{Cl-} = −15 mV) included (in mmol/L) 70 K-gluconate, 10 4-(2 Hydroxy-ethyl)piperazine-1-ethane-sulfonic acid sodium salt (HEPES), 4 Ethylene glycol bis(2-amino-ethyl-ether)-N,N,N′,N′-tetra-acetic acid (EGTA), 70 KCl, 2 $MgCl_2 \cdot 6H_2O$, 2 $CaCl_2 \cdot 2H_2O$, 4 Adenosine 5′-triphosphate (ATP) disodium salt hydrate, and 0.2 Guanosine 5′-triphosphate (GTP) sodium salt hydrate, with 0.25%-0.5% biocytin and in some cases 10 Lidocaine N-ethyl Bromide (QX-314, voltage-gated sodium channel blocker). A second solution (E_{Cl-} = −71 mV) included (in mmol/L) 130 K-gluconate, 10 HEPES, 11 EGTA, 2 $MgCl_2 \cdot 6H_2O$, 2 $CaCl_2 \cdot 2H_2O$, 4 ATP disodium salt hydrate, and 0.2 GTP sodium salt hydrate, with 0.25%-0.5% biocytin. A third solution (E_{Cl-} = -50 mV) included (in mmol/L) 117 Gluconic Acid, 117 CsOH, 11 CsCl, 10 HEPES, 11 EGTA, 2 $MgCl_2 \cdot 6H_2O$, 2 $CaCl_2 \cdot 2H_2O$, 4 ATP disodium salt hydrate, and 0.2 GTP sodium salt hydrate, with 0.25%-0.5% biocytin and in some cases 10 QX-314. All iterations were adjusted to 280-290 mOsm and pH 7.3. Solution one was used for recordings of optically generated IPSCs; QX-314 was utilized in some cases to address action potential contamination of synaptic current readouts. Solution two was used for recordings of current evoked action potential trains in SST-GFP neurons. Solution three was used for recordings of ChR2 current and ChR2-activation evoked action potentials in SST-GFP cells; QX-314 was utilized in some cases to address action potential contamination of ChR2 current readouts.

Access resistance (Ra) was measured for each cell prior to recording and periodically checked throughout experimentation. If Ra was observed to increase more than 20% during experimentation, recordings were terminated. Cells with Ra values > 25 MΩ were omitted from analysis. During recordings, patched cells were passively filled with biocytin to enable post-hoc

confirmation of cell type via staining of biocytin-filled cells with fluorescein-conjugated streptavidin (10 μg/mL). To perform post-hoc staining, slices were stored in 4% paraformaldehyde for 24 hours following experimentation, and PBS thereafter until staining.

Experiments involving selective activation of SST interneurons were performed by passing blue-range LED (460 nm) through a 60× objective. LED was either applied directly over the patched cell or from measured distances from the patched cell. LED strength was controlled via the X-Cite system and Lumen Dynamics software (20%, producing 1.5 mW continuously, Excelitas Technologies, Waltham, MA). A stimulus duration series was generated by applying LED at durations ranging from 0.1 to 2 ms, in 11 increments. The series was presented three times; therefore, measurements were made from averages of three stimulus presentations.

Experiments to characterize passive membrane properties and action potential firing patterns were performed by injecting a series of 400 ms current steps from a held potential of -60 mV (current steps ranged from -200 to 380 pA in 20 pA increments). Reported rheobase, time to first action potential at rheobase, as well as additional characteristics of the fired action potentials were determined from these recordings. Plots of voltage versus injected current for hyperpolarizing and non-action potential producing current steps were generated per cell to determine input resistance (slope of fitted line, mV/pA) and resting membrane potential (y-intercept of fitted line).

All recordings were made with a Multiclamp 700B amplifier (Molecular Devices, San Jose, CA) and digitized with data acquisition instrument Digidata 1440 (Molecular Devices) at 20 kHz with pClamp software (Molecular Devices).

Analyses were primarily performed via home written programs (Visual Basic in Excel; Microsoft Corporation, Redmond, WA), Clampfit (Molecular Devices), SPSS Statistics (IBM, Armonk, NY), and GraphPad Prism (GraphPad Software Inc., San Diego, CA). Data are reported as mean ± standard error of the mean (SEM). To test for differences between control, PMR, and distant groups across experimental paradigms, t-tests or repeated-measure analysis of variance (ANOVA) with post-hoc Bonferroni corrections for multiple comparisons when equal variance was assumed, or Welch corrections and post-hoc Dunnett's T3 multiple comparisons test when unequal variances were found. Results with $P < 0.05$ were considered significant.

2.3: Results

Whole-cell recordings from two cell types were performed in layer V of somatosensory cortex in *ex vivo* brain slices within PMR, "Distant", and homotopic control regions (*Figure 2.2*). All SST+ neurons were identified by fluorescence of ChR2-GFP reporter. All pyramidal neurons were identified via presence of apical dendrite under IR-DIC optics and confirmed to be non-fluorescent prior to recording. The utilized animal cohort comprised P12 - P21 control and lesioned SST-ChR2 transgenic female and male mice.

2.3.1. Intrinsic membrane properties of control versus PMR layer V pyramidal neurons: PMR group neurons exhibit lower rheobase, longer first spike rise tau values, and higher action potential firing frequencies.

For various reasons, it is critical to determine the condition of pyramidal neurons in PMR versus control. Firstly, we must confirm whether pyramidal neuron intrinsic functionality is

changed in developmental PMR so as to confirm that the reported differences in IPSC peak amplitude and area in layer V pyramidal neurons of PMR are in fact mediated by SST functional enhancement (Ekanem et al. 2019). Additionally, potential changes in pyramidal neuron intrinsic functionality could in itself be epileptogenic. To achieve these ends, we performed assessments of layer V pyramidal neuron intrinsic passive membrane and action potential properties. From these recordings, we were able to ascertain a number of characteristics per cell (comprehensively listed in *Table 2.1*.)

Results from this neuron cohort indicate that resting membrane potential of cells from the two groups were not different (mean values: Control -62.8±2.4 mV, PMR -66±1 mV, P =.26, *Figure 2.3C*), nor was input resistance (mean values: Control 184±0.04 MΩ, PMR 182±0.01 MΩ, P = .79, *Figure 2.3D*), spike amplitude, half width, max rise and decay rates, decay tau, and AHP amplitude (values reported in *Table 2.1*). Two main differences were observed in rheobase and first spike rise tau values. Rheobase appears significantly higher in controls compared to PMR (mean values: Control 39.4±4.4 pA, PMR 24.4±2.4 pA, P = .01, *Figure 2.3E*), and first spike rise tau appears significantly higher in PMR compared to controls (mean values: Control 3±0.7 ms, PMR 11.7±4.22 ms, P = .03, *Table 2.1*). Action potential frequencies as a function of injected current were also compared between groups (*Figure 2.3F*). Analysis revealed that there are significant differences of action potential firing frequencies between PMR and control, with frequencies appearing higher in PMR pyramidal neurons (two-way repeated measures ANOVA, effect of group P = .0002, effect of current $P < 0.0001$ *Figure 2.3F*).

2.3.2. Output from SST+ neurons to layer V pyramidal neurons recovers to control levels outside of epileptogenic PMR

Epileptogenic PMR has been reported to exhibit a terminus beyond which epileptiform activity is no longer easily evocable (Jacobs et al. 1999a). To assess whether the previously reported SST+ neuron functional enhancement observed within PMR is restricted therein (Ekanem et al. 2019), we obtained whole cell patch clamp recordings of inhibitory post-synaptic currents (IPSCs) in layer V pyramidal neurons distant to the microgyrus (≥2 mm), beyond the bounds of hyperexcitable PMR (distant site visualized in *Figure 2.2*). Currents were evoked by SST-ChR2 activation via application of a series of 11 increasing durations of LED (*Figure 2.4.1A*). We discerned that layer V pyramidal neuron IPSC peak amplitudes recorded outside PMR were equivalent to those recorded from control tissue (mean values at 2 ms LED: Control - $199.4.1 \pm 28.3$ pA, Distant -151.1 ± 27.6 pA, $P = .99$, *Figure 2.4.1B*). Expanded from what has been previously reported Ekanem et al. 2019, IPSC peak amplitudes recorded from PMR layer V pyramidal neurons were significantly higher than those observed from the control or distant populations (mean values at 2 ms: PMR -904.4 ± 124.7 pA, $P < .001$, *Figure 2.4.1B*). To illustrate the stark contrast of SST output within PMR and beyond its boundary, IPSCs from pairs of PMR and distant layer V pyramidal neurons were recorded within the same slices (*Figure 2.4.1C*). Again, IPSC peak amplitudes from PMR layer V pyramidal neurons were significantly larger than controls (PMR -1135.31 pA, n = 3; Distant -449.52 pA, n = 3; $P = .04$, *Figure 2.4.1C*). To confirm the observed differences were not mediated by differing ChR2 functionality between groups, we recorded directly from SST-ChR2 cells with blockade of glutamatergic and fast $GABA_A$ synaptic transmission, enabling us to measure ChR2 cationic current as evoked by LED short duration activation (*Figure 2.4.2A*). There were no differences in current peak amplitudes between groups indicating that ChR2 functions identically ($P = .44$,

Figure 2.4.2B). All observed differences are mediated by the synaptic relationship between SST+ neurons and layer V pyramidal neurons.

2.3.3. Search for mechanism: PMR group neurons exhibit shorter time to first action potential at rheobase and higher second spike halfwidth amplitudes

In pursuit of uncovering the unknown element driving SST functional enhancement, we performed assessments of SST+ neuron intrinsic passive membrane and action potential properties. Our previous report focused on discerning these properties in low threshold spiking (LTS) interneurons in rats as these have been particularly implicated in PMR-related altered functionality (George and Jacobs 2011). LTS neurons represent some SST+ neurons, although not all (Yavorska and Wehr 2016), which differs with the experiments presented within this work as optogenetic activation recruits SST+ neurons of all types. As such, analysis combines regular-spiking with LTS SST+ neurons. Despite the well documented presence of SST+ neurons with quasi-fast spiking phenotypes (Yavorska and Wehr 2016), all fast spiking neurons were excluded from analysis due to the reported error of ChR2 expression in parvalbumin+ fast spiking cells (Hu et al. 2013). It is critical to also note that insertion of ChR2 into the membranes of regular spiking and LTS SST+ neurons has been reported to cause them to rapidly enter depolarization block with high current injection in an irregular manner (Herman et al. 2014), a phenomenon regularly observed during experimentation. Finally, due to results reported in *section 2.3.2*, SST-GFP cells $\geq$ 2 mm distant to the microgyrus were included in this analysis to ascertain whether they are intrinsically similar to controls and distinct to PMR cells.

Described in *section 2.2* and identically to *section 2.3.1*, assessments of layer V SST-GFP neuron intrinsic passive membrane and action potential properties were performed. A comprehensive list of characteristics determined from these recordings is provided in *Table 2.1*.

Results indicate that resting membrane potential of cells from the three groups was not different (mean values: Control -59.3±1.7 mV, PMR -60.4±2.2 mV, Distant -62±2.9 mV, *P* = .29 *Figure 2.5C*), nor was input resistance (mean values: Control 272.9±0.02 MΩ, PMR 240.5±0.03 MΩ, Distant 237±0.04 MΩ, *P* = .66, *Figure 2.5D*), rheobase (mean values: Control 30.4±4.8 pA, PMR 24.2±5.9 pA, Distant 23.6±6.5 pA, *P* = .67, *Figure 2.5E*), spike amplitude, half width, max rise rate, rise and decay tau, and AHP amplitude (*Table 2.1*). Differences were found between groups in regard to the time to first action potential at rheobase, which was found to be significantly shorter in control SST+ neurons as compared to remaining groups (mean values: Control 116.6±10.6 ms, PMR 156.9±13 ms, Distant 159±0.94 ms, *P* = .02, *Figure 2.5F*). Additionally, second spike halfwidth amplitude (mean values: Control 39.6±1.5, PMR 43.9±0.9, Distant 43±1.7, one-way ANOVA, *P* = .03, *Table 2.1*) was found to be significantly different between groups, with significance falling between the PMR and control groups (Dunnett's T3 multiple comparisons test, *P* = .04, *Table 2.1*). Further, comparing action potential frequencies as a function of injected current in an action potential frequency versus current graph, it was revealed that there are significant differences of SST+ neuron firing frequencies between groups (*P* = .002, *Figure 2.5G*).

2.3.4. Search for mechanism: SST+ neurons of layer V PMR possess arbor with extended within layer reach compared to controls.

With confirmation that ChR2 functions the same between control and PMR SST+

neurons we continued investigations into the mechanism underlying SST output enhancement

onto layer V pyramidal neurons within PMR. ChR2 functionality, represented by number of

action potentials recorded from SST-ChR2 neurons evoked by local application of LED, no

difference between groups, $P = .97$, *Figure 2.6A,* consistent with our previous finding (Ekanem

et al. 2019).

We made use of inserted ChR2 to interrogate the range of activation for PMR versus

control SST+ neurons. The same SST+ neuron activating sequence of 11 increasing LED

durations used in *Figure 2.4* was applied at three, within-layer lateral distances from the patched

SST-GFP neuron. Glutamatergic and GABA$_A$ synaptic transmission was blocked with APV

(20uM, NMDA receptor antagonist), DNQX (10uM, AMPA receptor antagonist), and gabazine

(10-100 uM, GABA$_A$ receptor antagonist). Degree of direct activation at each of the three lateral

distances were normalized to the number of action potentials evoked with local LED per *Figure*

2.6A and found to be significantly higher in PMR SST-GFP neurons (significant effect of group,

$P < 0.0001$; effect of LED duration, $P < 0.0001$; interaction between group and LED duration, P

< 0.0001, *Figure 2.6D*, miniscule SEM values reported in Table 2.2). This indicates that SST+

neurons within layer V of PMR possibly exhibit arbors with extended within-layer reach.

Normalization was performed to address the raw data's tremendous variability. For full

disclosure, raw data means±SEM are included in Figure 2.7.

Two assessments were performed to determine what functional repercussions extended

SST+ neuron projections may have. First, we determined total GABA-mediated

neurotransmission, represented by electrically-evoked (e)IPSCs recorded in layer V pyramidal

neurons with blockage of glutamatergic synaptic transmission (*Figure 2.6E*). These data revealed

that eIPSC peak amplitudes are significantly higher in PMR than in controls at the longest

duration level used (mean values at 0.32 ms: control -469.67±87.2 pA, PMR -838.97± 219.7 pA,

significant effect of group *P = 0.028*, significant effect of stimulus duration *P < 0.001,*

Bonferroni multiple comparisons test reveals significant difference at longest stimulation

duration *P = .014, Figure 2.6F*). Secondly, we recorded IPSCs from layer V pyramidal neurons

as evoked by SST+ neuron activation at two of the three lateral sites, the same scheme per

Figure 2.6, but with recorded responses being synaptic in nature. Results indicate that SST+

neuron activation is able to evoke responses in layer V pyramidal neurons from further lateral,

within layer distances. Currents recorded from 1 and 2 (defined in *Figure 2.8A* insert) were

calculated as percentages of currents recorded with local LED application (*Figure 2.8C*). PMR

layer V pyramidal neurons exhibited higher percentages than controls indicating that SST-

activation has a stronger effect on these post synaptic neurons at these lateral sites (significant

effect of group, *P < 0.0001*; significant effect of LED duration, *P < 0.0001*; significant

interactions between group and LED duration, *P < 0.0001*; *Figure 2.8C,* miniscule SEM values

reported in Table 2.3). Through this study we can confirm that PMR SST+ neurons send within-

layer V axonal projections beyond their normal range exhibited in control cortex.

2.3.5. *Search for mechanism: SST+ neuron release probability is most likely identical between*

groups disqualifying it as a causal factor for any of the observed results.

   SST+ neuron probability of release was assessed as means to further investigate the

mechanism by which SST+ neurons put forth enhanced output onto layer V pyramidal neurons.

It is presently unknown whether presynaptic release probability of SST+ neurons within layer V

of PMR are altered in a significant, potentially pathological way.

To estimate release probability, we recorded IPSCs from layer V pyramidal neurons

evoked by a 25 Hz LED train. The chosen frequency of 25 Hz is appropriate because it is not

high enough to induce changes in presynaptic plasticity, such that occur with various types of

high frequency stimulation (Regehr 2012, Rowan et al. 2016). Five instances of LED at this

frequency were introduced above the patched cell, resulting in a sequence of 5 peaks (*Figure

2.9A*). IPSC peak amplitudes for peaks 1 – 5, per group, are presented in *Figure 2.9B*. Consistent

with *Figure 2.4*, currents recorded from layer V pyramidal cells were significantly higher than

those recorded from control and distant groups (significant effect of group, $P = .0002$, no

significant effect of peak $P = .85$ Figure 2.9B).

To ascertain the degree of facilitation or suppression, we compared peaks two through

five to the first (2 – 5 represented as percent of peak one, *Figure 2.9C*). Results indicate that

release probability is likely not different between the three tested groups. For all three groups,

peaks two through five exhibited identical percentages of peak one (no significant effect of group

$P = .96$, no significant effect of peak $P = .31$, *Figure 2.9C*). This result however is dually

inconclusive for the reason mentioned above, and also since we cannot presently account for

whether this effect is indeed synaptic or directly caused by ChR2 desensitization. To confirm

whether ChR2 activates to the same extent with each application of LED at the chosen frequency

of 25 Hz, we recorded ChR2 currents from SST+ neurons, while utilizing the same protocol as

with the pyramidal recordings (*Figure 2.9D*). ChR2 currents recorded in SST+ neurons were

different between groups ($P < 0.0001$) as well as between peaks ($P < 0.0001$), with significant

interactions between group and peak ($P < 0.0001$, *Figure 2.9D*). It is presently unknown how

current levels evoked at 25 Hz correlate with action potential evocation, a much more robust

measurement for SST-ChR2 activation (such as in *Figure 2.6A)*. So, there is a likelihood that

SST+ neurons are activated to the same extent at each instance of LED application at 25 Hz, despite different ChR2 current levels per peak and per group. Nevertheless, among this ChR2 current cohort, the percent of peak one for peaks two through five for all groups was determined to be identical across all groups and peaks (no effect of group $P = .99$, no effect of peak $P = 07$).

2.4: Discussion

In this endeavor to uncover the potential mechanism(s) that underlie SST+ neuron functional enhancement within PMR, several novel SST+ neuron-centric circuit paradigms were uncovered.

Introduced was a unique scheme for altered SST+ neuron positioning within layer V of developmentally malformed, epileptogenic cortex which likely contributes to their previously reported output enhancement onto same layer pyramidal neurons (Ekanem et al. 2019). Results herein indicate that arbors from SST+ neurons extend farther away from their cell bodies within layer V, and confirm that this arbor extension includes SST+ neuron axonal processes as postsynaptic layer V pyramidal neurons receive a greater percentage of functional input from SST+ neurons activated from farther away. It is of note that in rat, pyramidal neurons of layer V PMR exhibit longer dendritic branches, and therefore larger recipient surface areas (Di Rocco et al. 2002). This carries unique importance as the most common SST+ neuron subtype within layer V is reported to be the translaminar Martinotti cell that sends its axons superficially to external layers (Yavorska and Wehr 2016). It is unknown whether these layer V SST+ neurons are structurally aberrant Martinotti cells as output from layer V SST+ neurons onto external post-synaptic targets was not assessed. Alternatively, Martinotti cells could be supplanted in number by another subtype of SST+ neuron such as dendritically-targeting bitufted/double bouquet cells that exhibit a wide, horizontal, within-layer axon structure (Fishell and Rudy 2011).

Furthermore, release probability from SST+ neurons was estimated to be identical between experimental groups, which narrows down the candidate alterations to SST+ physiology that may contribute to their enhanced output within layer V of PMR. It seems there may be higher numbers of SST+ neuron synapses present in PMR, however whether this is from a population of neurons equal to or greater than control levels is presently unknown. Additionally, how this speculated increase in synaptic connections is established is unknown; perhaps this is a byproduct of aberrant synaptic pruning, a sign of immaturity (Paolicelli et al. 2011), which PMR has been implicated to be via other metrics (discussed in detail within *section 1.3.2*).

Compounded with the potential for increased synapses from SST+ neurons, comparing action potential firing frequencies as a function of injected current revealed that there are significant differences of SST+ neuron firing frequencies between groups. Sources of these differences are presently unknown however a previous report indicates that LTS interneurons within PMR exhibit higher maximum firing frequencies; these studies though were performed in rats aged P12 to P17 (George and Jacobs 2011). This same report indicates that SST+ neurons in PMR behave with a fast twitch like response tendency and greater degrees of fatigue in response to current injection; characteristics consistent with an overactive phenotype. It remains ambiguous if layer V SST+ neuronal dendritic processes are extended as well. Future studies may benefit from performing Sholl analysis on dendritic arborization of layer V SST+ neurons to these ends (O'Neill et al. 2015). It is also unknown if SST+ neurons of layer V exhibit extension of their processes beyond the terminus of PMR.

Developmentally malformed cortex exhibits staggered onsets of two common pathological characteristics, hyperexcitability and epileptogenesis, with the former preceding the latter in time (Jacobs et al. 1999a, Jacobs and Prince 2005, Zsombok and Jacobs 2007). Events

pertaining to the onset of hyperexcitability are therefore insufficient alone to trigger the generation of epileptiform events in our model. A previous report indicates that SST+ neurons are functionally enhanced onto layer V pyramidal neurons in a layer V-specific manner (Ekanem et al. 2019), but what role does this SST+ neuron-centric phenomenon play in pushing a hyperexcitable area such as is seen in early PMR, towards subsequent epileptogenesis in the developing brain? While this is presently unknown in certainty, we can at least look to a previous report to link changes in SST+ neuron densities over development to this FL to epileptogenesis timeline which demonstrates that SST+ neuron numbers within PMR significantly diminish at late developmental ages following the onset of epileptiform activity (Patrick et al. 2006). If our observed alteration to SST+ neuron function is therefore lost at late developmental stages as a result of depleted SST+ neuron densities, then it could be that SST+ neuron dysfunction may be unnecessary for the occurrence of epileptiform activity post onset, though there is also the possibility that this hypothetical loss of function could be epileptogenic in itself. Nevertheless, we are the first to report an interneuron function that returns to control levels beyond the terminus of epileptogenic PMR. As we do not yet know if SST+ neuron functional enhancement is epileptogenic, how its restriction to PMR pertains to overall network function is presently unknown.

Another novel finding in this work is the observed difference between first action potential rise tau values between layer V pyramidal neuron groups (Figure 1). With tau being equivalent to a neuron's resistance multiplied by its capacitance, longer tau durations among these neurons indicates increased capacitive capabilities, as input resistance is not different between groups. Neuron capacitance is a measure of how quickly a cell's membrane potential can respond to current changes, so higher capacitance of layer V pyramidal neurons within PMR,

the epileptogenic substrate of DCM, could have numerous interesting implications. One pertaining to how higher capacitance corresponds with decreased action potential velocity as there is a longer lag in voltage change in response to current changes. While slower action potentials seem logically inconsistent for a hyperexcitable neuronal substrate prone to the propagation of epileptiform activity (Prince 1985), it is consistent with delayed maturation, a characteristic inherent to neurons resident within PMR (Rosen et al. 1992, Super et al. 1997, Defazio and Hablitz 1999, Redecker et al. 2000). Decreased action potential velocity logically corresponds with slower action potential frequency which was indicated in previous reports to be the case in PMR layer V pyramidal neurons in rats aged P12 to P17 (George and Jacobs 2011) and in layers II/III regular spiking neurons of dysplastic cortex in rats aged one to four months (Luhmann et al. 1998). We also found significant differences of action potential firing frequencies between PMR and control, however frequencies appeared higher in PMR layer V pyramidal neurons (mice aged P12 to P21). These differences may be accounted for due to differences in species used, included age group, and even neocortical layer examined for experimentation.

The relevance higher layer V pyramidal neuron capacitance has to overall network function is called into question with the report that tonic $GABA_A$ receptor conductance can play a role in decreasing membrane tau in hippocampal CA1 pyramidal neurons (Wlodarczyk et al. 2013). We have observed enhanced pyramidal neuron responses to optogenetic activation of presynaptic PMR SST+ neurons, but we don't know yet whether these same GABAergic SST+ neurons are tonically more active within PMR. If this is the case, then tau values may approach control levels during normal network function due to increased spontaneous conductance through $GABA_A$ receptor channels. This seems likely given our demonstration that SST+

neurons exhibit extended within layer reach. While *Figure 2.6* does not proffer any suggestion as to whether the observed extended arbor are dendritic, axonal, or both, *Figure 2.8*, suggests that extension axonal of arbor is involved, which could present as increased branching and a higher number of synapse formation onto layer V pyramidal neurons. With that, increased tonic activity of SST+ neurons seem all the more likely.

That being said, we also found rheobase of layer V pyramidal neurons within PMR to be 20-42% higher than those of control homotopic cortex which is consistent with other reports that declare relatively lower rheobase values in layer V pyramidal neurons within neocortex that is epileptogenic and inflamed (Di Pasquale et al. 1997, Wu et al. 2016) though the underlying mechanisms are presumptively different to those that lead to the development of PMR, the epileptogenic and inflamed substrate of DCM (Jacobs et al. 1999a, Devinsky et al. 2013). This is relevant as disparate disease paradigms may actually exhibit important functional commonalities, which can be valuable in regard to treatment development across multiple disease modalities. The strength of our rheobase assessment via mean comparison is called into question as the range of values is 100-fold. While this may be biological, assessing for differences by way of averages may not be the most robust approach.

There are some inconsistencies between what we reported in this work and a previous study differentially performed in rats (George and Jacobs 2011). Firstly, analyses of SST intrinsic membrane properties in this report compiled results from both regular spiking and LTS cohorts, while previously only LTS interneurons were looked at. An unavoidable distinction since ChR2 inserts into all SST+ neurons regardless of firing type. Including a wider range of SST+ neuron subtypes could explain why some metrics that appeared significant in the previous report did not in the present one such as action potential firing frequency. For example, in the

present report, it appears that PMR SST+ (LTS and RS) neurons may exhibit lower action potential firing frequencies compared to the control and distant counterparts, while it was previously reported that firing frequency is increased in PMR LTS neurons (George and Jacobs 2011). It would be suitable in a follow up study to parse firing frequency changes between LTS and RS SST+ neurons to confirm whether these different populations are affected disparately in PMR. That being said, we observed that second spike halfwidth amplitudes are higher in PMR SST+ neurons. This being possibly indicative of a speedier upstroke period, is additionally incongruous with the observed lower firing frequencies. Secondly, irregularly rapid induction of depolarization block with high current injection or long LED activation is a documented feature of regular-spiking and LTS SST+ neurons containing ChR2 (Herman et al. 2014). As this is not in vivo work and depolarization block was not demonstrated to occur at the short LED durations utilized to activate SST+ neurons in this work (0.1 – 2 ms), LED experimentation could occur uninterrupted. Analysis also revealed that there are significant differences of action potential firing frequencies between PMR and control, with frequencies appearing higher in PMR pyramidal neurons. This is in conflict with the aforementioned previous reports. The frequency-current relationship was found to be identical between groups in our report consistent with one previous report (George and Jacobs 2011), but contradictory to another that reported a less steep rise (Luhmann et al. 1998).

In summary, this work introduces a unique scheme for SST+ neuron dysfunction within PMR. Much remains to be discovered pertaining to how SST+ neurons may modulate dysfunction within and outside of PMR. Nevertheless, these results indicate that the puzzle is far from completely solved.
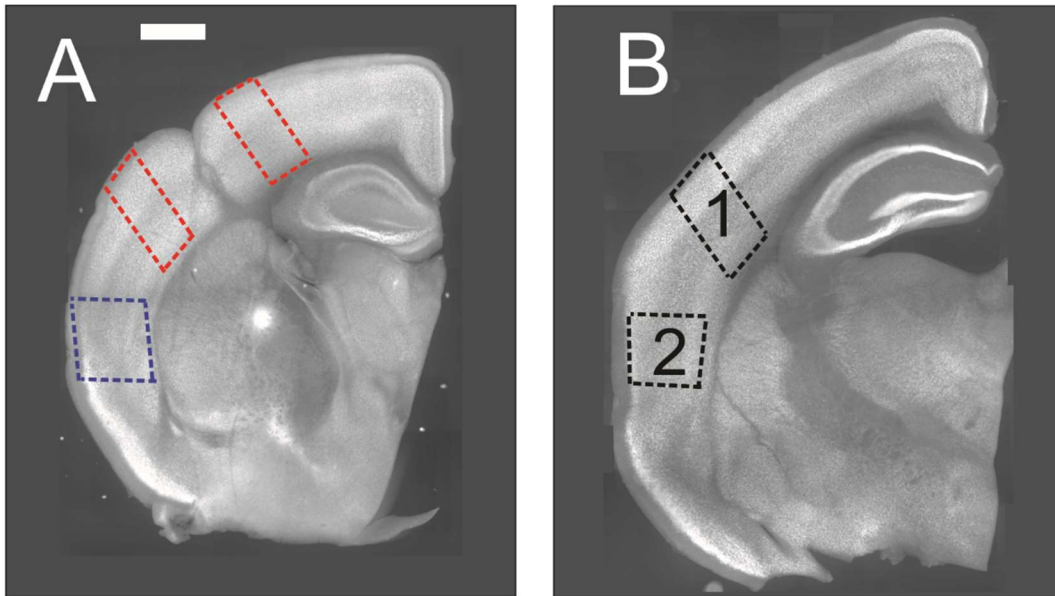
Figure 2.2 Examples of a prototypical *ex vivo* slice containing a freeze-lesion induced microgyrus **(A)** and a control *ex vivo* slice **(B)** used for recordings. Both slices are stained for NeuN.

Dotted boxes indicate the ranges within which all recordings were made.

(A) Red boxes represent PMR (0.5 mm - 1 mm away from microgyrus on either side). Blue box represents the >2 mm distant to microgyrus cohort referred to as Distant within this correspondence.

(B) Black boxes represent homotopic control correlates to (1) PMR and (2) "Distant" sites. All data recorded between sites 1 and 2 were statistically identical, and therefore grouped together to occupy the control cohort.

For simplicity, figures throughout this correspondence will abide by this color scheme. Control = grey, PMR = red, Distant = blue.

Scale bar in A for A-C = 800 μm
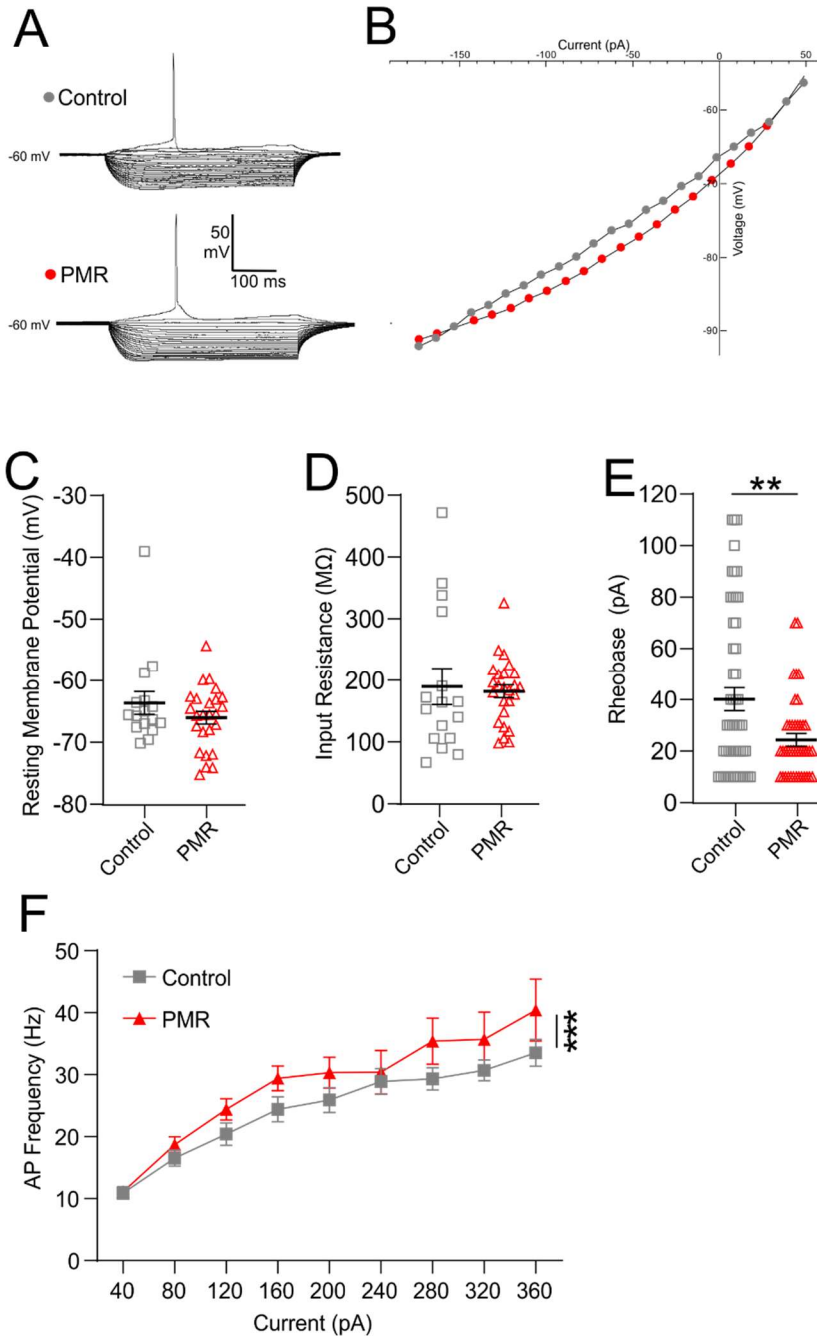
Figure 2.3: Rheobase is lower in control non-fluorescing, regular-spiking pyramidal neurons than those within PMR. Remaining intrinsic membrane properties are identical between groups.

(A) Membrane voltage responses to current steps from -200 pA to rheobase of control and PMR representative neurons

(B) I-V plots of representative traces in (A), visualizing the two cell's membrane voltage responses to injected current steps

(C) Individual values and mean±SEM of resting membrane potential for pyramidal neurons (control n = 14, PMR n = 25, unpaired t-test, P = 0.26)

(D) Individual values and mean±SEM of input resistance for pyramidal neurons (control n = 14, PMR n = 25, unpaired t-test, P = 0.79)

(E) Individual values and mean±SEM of rheobase for pyramidal neurons (control n = 52, PMR n = 41, unpaired t-test, P = 0.003)

(F) Plot of action potential firing frequency as a function of injected current. There are significant differences of group between control and PMR pyramidal neuron AP firing frequencies (control n = 47, PMR n = 41, one way ANOVA, effect of current P < 0.0001, effect of group P = 0.0002)

79

Parameter	Pyramidal neurons Control n = 50 / PMR n = 41	SST-GFP neurons Control n = 53 / PMR n = 50 / Distant n = 11	Parameter	Pyramidal neurons Control n = 50 / PMR n = 41	SST-GFP neurons Control n = 53 / PMR n = 50 / Distant n = 11
RMP (mV)	-62.8±2.4 / -66±1.0	-59.3±1.7 / -60.4±0.44 / -62±0.44	Rise to second half-amplitude time (ms)	0.5±0.1 / 0.7±0.3	0.29±0 / 0.31±0 / 0.34±0
Input Resistance (MΩ)	184±0.04 / 182±0.01	272.9±0.02 / 240.5±0.03 / 237±0.04	Max rate of rise to first half-amplitude (mV/ms)	241±16.9 / 203.7±19.2	203.7±15.3 / 235.7±15.9 / 168.7±15.6
Rheobase (pA)	39.4±4.4 / 24.4±2.4 *	30.4±4.8 / 24.2±5.9 / 23.6±6.5	Max rate of rise to second half amplitude (mV/ms)	158.6±11.8 / 141.9±13.2	170.2±14.4 / 189.2±13.4 / 148.5±18.9
Time to first spike at rheobase (ms)	135.3±11.5 / 144.6±8.1	115±10.4 / 156.9±13 * / 159±16.6	First spike rise tau (ms)	3±0.7 * / 11.7±4.2	4.7±2.2 / 3.2±0.7 / 3.1±0.9
Frequency at rheobase (Hz)	4.3±0.4 / 4.4±0.4	6.2±0.8 / 5.9±0.9 / 5±0.8	Second spike rise tau (ms)	3.4±1.4 / 4.3±2.3	2.9±0.5 / 5.4±1.3 / 3.1±0.2
Maximum firing frequency (Hz)	34.9±1.8 / 39.1±2.5	54.6±3.1 / 48.2±0.6 / 58.4±0.11	Decay time to first half amplitude (ms)	3.4±0.8 / 4.2±1.1	2.8±0.8 / 2.1±0.1 / 2.2±0.2
F/I slope (Hz/pA)	0.1±0.01 / 0.1±0.01	0.1±0.02 / 0.1±0.02 / 0.1±0.03	Decay time to second half amplitude (ms)	4±0.3 / 5.2±0.6	3.0±0.7 / 2.5±0.1 / 2.6±0.3
First spike amplitude (mV)	86.2±2.7 / 81±2.3	79.8±3.2 / 86.6±2.5 / 87.4±0.89	Max rate of decay to first half-amplitude (mV/ms)	-46.3±2.8 / -40.7±3.1	-49±6.9 / -60.9±4.3 / -51.1±6.9
Second spike amplitude (mV)	85.3±2.6 / 80.5±2.2	77.5±3.0 / 83.9±2.3 / 85.9±3.3	Max rate of decay to second half amplitude (mV/ms)	-37±2.3 / -33.5±2.7	-41.6±6.1 / -49.7±3.9 / -44.7±7
First spike halfwidth (ms)	2.3±0.2 / 2.8±0.4	2.5±0.8 / 1.7±0.1 / 1.9±0.2	First spike decay tau (ms)	5.3±2.9 / 3.2±1.2	1.9±0.3 / 1.6±0.2 / 1.6±0.1
Second spike halfwidth (ms)	2.7±0.2 / 3.4±0.4	2.7±0.7 / 2.1±0.2 / 2.3±0.3	Second spike decay tau (ms)	2.3±0.2 / 3.1±0.6	3.4±1.4 / 2.1±0.2 / 1.9±0.2
First spike half-width amplitude (mV)	45.4±1.2 / 40.8±1.2	40.9±1.6 / 45.4±1 / 43.7±1.9	First AHP amplitude (mV)	12.3±0.99 / 12.4±1.1	11.6±1.9 / 10.7±0.9 / 10.6±2.2
Second spike half-width amplitude (mV)	43±0.9 / 40.9±0.8	39.6±1.5 * / 43.9±0.9 / 43±1.7	Second AHP amplitude (mV)	9.8±0.8 / 10±0.9	12±1.9 / 11.2±1 / 9.6±1.6
Rise to first half-amplitude time (ms)	1.2±0.6 / 1.5±0.7	0.29±0 / 0.32±0 / 0.323±0			

Table 2.1 Comprehensive list of intrinsic passive and action potential properties of layer V pyramidal neurons and SST-GFP neurons. Values reported as mean±SEM; * indicates significant difference *(P < 0.05)*.

Pyramidal neuron p-values:
rheobase: p = 0.01
first spike rise tau: p = 0.03

SST-GFP neuron p-values:
time to first spike at rheobase: p= 0.02
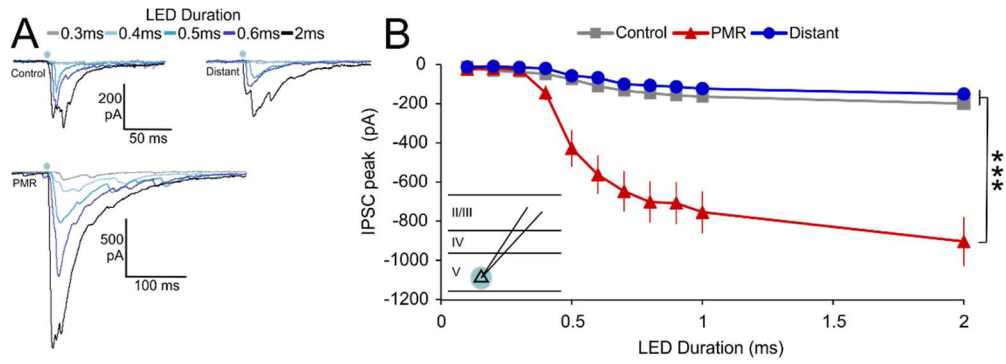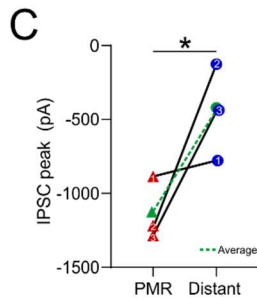second spike half-width amplitude: p = 0.04

Figure 2.4.1: Increased output from SST neurons, represented as IPSCs recorded from layer V pyramidal neurons, is limited to the epileptogenic PMR. At locations distant to the malformation (≥ 2 mm lateral to PMR), SST neuron to pyramidal neuron output is identical to control levels.

(A) Single cell representative examples of IPSC responses recorded from layer V pyramidal neurons in control, PMR, and distant tissue. SST-ChR2 activating LED was applied at multiple durations over the patched cell as per the graphic inset.

(B) Mean±SEM IPSC peak amplitudes of 37 control, 41 PMR, and 16 distant non-fluorescing pyramidal neurons(2-way repeated measures ANOVA, $p = .000$)

(C)IPSC peak amplitudes from same-slice PMR and distant pyramidal neuron pairs (2ms LED duration) (unpaired t-test, p = 0.04). Note pair 1, no change outlier.
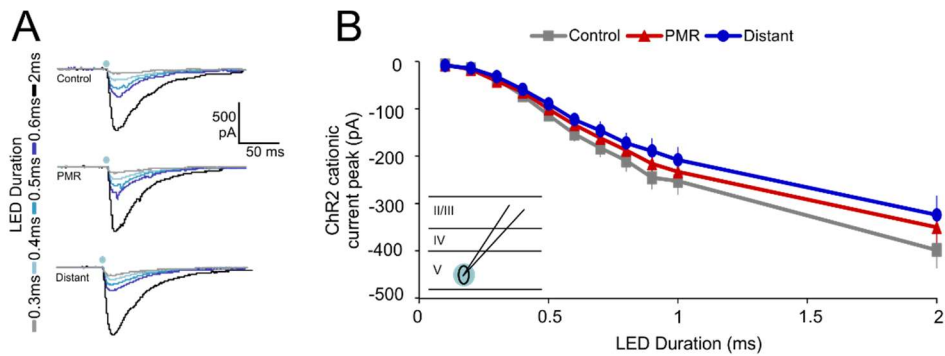
Figure 2.4.2: Differences reported in Figure 2.4 are not mediated by ChR2 as the option functions the same between the three groups.

(A) Single cell representative examples of ChR2 current responses recorded from layer V SST-GFP neurons in control, PMR, and distant tissue. SST-ChR2 activating LED was applied at multiple durations over the patched cell as per the graphic inset.

(B) Mean±SEM ChR2 non-selective cationic current peak amplitudes of 17 control, 11 PMR, and 10 distant fluorescing SST-ChR2 neurons (2 way repeated measures ANOVA, p = 0.446)
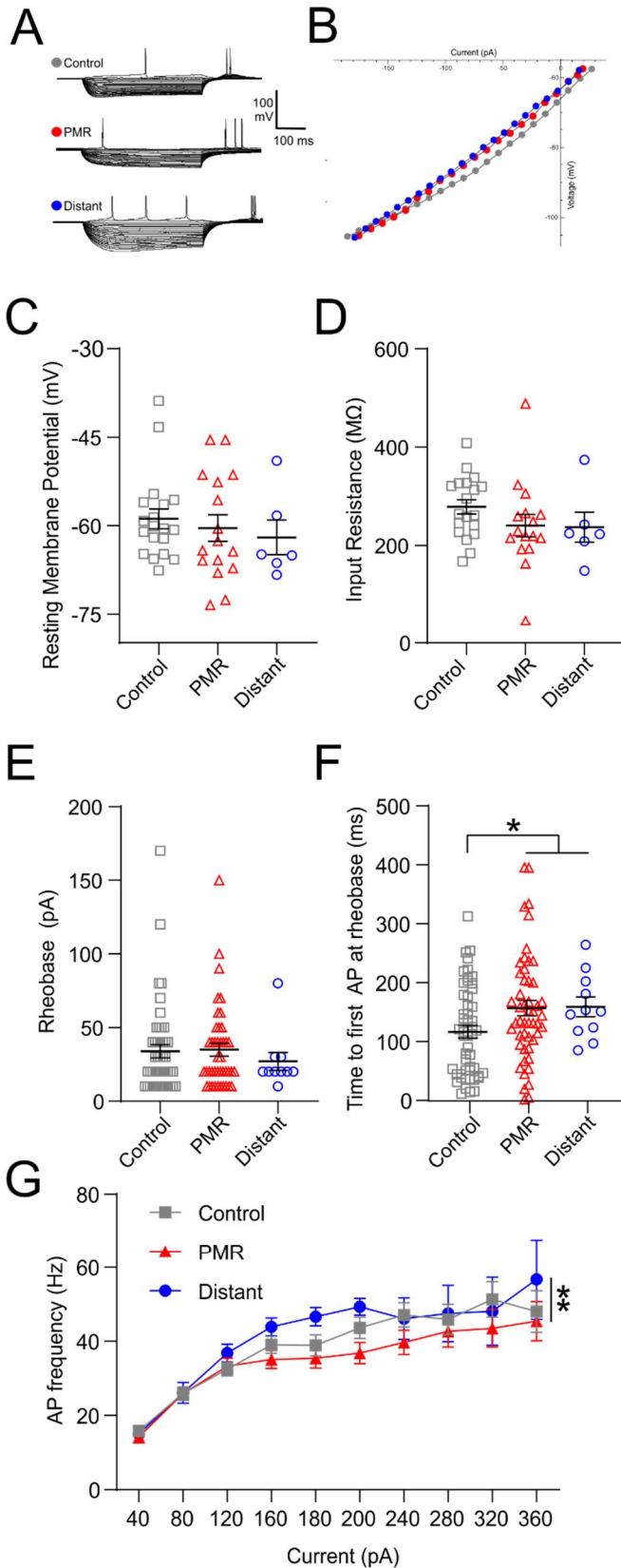
Figure 2.5: The time to first action potential at rheobase is lower in control non-fast spiking SST-GFP neurons than in PMR and distant groups. There are significant differences of action potential firing frequencies between groups. Lastly, remaining intrinsic membrane properties are identical across all groups.

(A) Membrane voltage responses to current steps from -200 pA to rheobase of control, PMR, and distant representative neurons

(B) I-V plots of representative traces in (A), visualizing the three cell's membrane voltage responses to injected current steps

(C) Individual values and mean±SEM of resting membrane potential for non-FS SST-GFP neurons (control n = 19, PMR n = 16, distant n = 6, one way ANOVA, P = 0.29)

(D) Individual values and mean±SEM of input resistance for non-FS SST-GFP neurons (control n = 19, PMR n = 16, distant n = 6, one way ANOVA, P = 0.66)

(E) Individual values and mean±SEM of rheobase for non-FS SST-GFP neurons (control n = 52, PMR n = 50, distant n = 11, one way ANOVA, P = 0.67)

(F) Individual values and mean±SEM of time to first action potential at rheobase for non-FS SST-GFP neurons (control n = 52, PMR n = 50, distant n = 11, one way ANOVA, P = 0.02)

(E) Plot of action potential firing frequency as a function of injected current. There are significant differences of group between control, PMR, and distant non-fast spiking SST-GFP neuron AP firing frequencies (control n = 49, PMR n = 38, distant n = 11, two way ANOVA, P = 0.002)

82

Figure 2.6. Non-fast spiking SST-GFP neurons within layer V of PMR may have an extended within-layer reach compared to those in homotopic control cortex.

(A) Mean±SEM action potential spikes evoked in SST-ChR2 neurons by local LED application as indicated by insert. Number of spikes evoked by LED is identical between groups (control n = 12, PMR n = 9, two way repeated measures ANOVA, no effect of group p = .974)

(B) SST-ChR2 activating LED was applied at three lateral distances within layer V away from the patched layer V SST-GFP cell. 1 = 100-200 um , 2 = 300-400 um, 3 = 500-600 um

(C) Single cell representative examples of action potential responses to 2 ms LED in layer V SST-GFP cells within control and PMR tissue

(D) Mean ±SEM action potential spikes normalized to local spike count at each LED duration and presented as percent of locally (two-way repeated measures ANOVA, p<0.0001 for n = 8 control, 7 PMR fluorescing SST+ neurons.) Minuscule SEM values do not appear on graph and are included in Table 2.2.

(E) Total GABAergic network electrical stimulation in a series of 5 durations was applied 100-200 um away from the patched layer V pyramidal cell. Single cell representative examples of current responses of one control and one PMR layer V pyramidal cell. Electrical artifact removed from depicted traces for neatness.

(F) Mean±SEM IPSC peak amplitudes of 18 control, 7 PMR non-fluorescing pyramidal neurons (2-way repeated measures ANOVA, effect of group p = 0.028, effect of stimulus duration p <0.0001 , Bonferroni multiple comparison test, difference at 0.32 ms, p = 0.014)

LED duration	Control 100-200 um			Control 300-400 um			Control 500-600 um		
	Mean %	SEM	N	Mean %	SEM	N	Mean %	SEM	N
0.4 ms	9.38	1.55	8	0	0	8	0	0	7
0.5 ms	50	1.00	8	0	0	8	0	0	7
0.6 ms	62.90	1.05	8	14.52	1.25	8	0	0	7
0.7 ms	64.29	1.10	8	17.14	1.32	8	0	0	7
0.8 ms	48.91	1.26	8	16.30	1.44	8	0	0	7
0.9 ms	56.60	1.33	8	14.15	1.54	8	0	0	7
1 s	70.75	1.13	8	19.81	1.58	8	0	0	7
2 s	77.53	1.52	8	35.39	1.57	8	7.70	1.79	7

LED duration	PMR 100-200 um			PMR 300-400 um			PMR 500-600 um		
	Mean %	SEM	N	Mean %	SEM	N	Mean %	SEM	N
0.4 ms	96.43	0.44	7	0	0	7	0	0	7
0.5 ms	76.45	0.89	7	0	0	7	0	0	7
0.6 ms	93.10	0.95	7	39.90	0.99	7	0	0	7
0.7 ms	109.09	1.18	7	42.86	1.09	7	3.90	2.18	7
0.8 ms	83.97	1.33	7	39.36	1.35	7	10.50	1.53	7
0.9 ms	84.07	1.39	7	44.51	1.22	7	17.31	1.41	7
1 s	86.45	1.15	7	50.99	1.24	7	19.95	1.40	7
2 s	91.24	1.35	7	56.68	1.22	7	17.97	1.43	7

Table 2.2 Minuscule SEM values from Figure 2.6D. As these do not show up on the graph, they are reported here.
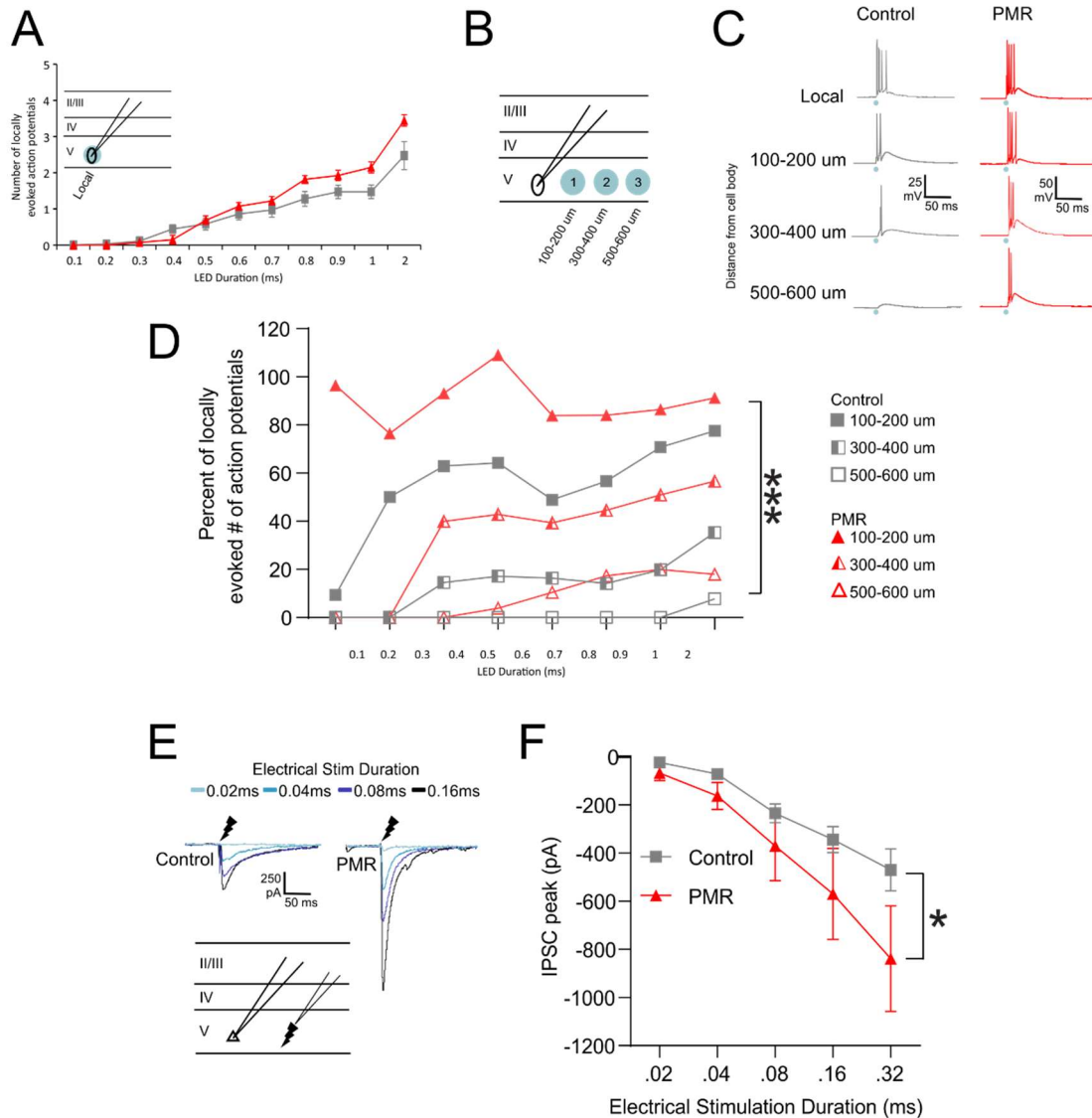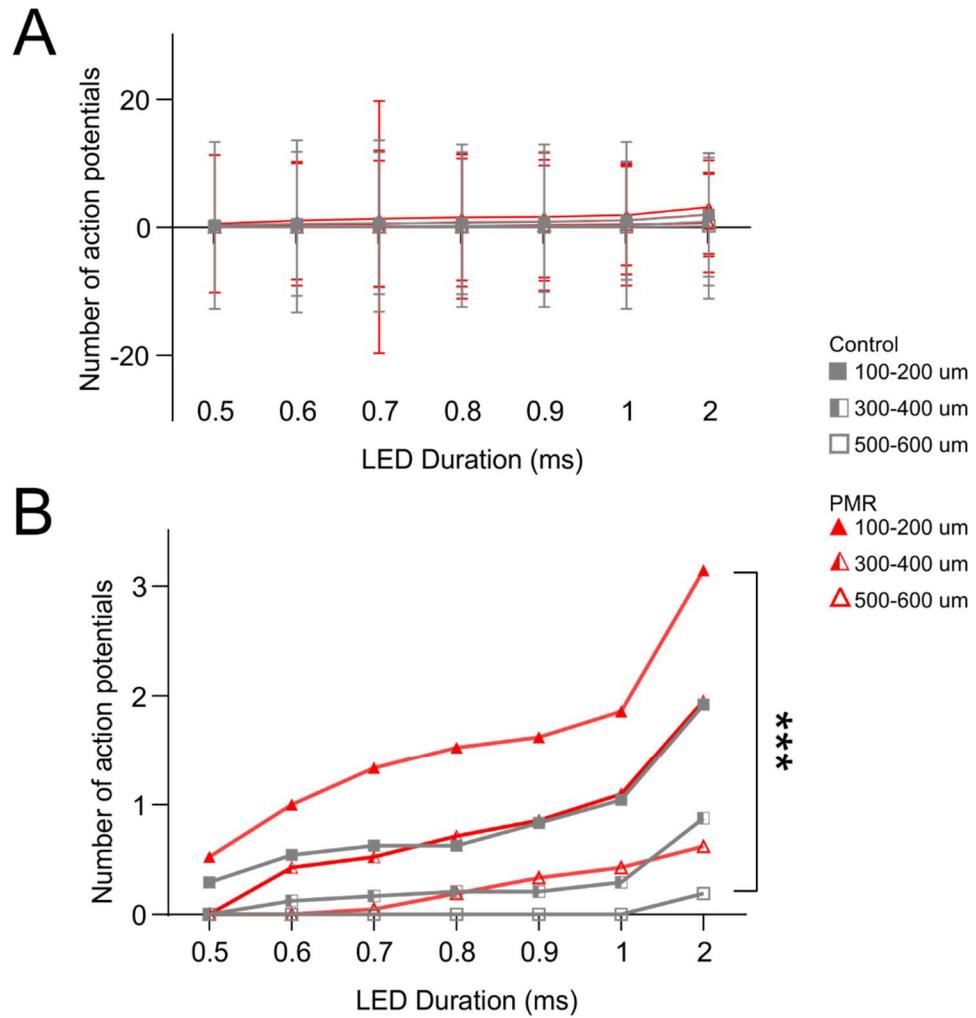
Figure 2.7 Non-fast spiking SST-GFP neurons within layer V of PMR may have an extended within-layer reach compared to those in homotopic control cortex.

(A) Original mean ±SEM action potential spikes evoked at each lateral distance from 0.5 ms. Note comically large error bars. To address this, data was normalized to number of action potentials evoked with local light application. Normalized data rresented in Figure 2.6D

(B) Data presented in A without error bars to illustrate population distribution. There are significant effects of group (P < 0.0001) and LED duration (P < 0.0001), two way repeated measures ANOVA, n = 8 control, 7 PMR fluorescing SST+ neurons.
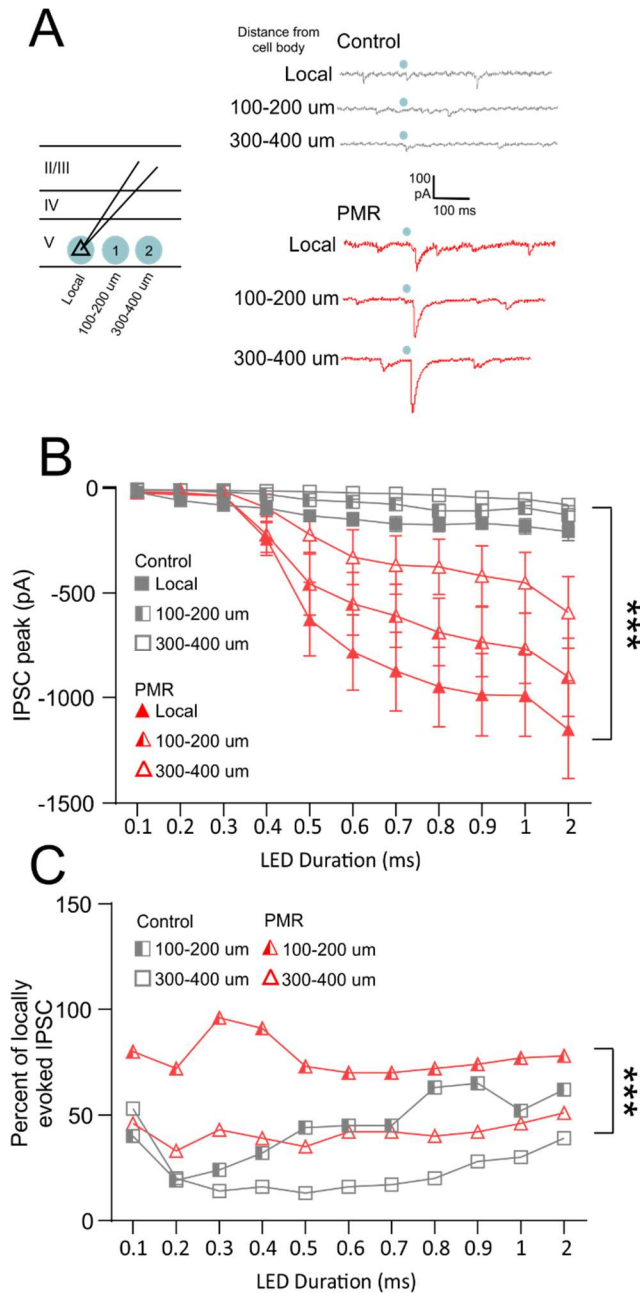
Figure 2.8. Additional functional corollary to SST neurons exhibiting an extended reach within layer V of PMR. Layer V pyramidal neurons exhibit a higher percentage of IPSC amplitude from laterally distant SST neuron activation

(A) SST-ChR2 activating LED was applied locally and at two lateral distances within layer V away from the patched layer V pyramidal neuron. 1 = 100-200 um , 2 = 300-400 um,

(B) Mean±SEM IPSC peak amplitudes recorded from layer V pyramidal neurons. Current peak amplitudes are significantly different across all groups and LED durations (two way repeated measures ANOVA, effect of group $P < 0.0001$, effect of LED duration $P < 0.0001$, significant interactions between group and LED duration $P < 0.0001$)

(C) To better represent the relationship between distance and SST neuron output onto layer V pyramidal neurons, percentages of local IPSC peak amplitude were determined for currents recorded at sites 1 and 2. Values are significantly different across groups and LED durations ((two way repeated measures ANOVA, effect of group $P < 0.0001$, effect of LED duration $P < 0.0001$, significant interactions between group and LED duration $P < 0.0001$). SEM values are minuscule and reported in Supplemental Table 2.3

LED duration	Control 100-200 um			Control 300-400 um		
	Mean %	SEM	N	Mean %	SEM	N
0.1 ms	40	0.1	12	53	0.19	12
0.2 ms	19	0.03	12	20	0.05	12
0.3 ms	24	0.06	12	14	0.03	12
0.4 ms	32	0.09	12	16	0.04	12
0.5 ms	44	0.17	12	13	0.06	12
0.6 ms	45	0.16	12	16	0.06	12
0.7 ms	45	0.18	12	17	0.07	12
0.8 ms	63	0.29	12	20	0.09	12
0.9 ms	65	0.31	12	28	0.12	12
1 s	52	0.22	12	30	0.11	12
2 s	62	0.3	12	39	0.2	12
LED duration	PMR 100-200 um			PMR 300-400 um		
	Mean %	SEM	N	Mean %	SEM	N
0.1 ms	80	0.17	19	46	0.06	19
0.2 ms	72	0.21	19	33	0.04	19
0.3 ms	96	0.23	19	43	0.07	19
0.4 ms	91	0.25	19	39	0.19	19
0.5 ms	73	0.19	19	35	0.12	19
0.6 ms	70	0.19	19	42	0.16	19
0.7 ms	70	0.18	19	42	0.17	19
0.8 ms	72	0.2	19	40	0.16	19
0.9 ms	74	0.2	19	42	0.17	19
1	77	0.2	19	46	0.17	19
2	78	0.19	19	51	0.17	19

Table 2.3 Minuscule SEM values from Figure 2.8C. As these do not show up on the graph, they are reported here.
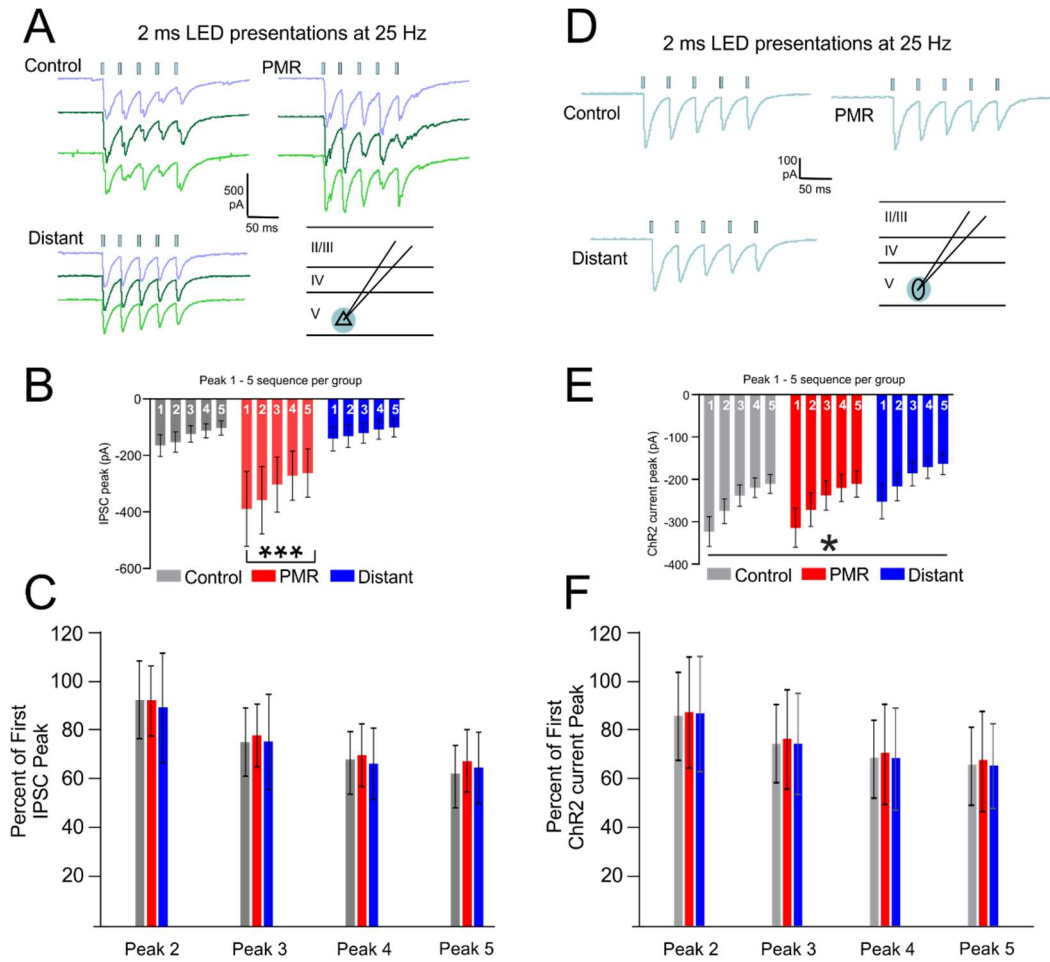
Figure 2.9 Estimated release probability of SST neurons as assessed by degree of sequence facilitation or suppression

(A) Five instances of SST-ChR2 activating LED was applied over patched layer V pyramidal neuron at frequency of 25Hz. Single cell representative examples of three evoked current peak sequences per group. Note qualitatively differing patterns of facilitation and depression per peak sequence.

(B) Mean±SEM Current peak amplitudes evoked per peak, per group. Consistent with previous results, PMR currents are significantly higher than those from control and distant groups (control n = 22, PMR n = 26, distant n = 10. two way ANOVA significant effect of group p = .0002, no effect of peak p = 0.85)

(C) Mean±SEM of percentage of first peak for peaks 2, 3, 4, and 5 of pyramidal neuron response to 25Hz LED activation of presynaptic SST neurons (control n = 22, PMR n = 26, distant n = 10. two way ANOVA, peak P = .31, group P = .96, interaction between peak and group $P > 0.99$).

(D) Five instances of SST-ChR2 activating LED was applied over patched layer V SST neurons at frequency of 25Hz. Single cell representative examples of evoked current peak sequences per group.

(E) Mean±SEM current peak amplitudes evoked per peak, per group. It is unknown how this correlates with the activation capabilities of ChR2 as action potential information is not included (control n = 16, PMR n = 11, distant n = 9. two way ANOVA, effect of group p < 0.0001, effect of peak number, p<0.0001, significant interactions between group and peak number p<0.0001)

(F) Mean±SEM of percentage of first peak for peaks 2, 3, 4, and 5 of ChR2 current peak recorded in SST-GFP neurons as means to determine consistency of ChR2 activation at 25 Hz. (control n = 16, PMR n = 11, distant n = 9. two way ANOVA, effect of group P = .99, effect of peak p = 0.68)

Chapter 3

Demonstrating parvalbumin neuron mediated microcircuit disinhibition of layer V beyond the terminus of developmentally malformed epileptogenic cortex.
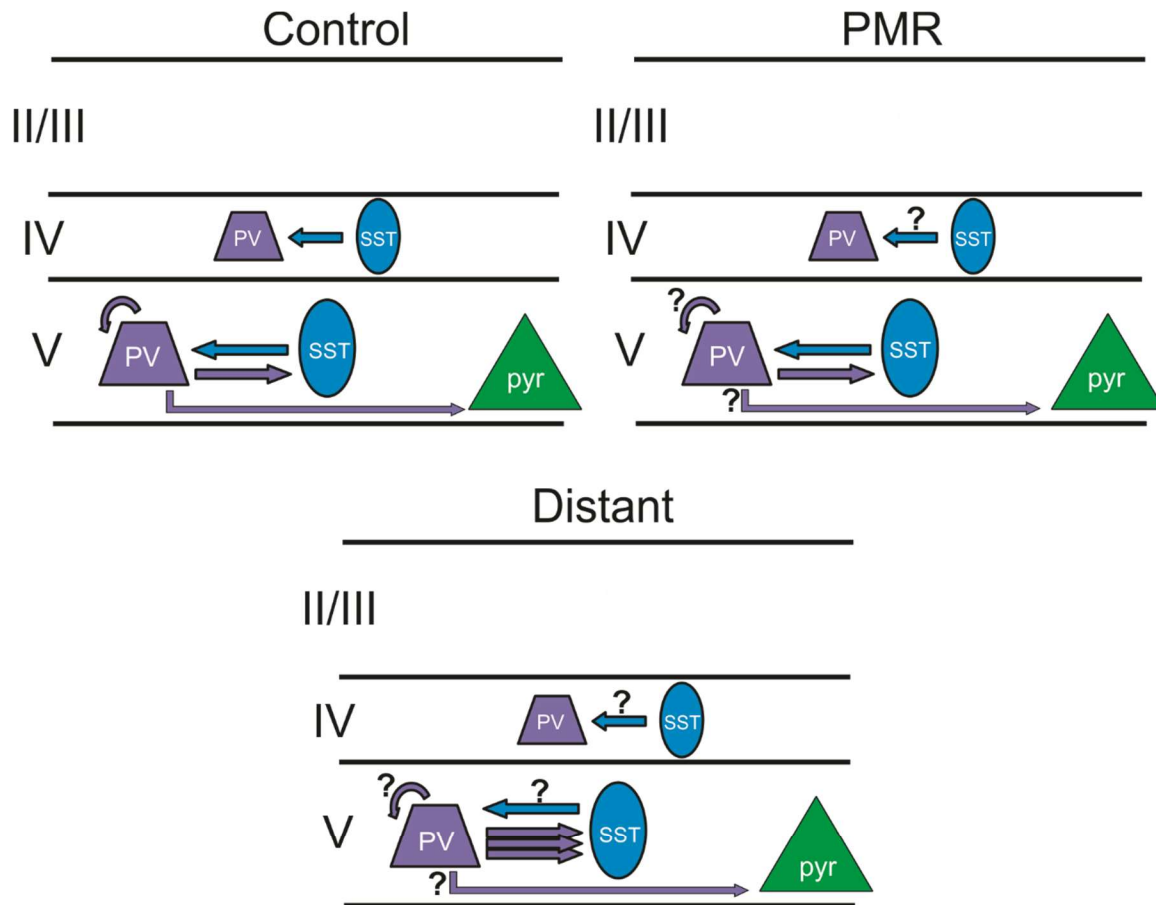
Figure 3.1 Graphical abstract representing results presented in Chapter 3. It is demonstrated primarily herein that output from SST neurons onto layer V FS neurons (presumably PV+) is not different between control, PMR, and "distant". Additionally, PV+ neurons exhibit enhanced output onto layer V SST+ neurons >2 mm from the microgyrus, beyond the terminus of epileptogenic PMR, demonstrating a novel disinhibitory pathway.

It is not presently known how PV neuron functionality may be changed onto layer V pyamidal neurons in PMR or at "distant" sites, nor how these circuit alterations pertain to PMR's epileptogenicity. Further, it is unknown how external SST+ neurons function in regard to postsynaptic PV+ neurons.

Chapter 3

Demonstrating parvalbumin neuron mediated microcircuit disinhibition and gamma oscillations of layer V beyond the terminus of developmentally malformed epileptogenic cortex.

3.1 Introduction

Through innumerable mechanisms unknown, drug resistant epilepsy and other such sequelae emerge from developmental cortical malformations (DCM). These Gestalt circumstances comprise unique territory that decades of international work have yet to completely elucidate. Nevertheless, with every report, the field inches ever closer to long sought answers. Our work within this sphere has presented the field with various novel results regarding altered cellular function within the DCM's epileptogenic substrate, the paramicrogyral region (PMR). Whether these alterations induce pathology is presently unknown, but it is critical to continue to investigate these altered circuit paradigms to these ends.

In this chapter, focus is shifted away from SST+ neurons to another class of GABAergic interneuron of greater cortical population density, parvalbumin (PV) interneurons. This subgroup encompasses somatic, perisomatic, and axonal targeting neurons possessing a fast-spiking (FS) action potential firing phenotype, which proffers these cells with powerful means of inhibition. There are indications that these neurons persist in an immature state for longer periods within PMR as conveyed in part by transient lessening of PV immunostaining within the microgyrus and PMR compared to controls (Rosen et al. 1998). PV expression typically erupts at later stages of post natal development (del Río et al. 1994) so within PMR, additional delays in PV locus initiation can indicate dysmaturity. Further, PV+ neurons of PMR have been observed to receive less inhibitory input compared to controls (Jin et al. 2014), which could yield enhanced output from these neurons, much like we have observed with SST+ neurons (Ekanem et al. 2019). It has

however been demonstrated that FS cells within PMR of freeze lesioned rats exhibit lower maximum firing frequencies compared to controls (George and Jacobs 2011). With these conflicting results, the thickets of this maze grow ever convoluted.

Presently, we aim to investigate a number of new questions to demystify the role PV+ neurons may play in this potentially pathological microcircuit relationship between SST+ neurons and their post-synaptic partners. In chapter 2, it was presented that there is higher total GABA$_A$ input to layer V pyramidal neurons (*Figure 2.6F*). With SST+ neurons exhibiting a more extended within layer reach, are they the culprit behind this observed increase or do PV+ neurons play a role? If SST+ neurons occupy a larger percentage of total GABA$_A$ neurotransmission, is their spontaneous or tonic behavior increased as their evoked behavior has been shown to be? Next, PV+ neurons within layer V receive inputs from SST+ neurons, other PV+ neurons, and even autaptic input from themselves (Deleuze et al. 2019). What are the circumstances of these distinct projections within PMR and outside of it?

We hypothesized that SST+ neuron output is enhanced onto all postsynaptic partners within PMR and that these levels return to control levels in regions distant (≥ 2 mm) to the microgyrus. In the particular case of SST to PV connectivity, we hypothesize that within PMR, enhanced output onto PV+ neurons results in a disinhibitory microcircuit paradigm. Additionally, we believe SST+ neurons within PMR exhibit higher spontaneous output onto their post synaptic partners, increasing their tonic GABAaR conductance. Lastly, we hypothesize that PV+ neurons exhibit diminished output onto their postsynaptic partners.

While the studies reported within this chapter are not all complete, results so far indicate that our hypotheses may have been largely incorrect. For starters, we demonstrate that output from SST+ neurons to layer V PV+ neurons is not enhanced within PMR and is in fact

equivalent to control levels, therefore microcircuit disinhibition was not demonstrated to occur. We do not know the nature of SST to PV+ neuron output in regions distant to the microgyrus. Attempts to determine whether SST+ neuron contribute a greater amount to $GABA_A$ neurotransmission were fruitless due to various technical issues explicated in detail. PV interneuron intrinsic membrane properties were identical across groups, except there appear to be some differences between control and PMR PV+ neurons in regard to action potential firing frequency likely consistent with the previous report (George and Jacobs 2011). Lastly, an unexpected result amidst a largely fruitless undertaking came about upon investigation of PV+ neuron function with ChR2-PV tissue. Technical issues therein were explicated in detail; however, we demonstrate that in regions distant to the microgyrus, PV+ neurons mediate a disinhibitory circuit via exhibit enhanced output onto layer V SST+ neurons. The PV to SST+ neuron relationship within PMR is presently unknown, but this result in particular broadens the epileptogenic possibilities of these GABAergic interneuron subtypes within and beyond PMR.

3.2 Materials and Methods

All animal and experimental protocols were conducted in accordance with the Virginia Commonwealth University Institutional Animal Care and Use Committee, which adhere to regulations including, but not limited to those set forth in the Guide for the Care and Use of Laboratory Animals, 8th Edition (National Research Council).

Animals

Three transgenic animal lines were generated. To achieve expression of the light-sensitive channelrhodopsin2 (ChR2) in SST-expressing interneurons or PV-expressing, SST-Cre mice (Jackson Laboratory, Farmington, CT; strain 013044) or PV-expressing interneurons, PV-Cre mice (Jackson Laboratory, strain 017320) respectively were bred with floxed ChR2 mice

(Ai32; Jackson Laboratory, strain 012569). To achieve expression of Archaerhodopsin (Arch) in SST-expressing interneurons, SST-Cre mice were bred with floxed Arch mice (Jackson Laboratory, strain 021188). Mice were housed with dam and litter siblings on a 12/12 hour light/dark cycle at 72°F, with continuous access to water and standard rodent chow.

Animal surgery

Transcranial freeze lesion surgery was used to induce bilateral microgyria over the somatosensory cortices of post natal day 1 (P1) female and male mouse pups. Mice were anesthetized through hypothermia and sustained in that state for the duration of the surgery via submersion in an ice-water slurry. Upon confirmed unresponsiveness via toe and tail pinch, skin overlying the skull was incised coronally from right to left temporal ridge at the midpoint between bregma and lambda to expose the skull above the somatosensory cortex. A rectangular probe ~0.2 mm in length cooled to −60° C was placed at the midpoints between the sagittal suture and temporal ridge on both hemispheres for 5 seconds. Sham mice had skin overlying the skull incised and skull exposed without placement of probe within time frames identical to the surgery cohort. Afterwards, the skin was sutured and the pup was rewarmed and returned to the dam. As this is survival surgery, the procedure was performed under sterile conditions. To further ensure survival, sham or freeze-lesion surgery was only performed on P1 mice weighing 1.3 mg or higher.

Ex Vivo Slice Preparation

Acute brain slices from female and male mice aged between P12 and P21 were prepared from freeze-lesioned mice and sibling controls. ChR2- and Arch-SST experiment controls consisted of 50% unoperated naïve and 50% sham mice. At all measures, sham and naïve cells

were not significantly different and were therefore both included in the control cohort. ChR2-PV experiment controls consisted of 100% sham mice.

Mice were rapidly anesthetized with an overdose of isoflurane until unresponsive to tail and toe pinches and decapitated after transcardial perfusion with cold (4° C) standard sucrose slicing solution containing (in mmol/L) 2.5 KCl, 1.25 NaH2PO4, 10 MgCl2, 0.5 CaCl2, 26 NaHCO3, 11 glucose and 234 sucrose (George and Jacobs 2011). In some cases, mice younger than P15 were not perfused prior to decapitation; no differences in slice health were observed between these and perfused cohorts. In the same standard sucrose slicing solution, 300 μm slices were obtained with a Leica VT1200S vibratome (Leica Biosystems; Wetzlar, Germany) and immediately stored in artificial cerebrospinal fluid (aCSF) containing (in mmol/L): 126 NaCl, 3.5 KCl, 1.25 NaH2PO4, 1.2 CaCl2, 1 MgSO4, and 26 NaHCO3, maintained at pH 7.3 with continuous infusion of 95% oxygen, 5% CO_2. Slices were maintained at 34° C for 1 hour and then cooled to and maintained at room temperature until time of recording.

Electrophysiological Recordings

Whole cell patch clamp cellular recordings were obtained from pyramidal and SST+ neurons within layer V of somatosensory cortex, 0.5-1.0 mm from the induced sulcus (PMR), ≥ 2 mm from the induced sulcus (distant), and homotopic cortex. Neuronal subtype was determined prior to recording based on neuronal morphology under differential interference contrast (DIC) optics, wherein confirmation of an apical dendrite was used to identify pyramidal neurons and fluorescence of green fluorescent protein (GFP) reporter associated with ChR2 or yellow fluorescent protein (YFP) reporter associated with Arch was used to identity SST+ neurons. Extracellular solution comprised aCSF with DL-2-amino-5-phosphonopentanoic acid (APV, NMDA receptor antagonist, 50 μmol/L) and 6,7-dinitroquinoxaline-2,3-dione (DNQX,

AMPA receptor antagonist, 20 μmol/L). Some experiments additionally included gabazine (SR-95531, GABA receptor antagonist, 20 μmol/L) with the above. Experiments involving electrical stimulation of local field were obtained with glass micropipettes (3-4.8 MΩ) containing blank aCSF. Whole cell patch clamp recordings were obtained using glass micropipettes (3-4.8 MΩ) containing one of three intracellular solutions. One, designated "high chloride" ($E_{Cl-} = -15$ mV) included (in mmol/L) 70 K-gluconate, 10 4-(2 Hydroxy-ethyl)piperazine-1-ethane-sulfonic acid sodium salt (HEPES), 4 Ethylene glycol bis(2-amino-ethyl-ether)-N,N,N′,N′-tetra-acetic acid (EGTA), 70 KCl, 2 MgCl$_2$ · 6H$_2$O, 2 CaCl$_2$ · 2H$_2$O, 4 Adenosine 5′-triphosphate (ATP) disodium salt hydrate, and 0.2 Guanosine 5′-triphosphate (GTP) sodium salt hydrate, with 0.25%-0.5% biocytin and in some cases 10 Lidocaine N-ethyl Bromide (QX-314). A second solution ($E_{Cl-} = -71$ mV) included (in mmol/L) 130 K-gluconate, 10 HEPES, 11 EGTA, 2 MgCl$_2$ · 6H$_2$O, 2 CaCl$_2$ · 2H$_2$O, 4 ATP disodium salt hydrate, and 0.2 GTP sodium salt hydrate, with 0.25%-0.5% biocytin. A third solution ($E_{Cl-} = -50$ mV) included (in mmol/L) 117 Gluconic Acid, 117 CsOH, 11 CsCl, 10 HEPES, 11 EGTA, 2 MgCl$_2$ · 6H$_2$O, 2 CaCl$_2$ · 2H$_2$O, 4 ATP disodium salt hydrate, and 0.2 GTP sodium salt hydrate, with 0.25%-0.5% biocytin and in some cases 10 QX-314. All iterations were adjusted to 280-290 mOsm and pH 7.3. Solution one was used for recordings of optically or electrically generated IPSCs in ChR2xSST, ChR2-PV, and Arch-SST tissue; QX-314 was utilized in some cases to address action potential contamination of synaptic current readouts. Solution two was used for recordings of current evoked action potential trains in FS neurons in ChR2-SST and Arch-SST tissue as well as LED evoked hyperpolarization events and spike suppression in Arch-SST tissue. Solution three was used for recordings of electrically generated IPSCs in Arch-SST tissue; QX-314 was utilized in all cases to address action potential contamination of synaptic current readouts.

Access resistance (Ra) was measured for each cell prior to recording and periodically checked throughout experimentation. If Ra was observed to increase more than 20% during experimentation, recordings were terminated. Cells with Ra values ≥ 25 MΩ were omitted from analysis. During recordings, patched cells were passively filled with biocytin to enable post-hoc confirmation of cell type via staining of biocytin-filled cells with fluorescein-conjugated streptavidin (10 μg/mL). To perform post-hoc staining, slices were stored in 4% paraformaldehyde for 24 hours following experimentation, and PBS thereafter until staining.

Experiments involving selective activation of SST or PV interneurons were performed by passing blue-range LED (460 nm) through a 60× objective. LED was either applied directly over the patched cell or from measured distances from the patched cell. LED strength was controlled via the X-Cite system and Lumen Dynamics software (20%, producing 1.5 mW continuously, Excelitas Technologies, Waltham, MA). A stimulus duration series was generated by applying LED at durations ranging from 0.1 to 2 ms, in 11 increments. The series was presented three times; therefore, measurements were made from averages of three stimulus presentations.

Experiments to characterize passive membrane properties and action potential firing patterns were performed by injecting a series of 400 ms current steps from a held potential of -60 mV (current steps ranged from -200 to 380 pA in 20 pA increments). Reported rheobase, time to first action potential at rheobase, as well as additional characteristics of the fired action potentials were determined from these recordings. Plots of voltage versus injected current were generated per cell to determine input resistance (slope of fitted line, mV/pA) and resting membrane potential (y-intercept of fitted line).

Experiments involving electrical stimulation of local field were performed by placement of a stimulating electrode 100-200 μm lateral to the patched cell, within layer V. Threshold was determined as the current amplitude at a duration of 0.02 ms required to elicit a response in the patched cell 50% of the time. An duration series was generated by applying electrical stimuli at durations ranging from 0.02 ms (half-threshold) to 0.32 ms, in 5 increments. The series was presented three times; therefore, measurements were made from averages of three stimulus presentations.

All recordings were made with a Multiclamp 700B amplifier (Molecular Devices, San Jose, CA) and digitized with data acquisition instrument Digidata 1440 (Molecular Devices) at 20 kHz with pClamp software (Molecular Devices).

Statistical Analysis

Analyses were primarily performed via home written programs (Visual Basic in Excel; Microsoft Corporation, Redmond, WA), Clampfit (Molecular Devices), SPSS Statistics (IBM, Armonk, NY), and GraphPad Prism (GraphPad Software Inc., San Diego, CA). Data are reported as mean ± standard error of the mean (SEM). To test for differences between control, PMR, and distant groups across experimental paradigms, t-tests or repeated-measure analysis of variance (ANOVA) with post-hoc Bonferroni corrections for multiple comparisons when equal variance was assumed, or Welch corrections and post-hoc Dunnett's T3 multiple comparisons test when unequal variances were found. Results with $P < 0.05$ were considered significant.

3.3 Results

Whole-cell recordings from three cell types were performed in layer V of somatosensory cortex in *ex vivo* brain slices. In Arch-SST or ChR2-PV tissue, SST and PV+ neurons

respectively were identified by fluorescence of Arch-YFP or ChR2-GFP reporter. All pyramidal

neurons were identified via presence of apical dendrite under IR-DIC optics and confirmed to be

non-fluorescent prior to recording. The utilized animal cohort comprised P12 - 21 control and

lesioned SST-ChR2, SST-Arch, PV-ChR2 transgenic female and male mice. Effectiveness or

ineffectiveness of utilizing Arch-SST and ChR2-PV tissue to investigate cell circuitry at this age

group will be interspersed throughout.

3.3.1 Intrinsic membrane properties of fast-spiking neurons are identical between groups, apart

from action potential frequency which is significantly different between groups, and first and

second spike half-width amplitudes, which are higher in PMR.

SST+ neurons, have multiple post synaptic partners, so an important step to the continued

dissection of altered SST+ neuron circuit function in freeze lesioned cortex is to evaluate them

all. After pyramidal neurons, PV+, FS neurons are the next candidate in terms of population

density, so assessments of whether layer V PV+ neurons differ between control, PMR, and

distant groups were performed. Previous work has indicated through multiple methodologies that

PV FS cell function may be altered within PMR (George and Jacobs 2011, Jin et al. 2014). In an

effort to elucidate any alterations that may be occurring to FS cells within PMR it important to

begin with an assessment of their intrinsic membrane properties.

This figure shows only preliminary data. That collected so far yields results that indicate

no differences between resting membrane potential of cells from the two groups (mean values:

Control -62.8±2.4 mV, PMR -66±1 mV, *Figure 3.2C*), nor input resistance (mean values:

Control 184 MΩ, PMR 182 MΩ, *Fig 3.2D*). While these measurements regrettably do not

include any cells from the "distant" cohort all other included measurements do. Results indicate

there to be no differences in rheobase (mean values: Control 39.4±4.4 pA, PMR 24.4±2.4 pA, *P* = .01, *Figure 3.2E*), spike amplitude, half width, max rise and decay rates, decay tau, and AHP amplitude (*Table 3.1*). Differences were observed among the first and second spike half width amplitudes. Mean values are as follows: first spike half width amplitude (Control 39.7±1.4 pA, PMR 44.5±1.2, Distant 41.8±1.7 pA, one-way ANOVA *P* = .034, Dunnett's multiple comparisons test Control vs. PMR *P* = .04) and second spike half width amplitude (Control 39.2±1.3 pA, PMR 44.2±1.1, Distant 41.4±1.6 pA one-way ANOVA p = 0.015, Dunnett's multiple comparisons test Control vs. PMR *P* = .02).

3.3.2 Output from SST+ neurons to fast spiking neurons is statistically identical between PMR and controls. SST+ neuron-mediated disinhibition does not occur within PMR.

To ascertain whether SST+ neuron output to layer V PV+ neurons is enhanced as it is onto layer V pyramidal neurons, IPSCs were recorded from layer V pyramidal neurons in ChR2-SST tissue as evoked by two conditions. Condition 1 yielded IPSCs evoked by a series of 5 increasing durations of threshold electrical stimulus applied 100-200 um lateral and within layer to the patched cell. Condition 2 added a simultaneous LED component (to stimulate SST+ neurons) which was applied from the same lateral site as the electrical stimulus. Several iterations of these conditions were attempted, as summarized in *Table 3.2.*

As the electrically evoked IPSC recorded from layer V pyramidal neurons comprises total GABA$_A$ input, of which SST+ and PV+ interneurons dominate, adding SST+ neuron activating LED during electrical stimulation would theoretically cause a reduction in the observed IPSC peak amplitude if they exhibited enhanced output onto PV+ neurons within PMR; an elegant demonstration of microcircuit disinhibition. Comparing percent change of condition 2 to

condition 1 would provide us with a robust means to determine the answer to this question, however, condition 2 yielded tremendous increases in IPSC peak amplitude in both control and PMR groups in all experiment iterations (*Figure 3.3C; Figure 3.3.2a C, Figure 3.3.3a C*). As such, the percent changes between peaks evoked at condition 1 versus condition 2 were equivalent at all electrical stimulus durations tested (Iteration #1: *Figure 3.3D* no effect of group $P = .83$; Iteration #2: *Figure 3.3.2b* no effect of group $P = .35$, Iteration #3: *Figure 3.3.3b* no effect of group $P = .52$).

With the knowledge that significant differences arise between control and PMR pyramidal neuron IPSC peak amplitudes with 0.5 ms durations of LED application (Ekanem et al. 2019), it is possible that a combination of the electrical stimulus with an LED duration different from the 20 ms used in these studies would have been optimal. Nevertheless, with shortened LED durations at a lower wattage, it could theoretically be possible to ascertain whether microcircuit disinhibition is occurring within traces.

A more direct assessment to the same ends was performed comprising whole cell patch clamp recordings of inhibitory post synaptic currents (IPSCs) in layer V FS neurons within PMR and homotopic control cortex. Currents were evoked by SST-ChR2 activating application of a series of 11 increasing durations of LED (*Figure 3.4A*). We discerned that layer V FS IPSC peak amplitudes recorded in PMR were equivalent to controls ($P = .59$, *Figure 3.4B*). Recorded IPSCs in both groups exhibited similar ranges as illustrated by the plotted current peak amplitudes recorded with 2ms LED application (mean values: Control -122.5 ± 0.58, PMR -136.8 ± 0.62, $P = .76$, *Figure 3.4C*). A power analysis was performed with these means to confirm the validity of these results; calculations indicate sample sizes of 5 cells per group to be sufficient for a power of 0.80. The following formulas were utilized for calculation wherein n_1 is equivalent to the

sample size required in each group, Z refers to the confidence interval (95%), σ refers to pooled standard deviation, ES refers to effect size, and μ refers to the utilized means (Brant (web resource), Glen (web resource), Sullivan (web resource)).

$$n_i = 2\left(\frac{Z\sigma}{ES}\right)^2$$

$$ES = \frac{|\mu_1 - \mu_2|}{\sigma}$$

$$\sigma = \sqrt{\frac{SD_1^2 + SD_2^2}{2}}$$

These results are in part consistent with previous findings that indicate IPSC input to be diminished onto PV+ neurons within PMR (Jin et al. 2014). Finally, the possibility that SST+ neuron to FS output may not be altered at sites distant to the microgyrus is not ruled out by this outcome; this information is needed in order to fully understand the relationship between SST+ neurons to PV+ neurons. An elaboration on this study could be to assess this metric within layer IV since SST+ neurons therein primarily target same layer PV-FS neurons (Xu et al. 2013).

3.3.3 Unsuccessful experimentation: using Archaerhodopsin3-SST tissue to study SST+ neuron function

Reported in *section 2.3.4*, GABA$_A$ input to layer V pyramidal cells is greater within PMR than in control cortex. As SST+ neurons are not the only source of inhibitory afference to the network, it is critical to determine whether this effect is mediated by SST+ neurons, other GABAergic subtypes, or is multifactorial in nature. Archaerhodopsin-3 (Arch)-Cre transgenic mice provided us with the opportunity to functionally silence a neuronal subtype of our choice.

Expressing Arch, a light activated proton extrusion pump in SST+ neurons provides the means to interrogate contribution from other GABAergic cell types to layer V pyramidal neurons without the overshadowing influence of SST+ neurons. SST-Arch cells were identified by fluorescence of GFP reporter.

Assessments of Arch functionality revealed that this opsin has some rather curious characteristics. Firstly, hyperpolarization is it not required for its cell silencing functionality. It is instead dependent on the alkalization of presynaptic boutons which thereby prevents vesicular release (El-Gaby et al. 2016). Despite that, measuring LED-evoked hyperpolarizing current importantly enables the confirmation of Arch insertion into SST+ neurons, which we were able to demonstrate (*Figure 3.5A*). SST+ neurons, many of which express T-type calcium channels, fire rebound action potentials upon relief of hyperpolarization. Consistent with that, some SST-Arch neurons would fire these rebound spikes following removal of Arch-activating LED (4 out of 11 evaluated cells fired rebound spikes, traces from one no rebound cell and one rebound cell shown, *Figure 3.5A)*. As expected (Weiss and Zamponi 2019), there seemed to be a relationship between the magnitude of Arch-mediated hyperpolarization and occurrence of rebound spikes as the cells which exhibited rebound demonstrated hyperpolarizing currents greater than or equal to 30 mV (not shown). This could possibly be an artifact of differing ratios of Arch pump per unit membrane due to variably sized cells. Nevertheless, and despite rebound not occurring in every SST-Arch neuron, this spiking behavior can elicit appreciable responses in local pyramidal neurons (*Figure 3.5C*). That in addition to Arch pump function possibly leading to a gradual increase in the extracellular concentration of protons (Glock et al. 2015), Arch may just be suitable as an investigative probe into short timescale neuronal phenomena, rather than for in vivo use as these would undeniably have confounding effects on overall network function.

The effectiveness of Arch-mediated silencing of SST+ neurons was ascertained through an experimental paradigm wherein Arch activating LED of varying durations (5 to 200 ms) was applied over a cell in the middle of an injected depolarizing current step (*Figure 3.5B*). Curiously and regardless of utilized LED duration, silencing of action potentials was only possible in 50% of cells tested (3 out of 6 evaluated cells exhibited spike suppression, suppression examples with 100 and 150 ms LED shown from two SST-GFP neurons, *Figure 3.5B*). This rate of silencing is of import as it calls into question the effectiveness of utilizing Arch in our experimentation; were this rate to be reflected by the total SST-Arch population and if no effects were observed, is this because Arch is an insufficient probe, or is the effect biological? Secondly, and as indicated above, this further supports the possibility that Arch is differentially effective across neuron subtypes, whether distinguishing characteristics be cell size or other unanticipated distinction. Arch pump insertion seems to be wholly unlike that of ChR2 which is highly dense due to exceptionally low single channel conductance (Feldbauer et al. 2009). That being said, human error must be taken into account as the possibility of mistakenly patching onto a cell neighboring a fluorescently marked one remains high.

3.3.3.1 Non-SST+ neuron IPSC amplitudes are not different between control and sham, however this may be a false result due to mis-applied technique

Results from experimentation utilizing Arch-SST tissue are presently inconclusive since it is unknown whether the LED durations we used were appreciably effective (2 out of the 6 neurons screened for Arch mediated spike suppression exhibited successful silencing at LED durations below 100 ms, not shown). Identically to what was described in *section 3.3.1 e*lectrically evoked IPSCs (condition 1) and IPSCs evoked electrically with added LED

component were recorded from layer V pyramidal neurons. Condition 2 in these recordings comprised of pre-electrical LED of 5 ms then 35 ms LED respectively, to occur with electrical stimulation and following (*Figure 3.6A and B*). To isolate non-SST IPSC, currents recorded with LED component (Arch IPSC) were subtracted from total IPSC (*Figure 3.6D*). This manipulation demonstrates that there is no significant effect of group between control and PMR and that non-SST IPSCs recorded from layer V pyramidal neurons are identical between groups ($P = 0.14$, *Figure 3.6D*). Again, it is undetermined if this is due to ineffective LED durations or if this is a true result. As such, these experiments need to be redone with durations of Arch activating light equal to or exceeding 100 ms.

3.3.4 *Using Chr2-pv to study PV function at P12-P21. Failures and Successes.*

The ChR2-SST transgenic line clearly became paramount in our investigations of SST+ neuron function. Since of course SST+ neuron-mediated circuit alterations may not comprise the whole story, we looked to the ChR2-PV transgenic line to help answer some new questions regarding PV+ neuron function, however significant, project-terminating setbacks arose which I will highlight here to help inform any future attempts.

Parvalbumin expression has been reported to initiate at P12/P13 and progress from there into maturity in adult stages around P60 (del Río et al. 1994, Gonchar et al. 2007, Banerjee et al. 2016). This is an exceedingly critical factor when considering using PV as a promoter to knock in or out expression of a choice protein. In our case, wherein studies fall between P12 and P21, an age range occupying the nascent stages of PV locus initiation, using a PV-Cre line to express ChR2 is simply not ideal. Regrettably this was demonstrated after months of nearly fruitless use

of mice within this age group wherein GFP-reporter fluorescence ended up being scant to non-existent, indicating negative presence of the intended knock-in protein.

An additional confound involves layer-selective presentation of PV-Cre mediated knock in proteins. A group reported that they were unable to observe any light activation of layer V FS cells in barrel cortex of 7 'adult' PVCre-ChR2floxed animals tested (Cardin et al. 2009). This is unusual as developmental immunoreactivity assays dictate that PV expression initiates within layer V and expands to "upper and inner cortical layers" from there "at subsequent developmental stages" (del Río et al. 1994). Still since this is the case with PV-Cre animals, studies that have been successfully utilized these transgenic lines in young age cohorts conducted all experimentation within layers II/III and/or IV (Xue et al. 2014). Even so, it is of critical importance to emphasize that the group reporting a null presentation of ChR2 in layer V were utilizing adult mice, presumed to be older than P21 although the specific age range used is not reported.

3.3.4.1 Output from PV to low threshold spiking neurons is enhanced at areas distant to the microgyrus (≥ 2 mm). Control and PMR groups are identical. Preliminary indications of PV-evoked gamma oscillations.

Nevertheless, persistent attempts did yield one very exciting and paradigm shifting result! Investigations of PV+ neuron to LTS neuron connectivity within our three groups has revealed IPSC peak amplitudes, evoked by ChR2-PV activation via application of a series of 8 increasing durations of LED (*Figure 3.7A*) are significantly higher among in layer V LTS neurons distant to the microgyrus (≥2 mm, mean values at 5 ms: Control -66.68±43.43 pA, PMR -76.53±34.31 pA, Distant -326.67±122.17, $P < 0.0001$, *Figure 3.7B*). This completely flips the page on what has

been hypothesized to occur within and beyond the terminus of PMR. As per section 3.3.1, we demonstrated that microcircuit disinhibition does not occur within PMR. Instead, it occurs outside of PMR and is mediated by PV interneurons rather than the previously assumed SST+ neurons. This is extremely novel and I deeply regret that I will not be able to increase the number of n's so this can be published as soon as possible.

Figure 3.7A also introduces a curious premise for consideration. As can be seen in the single cell current examples, 5 ms LED activation of presynaptic PV+ neurons yield a multipeaked, qualitatively sustained response recorded from post-synaptic LTS neurons that is not seen at longer LED durations. These responses appear to be high frequency, and possibly in the gamma range (20-150 Hz), which is perhaps indicative of a known connectivity schematic for PV+ neurons which are known to synapse onto other PV+ neurons and onto themselves and can thusly amplify or self-induce gamma oscillations (Cardin et al. 2009, Deleuze et al. 2019). This occurs in all groups, but perhaps a future investigator may determine if PV+ neuron elicited gamma frequencies are higher in the distant population, which could be interesting particularly when considering "distant" as a non-PMR pathological substrate in DCM.

It is important to note that LED activates cell bodies and their projections, so the PV inputs responsible for this layer V phenomenon could originate or be contributed to from external layers such as layers II/III. Perhaps it would suit a future investigator to assess layer II/III PV+ neuron relationships with their layer V partners.

3.4 Discussion

These results, while preliminary, dramatically shift the original framework of thinking away from one unilaterally dominated by SST+ neuron dysfunction, to a more diversified model

of distributed GABA$_A$ dysfunction wherein PV+ neurons play a significant role. Still though, it is unknown how all of our observations pertain to epileptogenesis. Recent investigations into such have introduced to the field a modernized perspective into the nature of seizure originating regions. Detailed in *section 1.1.2*, the familiar hypersynchrony theory is challenged by a slightly more complex schematic comprising the pairing of high-frequency, high synchrony "centers" or cores with low frequency, desynchronized "surrounds". This paired system is said to feature an endogenous curb on seizure propagation through strong inhibitory projections from the core out to the penumbra. While factors priming for and inciting initiation are still unknown, it appears that once an epileptogenic state is generated, the implication is that the low frequency penumbra(s) have to be overridden in some way for propagation to commence. Due to resident neuron's unique smatterings of innumerable ion channels, it makes sense that 'propagation' is dynamic attrition warfare between excitation and inhibition.

There are some curious ways we may tie our findings into this schematic for epileptogenesis. Regarding PV interneurons, we were unable to address how their output is altered onto postsynaptic partners within PMR. Still, given the knowledge that PV FS interneurons of layer V are strongly autaptic (Deleuze et al. 2019), if factors such as lessened inhibitory input (Jin et al. 2014) onto PV+ neurons result in indiscriminately enhanced output from them onto all of their non-PV+ postsynaptic partners, then what implications would that have for the integrity of the center-surround system's endogenous restraints? This premise though is somewhat in logical contrast with demonstrations within this and another report of layer V FS neurons of PMR presenting with lower maximum firing frequencies (George and Jacobs 2011). It will be interesting to uncover the computation of lower intrinsic firing frequency occurring in conjunction with theorized output enhancement within PMR.

To link SST+ neurons into the center-surround epileptogenicity scheme, chapter 2 reports that these cells exhibit arbors that exert functional influence to lengthier within-layer ranges. Could it be that SST+ neurons recruited within one epileptogenic, high frequency core could have synapses with other spontaneously forming high frequency cores thereby silencing them and possibly making its own more prone to propagate? Still moving towards interpretation based on substantial results, we initially demonstrated that SST+ neuron function drops down to control levels beyond the terminus of PMR. While these results were evoked experimentally, results in this section indicate that PV+ neurons put forth enhanced output onto this cohort of SST+ neurons. As epileptiform activity is not easily evocable from this range, we firstly have a hint that perhaps PV neuron functional enhancement cannot underlie epileptogenicity and secondly, we have an indication that diminishment of SST+ neuron output outside of PMR may hold up *in vivo* and be mediated by action of PV+ neurons. If the wild speculation mentioned at the top of this paragraph is true (SST+ neurons assisting with the propagation of aberrant excitatory activity), then perhaps PV+ neuron-mediated silencing of them beyond the terminus of PMR underlies why epileptogenesis does not occur within this region.

To reiterate, beyond the terminus of PMR, SST+ cells may be functionally constrained within control-like domains due to PV+ neuron intervention. So, in this case, if there is any generation of high frequency core activity, PV+ neurons therein may be recruited and proceed to inhibit propagation by way of this disinhibitory mechanism. Again, this is all speculation, but how fascinating if disinhibition ends up being anti-epileptogenic in this context, when initially it was thought to be a mandate for the initiation of epileptic events (Prince 1985). The two may not be mutually exclusive; disinhibition could both promote and prevent epileptogenesis depending on the context.

There is also the preliminary demonstration of PV neuron mediated induction of gamma oscillations to take into account. This is unconfirmed, but if PV+ neurons can self-incite higher frequency gamma outside of PMR, is it somehow easily spread and morphed into widespread gamma oscillations? Previous work indicates that higher frequency gamma activity is associated with increases in selective auditory and tactile attention (Ray et al. 2008). Therefore, what effect could 'higher' ranges of gamma activity focally sequestered the 'distant' substrate, outside PMR, have on cognitive function? Could it be possible for this postulated higher band gamma activity to be more persistent outside of PMR? What effects could persistent high band gamma have on cognitive activity?

The work discussed in chapters 2 and 3, and in the above hypothetical speculations pertain to connectivity schemes within layer V, so ambiguity remains regarding the relationship between SST+ neurons and PV+ neurons in external layers. This is speculation, but perhaps it can be inferred from Chapter 2's results that strong connections from SST+ neurons in PMR persist with their most prominent and highly active within-layer post-synaptic partner. It has been demonstrated that pyramidal neurons in layer V of PMR receive a greater magnitude of excitatory inputs compared to controls, while there were no differences in the same observed onto those within layers II/III of PMR (Brill and Huguenard 2010). While we have not assessed selective SST+ neuron input onto pyramidal neurons in layers II/III as we have with those in layer V (Ekanem et al. 2019), this work suggests that there may be an activity-dependence to the observed selectivity of within-layer SST+ neuron output enhancement. Layer IV of neocortex features regular connectivity from SST+ neurons to PV+ neurons (Xu et al. 2013). If this postulated effect is activity based, enhanced outputs from SST+ neurons to PV+ neurons within layer IV becomes all the more probable as PV+ neurons therein receive a great deal of

thalamocortical input (Porter et al. 2001). This is critical to the epileptogenicity of the circuit, as layer IV PV+ neurons typically contribute enormously to the protection against propagation of aberrant excitation, such as may occur during an epileptiform discharge, through strong feed-forward inhibition onto spiny stellate and pyramidal cells therein (Sun et al. 2006). With thalamocortical inputs, such as from the ventrobasal thalamus having been demonstrated to be epileptogenic with its main cortical output (the primary somatosensory cortex, Sun et al. 2005), investigation into the nature of the layer IV connectivity patterns from presynaptic SST+ becomes critical as loss of layer IV PV functionality would clearly be epileptogenic. Additional questions such as what population of SST+ neuron dominates within layer IV remain unanswered; this could be important if the different subtypes, primarily RS or LTS, are affected differentially within PMR (discussed in *Section 2.4*). Much work has been done to ascertain the effects the microgyrus has on LTS neurons (George and Jacobs 2011), but much remains to be uncovered about their RS counterparts.

It is of note that these speculations are being made under glaring ignorance of whether these observed, experimentally evoked phenomena directly cause or are even appreciably correlated to the pathogenic aberrance in overall network function inherent to PMR, which includes epileptogenesis. That being said, interneurons have been directly implicated to be involved in the initiation and termination of seizure events in vivo. For example, in freeze lesioned mice, optogenetic activation of pan-GABAergic neurons was demonstrated to reliably stop spontaneous slow-wave sleep associated seizure events (Sun et al. 2016); though the specific roles each GABAergic subtype carries in this phenomenon was not investigated. Even in naïve mice, selective recruitment of SST+, PV+, and even VIP+ neuron subtypes initiate, maintain, or terminate *in vivo*, optogenetically induced seizures in interesting ways (Khoshkhoo

et al. 2017). It is known that these interneurons are involved, but how exactly they contribute to these pathologies is a critical component presently left unanswered. Importantly, this work, while incomplete, continues to push this puzzle towards completion.
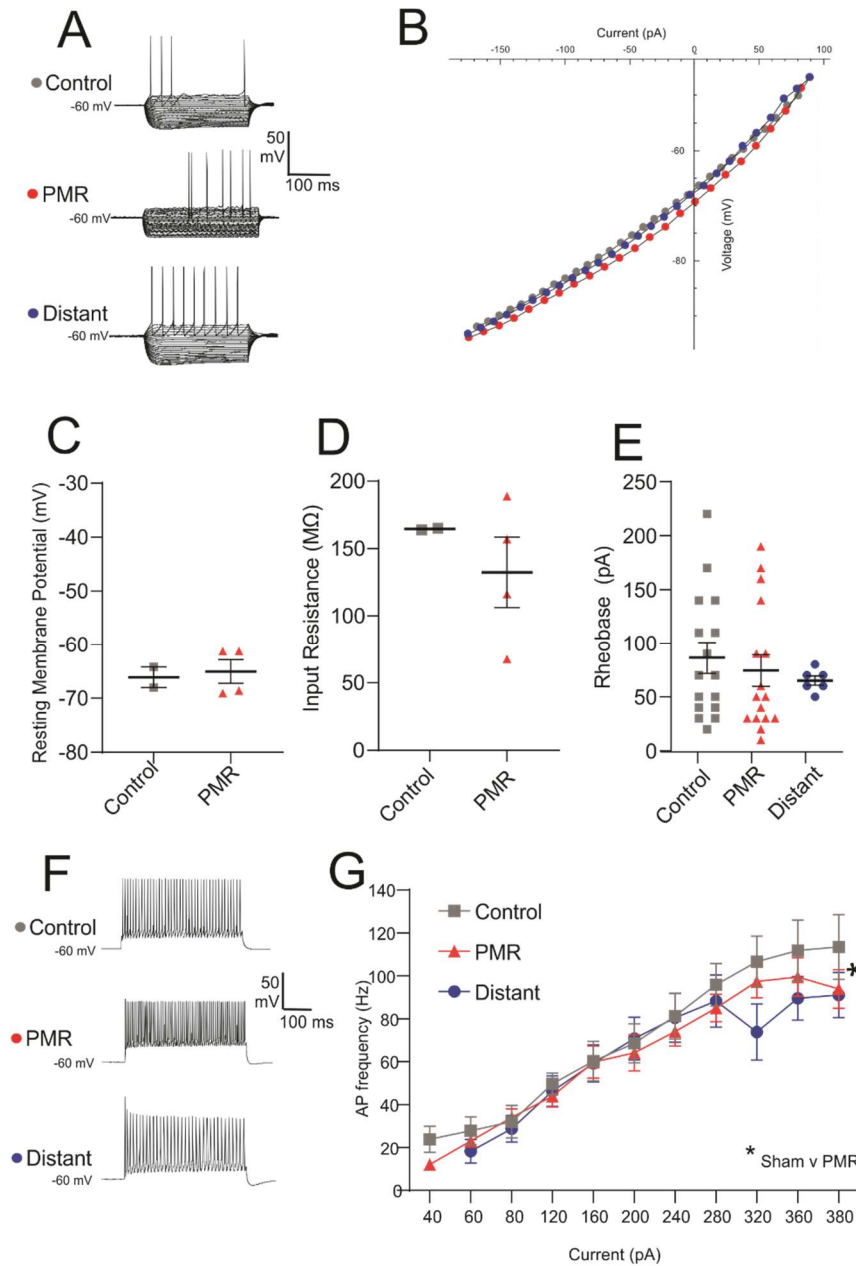
Figure 3.2: AP firing frequency of fast-spiking cells is significantly different between PMR and Sham. All remaining intrinsic properties have no differences between groups.

(A) Membrane voltage responses to current steps from -200 pA to rheobase of control, PMR, and distant representative neurons

(B) I-V plots of representative traces in (A), visualizing the two cell's membrane voltage responses to injected current steps

(C) Individual values and mean±SEM of resting membrane potential for fast spiking neurons (control n = 2, PMR n = 4, unpaired t-test, P = 0.83) Distant group was not included in statistical analysis due to insufficient n's.

(D) Individual values and mean±SEM of input resistance for pyramidal neurons (control n = 2, PMR n = 4, unpaired t-test, P = 0.37) Distant group was not included in statistical analysis due to insufficient n's.

(E) Individual values and mean±SEM of rheobase for pyramidal neurons (control n = 16, PMR n = 16, distant n = 6, one way ANOVA, P = 0.57)

(F) Membrane voltage responses to 380 pA current steps of control, PMR, and distant representative neurons

(G) Plot of action potential firing frequency as a function of injected current. There are significant differences of group between control and PMR fast spiking AP firing frequencies (control n = 16, PMR n = 14, two way ANOVA, effect of current P < 0.0001, effect of group P = 0.0483). Distant group was not included in statistical analysis due to insufficient n's, but included in graph for visualization purposes.

112

Parameter	Fast-spiking neurons Control n = 16 PMR n = 16 Distant n = 6		
Resting Membrane Potential (mV)	163.8±0.002 132.4±0.026 175.4 (no sem)	Rise to second half-amplitude time (ms)	0.277±0.015 0.317±0.011 0.299±0.016
Input Resistance (MΩ)	-65.7±1.2 -65.1±2.2 -65.9 (no sem)	Max rate of rise to first half-amplitude (mV/ms)	257.5±23.6 303.1±23.4 231.9±17
Rheobase (pA)	86.3±14.4 74.4±14.7 65±4.3	Max rate of rise to second half amplitude	244.8±24.1 293.8±23.7 218.9±12.9
Time to first spike at rheobase (ms)	130.9±33.7 127.2±26.3 41.4±15.9	First spike rise tau (ms)	9.5±7.1 29.3±20.3 2.7±0.8
Frequency at rheobase (Hz)	8.3±1.7 8±1.7 12.1±4.4	Second spike rise tau (ms)	3.7±2.5 6±4.4 6.4±4.3
Maximum firing frequency (Hz)	110±11.5 101.6±6.7 101.3±12	Decay to first half amplitude time (ms)	1.2±0.1 1.1±0.1 1.2±0.1
F/I slope (Hz/pA)	0.4±0.08 0.6±0.22 0.2±0.03	Decay to second half amplitude time (ms)	1.2±0.1 1.1±0.1 1.3±0.1
First spike amplitude (mV)	79.2±2.7 83.4±4.3 83.6±3.4	Max rate of decay to first half-amplitude (mV/ms)	-117.1±16.2 -139.2±16.6 -96.9±8.4
Second spike amplitude (mV)	78.4±2.4 82.9±4.3 82.9±3.1	Max rate of decay to second half amplitude (mV/ms)	-112.2±16.8 -135.6±17.3 -94±8.5
First spike halfwidth (ms)	0.9±0.1 0.8±0.1 0.9±0.1	First spike decay tau (ms)	0.7±0.1 0.6±0.1 0.7±0.1
Second spike halfwidth (ms)	0.9±0.1 0.8±0.1 1±0.1	Second spike decay tau (ms)	0.7±0.1 0.6±0.1 0.8±0.1
First spike half-width amplitude (mV)	39.7±1.4 * $p = 0.04$ 44.5±1.2 41.8±1.7	First AHP amplitude (mV)	4.8±2.3 3.7±1.5 1.2±0.4
Second spike half-width amplitude (mV)	39.2±1.3 * $p = 0.02$ 44.2±1.3 41.4±1.6	Second AHP amplitude (mV)	5.5±2.3 4±1.4 1.4±0.5
Rise to first half-amplitude time (ms)	0.279±0.019 0.320±0.006 0.29±0.014		

Iteration	Condition 1 "E"	Condition 2 "EL" and/or "LEL"
1. "High Cl" K Gluc-based internal solution (Ecl = -15) IPSCs at holding = -70 mV APV and DNQX in bath to block EPSCs	Series of 5 or 6 increasing durations 0.02-0.32/0.64 ms of threshold electrical stimulation	EL = Simultaneous Electrical stim series + 20 ms LED and/or LEL = Pre-Electrical 20 ms LED followed by simultaneous Electrical stim series + 20 ms LED
2. "Regular" K Gluc-based internal solution (Ecl = -15) EPSCs at holding = -70 mV IPSCs at holding = +10 mV no APV and DNQX in bath		
3. Cs Gluc-based internal solution (Ecl = -50) IPSCs at holding = +10 mV APV and DNQX in bath to block EPSCs		

Table 3.2: Three iterations of the same experiments aimed to attempt demonstrations of SST neuron mediated disinhibition.
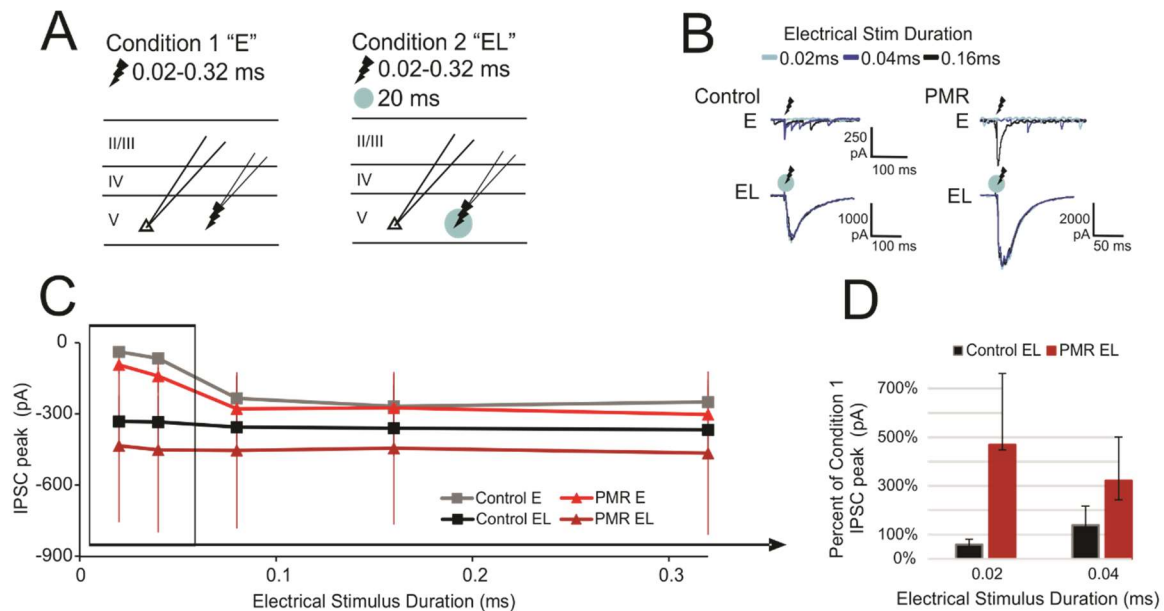
Figure 3.3.1: Table 3.2 Iteration #1: Output from SST neurons to layer V fast spiking neurons is not different between controls and PMR.

(A) This experiment comprised the comparison of two experimental paradigms. Condition 1 involved recording eIPSCs from a layer V pyramidal neuron, evoked by electrical stimulation in a series of 5 increasing durations, 100-200 um lateral to the cell and within the same layer. Condition 2 involved simultaneous electrical stimulation and 20 ms LED activation of SST neurons. Both stimuli were applied at the same location (100-200 um) lateral to patched pyramidal neuron.

(B) Single cell representative examples of IPSC responses recorded from layer V pyramidal neurons in control and PMR conditions 1 and 2.

(C) Mean±SEM IPSC peak amplitudes of 10 control and 10 PMR layer V pyramidal neurons neurons (2-way repeated measures ANOVA, no effect of group $p = 0.08$, no effect of stimulus duration p = 0.83)

(D) Example of intended method of comparison between the two conditions. Percent of condition 1 was determined for condition 2 between groups (2ms LED duration) (2-way repeated measures ANOVA, no effect of group, $p = .16$, no effect of stimulus duration p = 0.78).
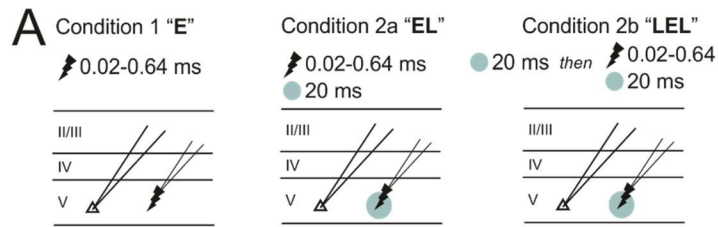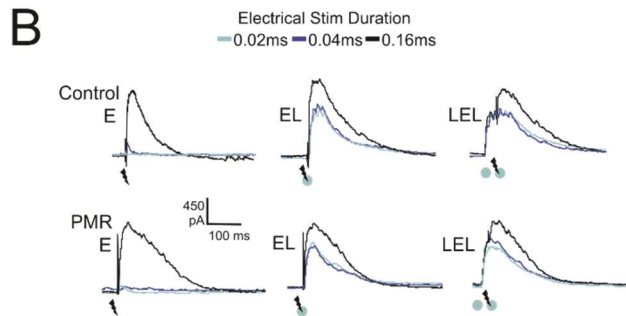
A Condition 1 "**E**"   Condition 2a "**EL**"   Condition 2b "**LEL**"

Figure 3.3.2a: Table 3.2 Iteration #2: Output from SST neurons to layer V fast spiking neurons is not different between controls and PMR.

(A) This experiment comprised the comparison of three experimental paradigms. Condition 1 involved recording eIPSCs from a layer V pyramidal neuron, evoked by electrical stimulation in a series of 6 increasing durations, 100-200 um lateral to the cell and within the same layer. Condition 2a EL involved simultaneous electrical stimulation and 20 ms LED activation of SST neurons. Condition 2b LEL involved pre-application of 20ms LED followed by simultaneous electrical stimulation and 20 ms LED activation of SST neurons. Both stimuli were applied at the same location (100-200 um) lateral to patched pyramidal neuron.

(B) Single cell representative examples of IPSC responses recorded from layer V pyramidal neurons in control and PMR conditions 1, 2a, and 2b.
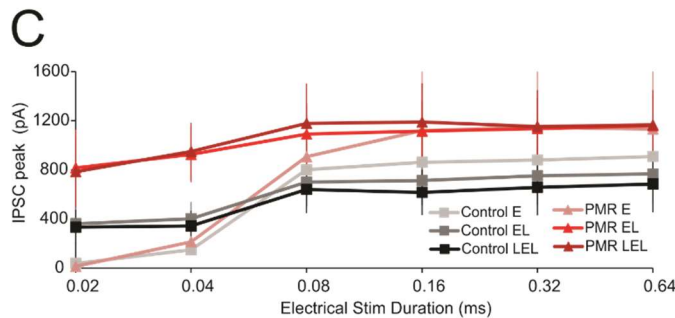
(C) Mean±SEM IPSC peak amplitudes of 4 control and 4 PMR layer V pyramidal neurons neurons (2-way repeated measures ANOVA, there is an effect of group $p < 0.0001$, there is an effect of stimulus duration $p < 0.0001$; specifically between the E and EL/LEL conditions.

116

Figure 3.3.2b Example of intended method of comparison between the two conditions. Percent of condition 1 was determined for conditions 2a and 2b between groups (2ms LED duration) (2-way repeated measures ANOVA, there is no effect of group, $p = 0.35$, there is an effect of stimulus duration $p = 0.01$).

A Condition 1 "E"
⚡ 0.02-0.64 ms

Condition 2 "EL"
⚡ 0.02-0.64 ms
🔵 20 ms

B Electrical Stim Duration
— 0.02ms — 0.04ms — 0.16ms

Control
E

PMR
E

300 pA / 50 ms

500 pA / 100 ms

EL

EL

C

IPSC peak (pA)

Control E   PMR E
Control EL   PMR EL

Electrical Stim Duration (ms)

Figure 3.3.3a: Table 3.2 Iteration #3: Output from SST neurons to layer V fast spiking neurons is not different between controls and PMR.

(A) This experiment comprised the comparison of two experimental paradigms. Condition 1 involved recording eIPSCs from a layer V pyramidal neuron, evoked by electrical stimulation in a series of 6 increasing durations, 100-200 um lateral to the cell and within the same layer. Condition 2 involved simultaneous electrical stimulation and 20 ms LED activation of SST neurons. Both stimuli were applied at the same location (100-200 um) lateral to patched pyramidal neuron.

(B) Single cell representative examples of IPSC responses recorded from layer V pyramidal neurons in control and PMR conditions 1 and 2.

(C) Mean±SEM IPSC peak amplitudes of 3 control and 4 PMR layer V pyramidal neurons neurons (2-way repeated measures ANOVA, there is an effect of group $p = 0.04$, and there is an effect of stimulus duration $p = 0.03$)
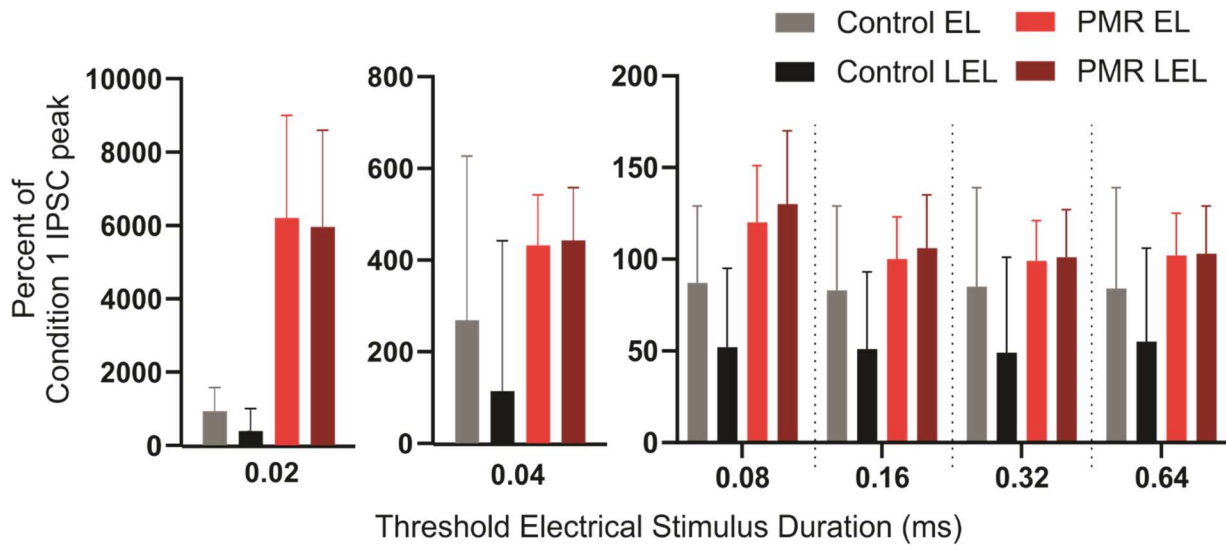
118
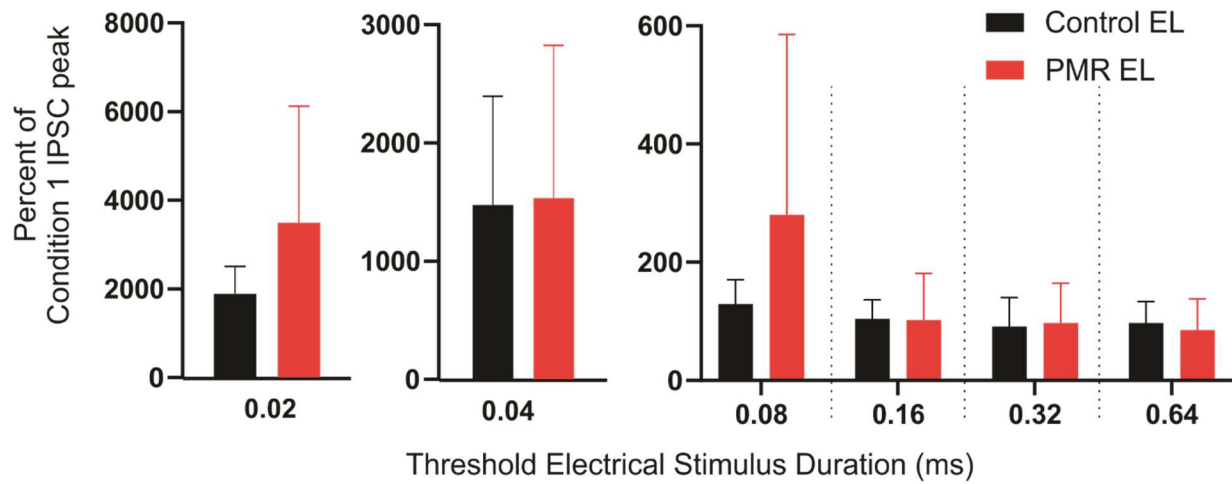
Figure 3.3.3b Example of intended method of comparison between the two conditions. Percent of condition 1 was determined for condition 2 between groups (2ms LED duration) (2-way repeated measures ANOVA, there is no effect of group, $p = 0.52$, there is an effect of stimulus duration $p = 0.01$).
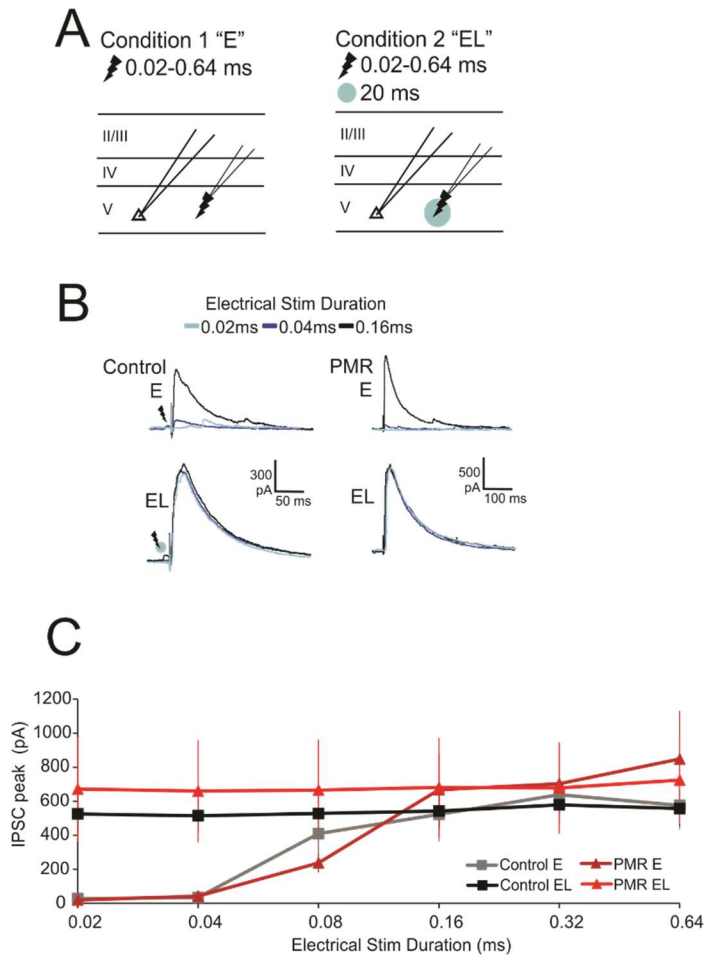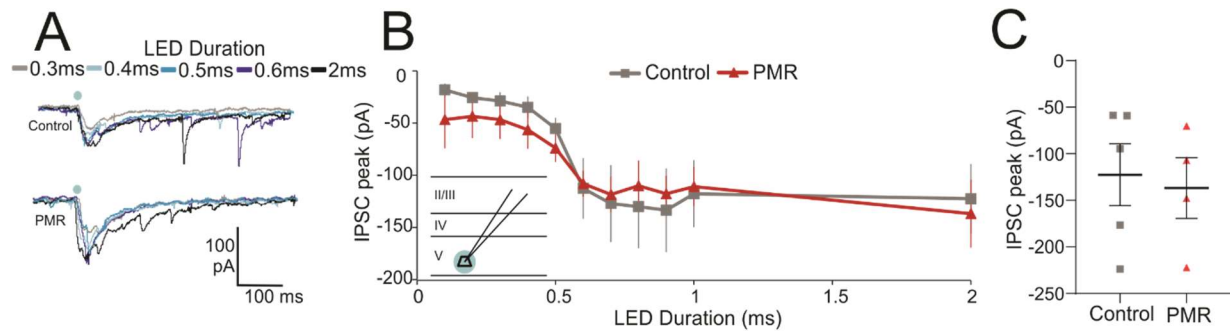
Figure 3.4: Output from SST neurons to layer V fast spiking neurons is not different between controls and PMR.

(A) Single cell representative examples of IPSC responses recorded from layer V fast-spiking neurons in control and PMR. SST-ChR2 activating LED was applied over the patched cell as per the graphic inset in **B**

(B) Mean±SEM IPSC peak amplitudes of 5 control and 4 PMR fast-spiking neurons (2-way repeated measures ANOVA, no effect of group, $p = 0.59$)

(C) IPSC peak amplitudes from control and PMR fast spiking neurons to illustrate range of responses (2ms LED duration) unpaired Student's t-test, $p = 0.76$).

Figure 3.5: Insertion of Archaerhodopsin into SST neurons enables selective silencing of this interneuron subgroup.

(A) Single cell representative examples of hyperpolarizing current evoked by application of 565nm LED over patched layer V fluorescing SST-Arch neurons. 100 and 150 ms durations shown. Not every cell that expresses Arch is able to hyperpolarize far away from the holding level to elicit rebound. This could be indicative of varying ratios of Arch channels to total membrane due to differently sized cells.
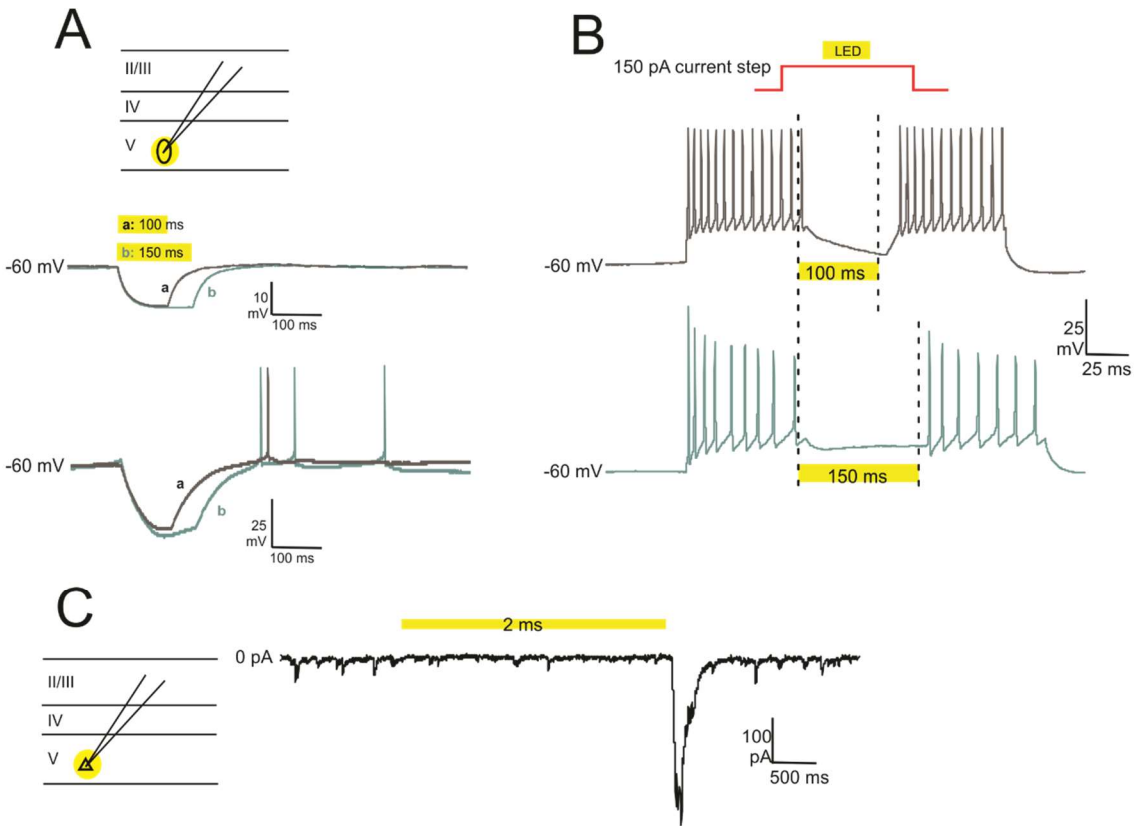
(B) Single cell representative examples of Arch-activation mediated cessation of ongoing action potentials. Patched fluorescing SST-Arch cells were injected with 150 pA of current for 300 ms (top) and 450 ms (bottom). In the middle of each period, LED was continuously exposed for either 100 ms (top) and 150 ms (bottom). Despite continuous injection of depolarizing current, LED application was sufficient to temporarily terminate action potentials with spikes returning upon removal of LED. Effective silencing of action potentials only occurred in 50% of cells tested adding further credence to the possibility that some cells have insufficient insertion of Arch into their membranes.

(C) When recording from a pyramidal neuron, applying 565 nm LED over the patched cell will evoke a large current upon removal of LED stimulus. This indicates that SST neuron rebound is sufficient to stimulate post-synaptic neurons.
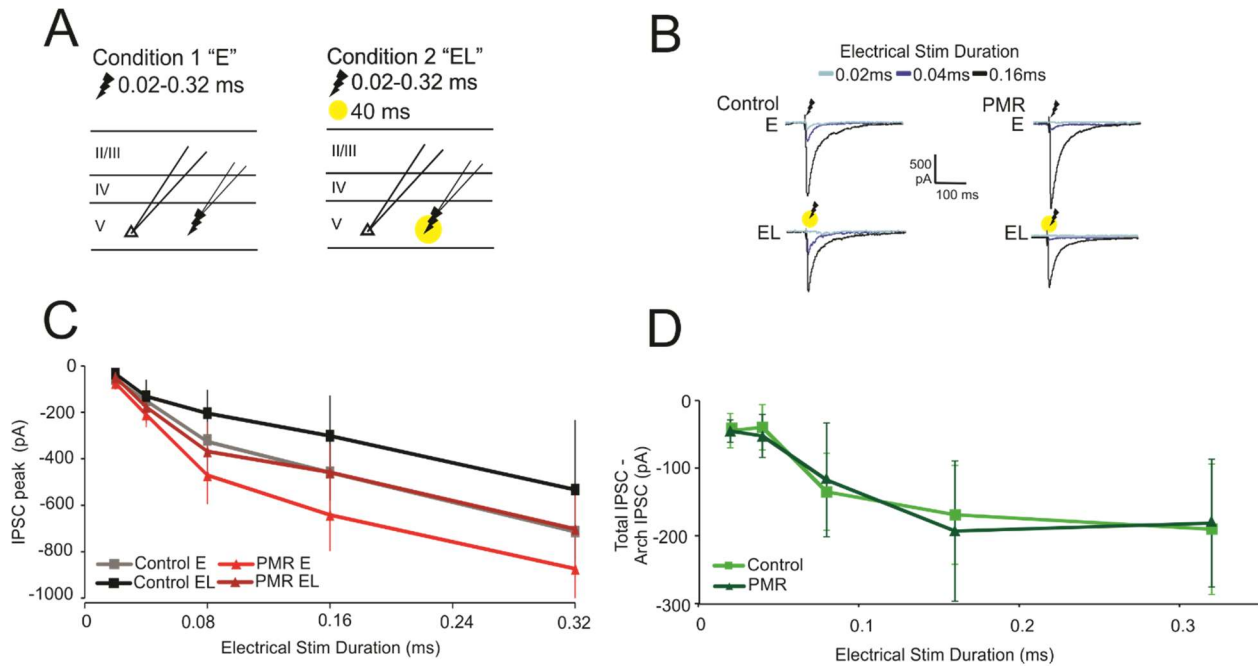
Figure 3.6: IPSC remaining after silencing SST component is not different between control and PMR. SST neurons contribute the same magnitude of inhibition to total GABAergic neurotransmission. Or are these data flawed due to the experimental design?

(A) This experiment comprised the comparison of two experimental paradigms. Condition 1 involved recording eIPSCs from a layer V pyramidal neuron, evoked by electrical stimulation in a series of 5 increasing durations, 100-200 um lateral to the cell and within the same layer. Condition 2 involved simultaneous electrical stimulation and 40 ms LED silencing of SST neurons (5 ms pre, 35 ms post electrical). Both stimuli were applied at the same location (100-200 um) lateral to patched pyramidal neuron.

(B) Single cell representative examples of IPSC responses recorded from layer V pyramidal neurons in control and PMR conditions 1 and 2.

(C) Mean±SEM IPSC peak amplitudes of 4 control and 8 PMR layer V pyramidal neurons neurons (2-way repeated measures ANOVA, no effect of group $p = 0.14$)

(D) Example of intended method of comparison between the two conditions. Arch-SST IPSC was subtracted from total IPSC to yield non-SST IPSC peak amplitudes between control and PMR (2-way repeated measures ANOVA, no effect of group, $p > 0.999$, no effect of stimulus duration $p > 0.999$).
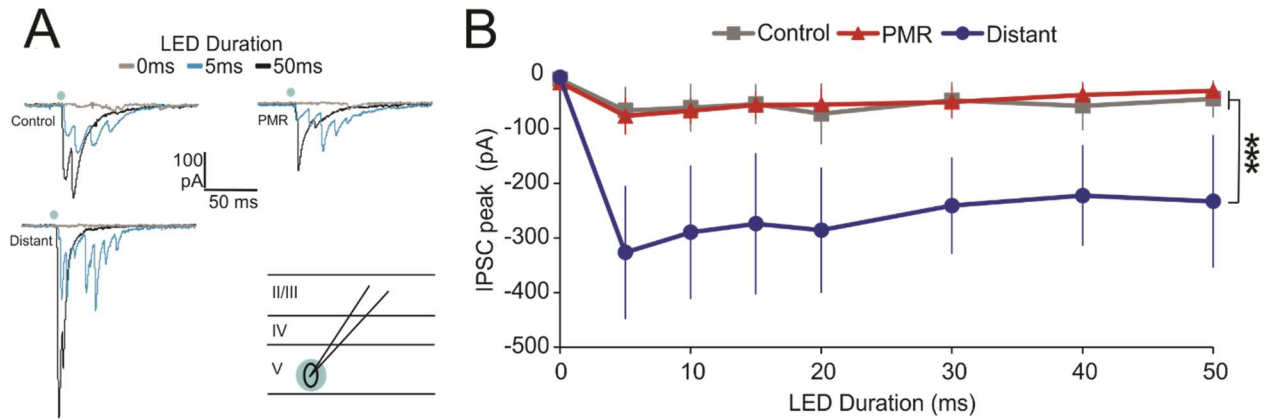
Figure 3.7: Output from PV neurons to layer V low-threshold spiking neurons is significantly higher in distant populations compared to both control and PMR.

(A) Single cell representative examples of IPSC responses recorded from layer V fast-spiking neurons in control and PMR. SST-PV activating LED was applied over the patched cell as per the graphic inset. Note distinctly multi-peaked current traces at 5 ms LED duration.

(B) Mean±SEM IPSC peak amplitudes of 2 control, 3 PMR, and 3 distant low threshold spiking neurons (2-way repeated measures ANOVA, significant effect of group, $p < .0001$)

"… 'You', your joys and sorrows, your memories and ambitions, your sense of personal identity and free will are, in fact, no more than the behaviour of a vast assembly of nerve cells…[I]t seems to me that this is not so astonishing a statement for a scientist to make. Isn't this what reductionist science has always believed?"

Francis Crick, Ph.D.

Chapter 4:

***Summary and Supplemental Discussion: Convergent evolution of fragility. Ramblings on the
selective, developmental vulnerability of interneuron subtypes.***

Figure 4.1 Summary of novel findings

      I have run out of time and cannot fully expound on this topic per my lofty intentions.

Still, I will close out this document with a summary of findings and list a few considerations I've

been quietly keeping to myself during my time in this graduate program.

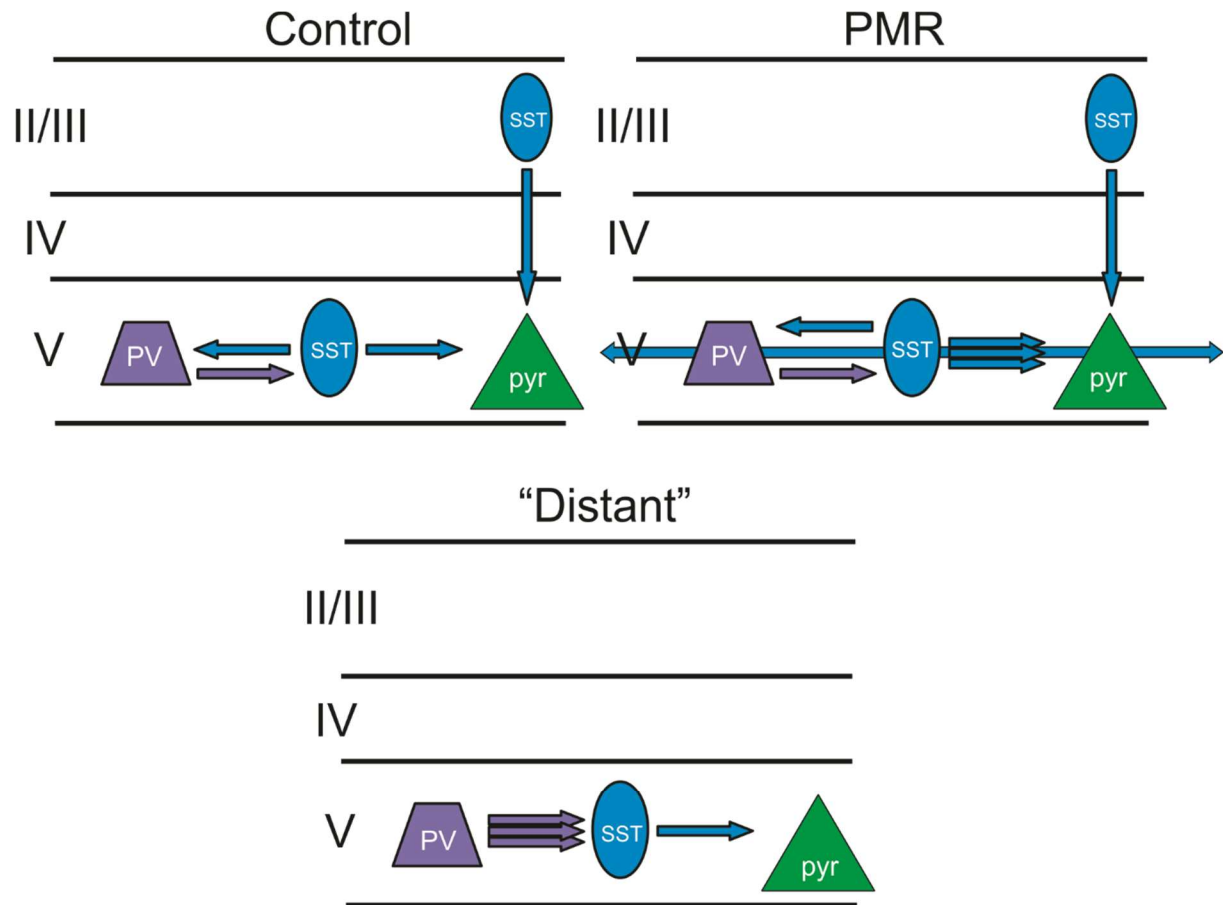I consider myself quite lucky to have been able to uncover a potentially pathological novel circuit paradigm in and outside of epileptogenic PMR. Discoveries are as follows: in PMR, layer V SST+ neuron arbors spread to further within-layer distances. Extended arbors include axons that exhibit enhanced output onto distant same-layer pyramidal neurons. SST+ neurons exhibit control levels of output onto a second post-synaptic partner, FS PV+ neurons. From PV+ neurons, SST+ cells receive control level inputs.

Outside of PMR, "distant" to the microgyrus, SST+ neurons exhibit control levels of output onto same layer pyramidal neurons. From PV+ neurons, SST+ neurons receive enhanced inputs; a novel disinhibitory relationship in a region previously assumed to function identically to controls.

How epilepsy, cognitive dysfunction, and etc. emerge from these circumstances remains unknown, however it seems clear that SST+ and PV+ cells seem to demonstrate a particular vulnerability in this developmental disorder. Is there an evolutionary tradeoff between fine-scale electrical specialization and fragility under duress?

GABAergic neurons, compared to say pyramidal neurons, seem to each independently exhibit a particular fragility, or vulnerability to change in the context of developmental disorders. It never quite made sense to me until I learned to patch clamp and became familiarized with these different cell types in a more 'hands on' way. Though the phrase 'hands on' is comically inaccurate considering the range of manipulation an electrophysiologist has falls strictly within the several picometer width opening of a glass capillary pipette. Nevertheless, interacting with these neurons sparked curiosity into the surface area to membrane protein ratios (receptor, ion channel, transport pump, etc.) of these cells and how that possibly may contribute to a neuron's

propensity to 'change' under various forms of developmental duress. I vaguely recall from the didactic classes I took early on and random google searches that ion channels in a neuron's membrane typically have a density of 1 channel per square micrometer. Perhaps that is true for pyramidal neurons, but it couldn't possibly apply for all neuron types. GABAergic neurons, which tend to be smaller than pyramidal cells, require insertions of certain specialized membrane proteins, in addition to what I suppose what I could call the 'regular suite'. These additional components provide them with electrophysiological specializations such as how unique expression of Kv3.1b and Kv3.2 channels contribute to a PV+ neuron's "fast-spiking" phenotype (Du et al. 1996, Martina et al. 1998).

To sum up in the simplest step in logic that I can muster this late night, if all neurons have a standard package of protein insertions, and interneurons include added components in their relatively diminutive areas of membrane, then their ratio of membrane to protein becomes very small. Pyramidal neurons, which would have larger relative ratios do not exhibit vulnerability to the same extent as their GABAergic counterparts. So, is it safe to assume that having a higher membrane to inserted protein ratio yields a higher degree of robustness in the context of developmental injury or stress? Perhaps this is obvious, but I spent many a wander down an isolated and yellowed Sanger hallway wondering if it was ever worth bringing up. I suppose now is as good a time as any.

List of References

Acsády, L., T. J. Görcs and T. F. Freund (1996). "Different populations of vasoactive intestinal polypeptide- immunoreactive interneurons are specialized to control pyramidal cells or interneurons in the hippocampus." Journal of Neuroscience **16**(10): 1552.

Adesnik, H., W. Bruns, H. Taniguchi, J. Z. Huang and M. Scanziani (2012). "A neural circuit for spatial summation in visual cortex." Nature **490**(7419): 226.

Adesnik, H., W. Bruns, H. Taniguchi, Z. J. Huang and M. Scanziani (2012). "A neural circuit for spatial summation in visual cortex." Nature **490**(7419): 226-231.

Ak, H., B. Ay, T. Tanriverdi, G. Z. Sanus, M. Is, M. Sar, B. Oz, C. Ozkara, E. Ozyurt and M. Uzana (2007). "Expression and cellular distribution of multidrug resistance-related proteins in patients with focal cortical dysplasia." Seizure **16**(6): 493-503.

Ali, A. B. and A. M. Thomson (1998). "Facilitating pyramid to horizontal oriens- alveus interneurone inputs: dual intracellular recordings in slices of rat hippocampus." J Physiol **507**(1): 185.

Allen, K. and H. Monyer (2015). "Interneuron control of hippocampal oscillations." Curr Opin Neurobiol **31**: 81-87.

Almoguera, B., E. McGinnis, D. Abrams, L. Vazquez, A. Cederquist, P. M. Sleiman, D. Dlugos and H. Hakonarson (2019). "Drug-resistant epilepsy classified by a phenotyping algorithm associates with NTRK2." Acta Neurol Scand **140**: 8.

Angulo, M. C., A. S. Kozlov, S. Charpak and E. Audinat (2004). "Glutamate released from glial cells synchronizes neuronal activity in the hippocampus." Journal of Neuroscience **24**(31): 6920 -6927.

Araujo, D., D. B. de Araujo, O. M. Pontes-Neto, S. Escorsi-Rosset, G. N. Simao, L. Wichert-Ana, T. R. Velasco, A. C. Sakamoto, J. P. Leite and A. C. Santos (2006). "Language and motor FMRI activation in polymicrogyric cortex." Epilepsia **47**(3): 589-592.

Armbruster, M., D. Hampton, Y. Yang and C. G. Dulla (2014). "Laser-scanning astrocyte mapping reveals increased glutamate-responsive domain size and disrupted maturation of glutamate uptake following neonatal cortical freeze-lesion." Frontiers in Cellular Neuroscience **8**(277): 1-15.

Aronica, E., J. A. Gorter, G. H. Jansen, C. W. M. van Veelen, P. C. van Rijen, S. Leenstra, M. Ramkema, G. L. Scheffer, R. J. Scheper and D. Troost (2003). "Expression and cellular distribution of multidrug transporter proteins in two major causes of medically intractable epilepsy: focal cortical dysplasia and glioneuronal tumors." Neuroscience **118**(2): 417-429.

Ascoli, G. A., L. Alonso-Nanclares, S. A. Anderson, G. Barrionuevo, R. Benavides-Piccione, A. Burkhalter and e. al. (2008). "Petilla terminology: nomenclature of features of GABAergic interneurons of the cerebral cortex." Nature Reviews Neuroscience **9**(7).

Atallah, B. V., W. Bruns, M. Carandini and M. Scanziani (2012). "Parvalbumin-expressing interneurons linearly transform cortical responses to visual stimuli." Neuron **73**(1): 159-170.

Banerjee, A., R. V. Rikhye, V. Breton-Provencher, X. Tang, C. Li, K. Li, C. A. Runyan, Z. Fu, R. Jaenisch and M. Sur (2016). "Jointly reduced inhibition and excitation underlies circuit-wide changes in cortical processing in Rett syndrome." Proc Natl Acad Sci U S A **113**(46): E7287-E7296.

Banerjee, P. N., D. Filippi and W. A. Hauser (2009). "The descriptive epidemiology of epilepsy—A review." Epilepsy Research **85**(1): 31-45.

Barkovich, A. J. (2010a). "Current concepts of polymicrogyria." Neuroradiology **52**(6): 479-487.

Barkovich, A. J. (2010b). "MRI analysis of sulcation morphology in polymicrogyria." Epilepsia **51**(Supp1): 17-22.

Barkovich, A. J., R. Guerrini, R. I. Kuzniecky, G. D. Jackson and W. B. Dobyns (2012). "A Developmental and Genetic Classification for Malformations of Cortical Development: Update 2012." Brain **135**(Pt 5): 1348-1369.

Barkovich, A. J. and B. O. Kjos (1992). "Gray matter heterotopias: MR characteristics and correlation with developmental and neurologic manifestations." Radiology **182**: 493-499.

Barth, P. G. (1987). "Disorders of neuronal migration." Can J Neurol Sci **14**: 1-16.

Bartos, M., I. Vida, M. Frotscher, A. Meyer, H. Monyer and P. Jonas (2002). "Fast Synaptic Inhibition Promotes Synchronized Gamma Oscillations in Hippocampal Interneuron Networks." Proc Natl Acad Sci U S A **99**(20): 13222-13227.

Batista-Brito, R. and G. Fishell (2009). "Chapter 3 The Developmental Integration of Cortical Interneurons into a Functional Network." Curr Top Dev Biol **87**: 81-118.

Bell, G. S., A. Neligan and J. W. Sander (2014). "An unknown quantity—The worldwide prevalence of epilepsy." Epilepsia **55**(6): 958-962.

Berg, A. T. and M. M. Kelly (2006). "Defining Intractability: Comparisons Among Published Definitions." Epilepsia **47**(2): 6.

Bethmann, K., J.-M. Fritschy, C. Brandt and W. Löscher (2008). "Antiepileptic drug resistant rats differ from drug responsive rats in GABAA receptor subunit expression in a model of temporal lobe epilepsy." Neurobiol. Dis. **31**: 169-187.

Bielschowsky, M. (1916). "Uber Mikrogyrie." J Psychol Neurol **22**: 1-47.

Bladin, C. F., A. V. Alexandrov, A. Bellavance, N. Bornstein, B. Chambers, R. Cote, L. Lebrun, A. Pirisi and J. W. Norris (2000). "Seizures after stroke: a prospective multicenter study." Arch.Neurol. **57**(11): 1617-1622.

Bland, B. H., J. Konopacki and R. H. Dyck (2002). "Relationship between membrane potential oscillations and rhythmic discharges in identified hippocampal theta- related cells." J Neurophysiol **88**(6): 3046.

Blazquez-Lorca, Woodruff, Inan, Anderson, Yuste, DeFelipe and Merchan-Perez (2014). "Spatial distribution of neurons innervated by chandelier cells." Brain Struct Funct **220**(5): 2817-2834.

Blumcke, I., H. V. Vinters, D. Armstrong, E. Aronica, M. Thom and R. Spreafico (2009). "Malformations of cortical development and epilepsies: neuropathological findings with emphasis on focal cortical dysplasia." Epileptic.Disord. **11**(3): 181-193.

Boer, K., W. G. M. Spliet, P. C. van Rijen, S. Redeker, D. Troost and E. Aronica (2006). "Evidence of activated microglia in focal cortical dysplasia." Journal of Neuroimmunology **173**(1-2): 188-195.

Borggraefe, I., M. Tacke, L. Gerstl, S. Leiz, R. Coras, I. Blümcke, A. Giese, B. Ertl-Wagner, C. T. Thiel, S. Noachtar and A. Peraud (2019). "Epilepsy surgery in the first months of life: a large type IIb focal cortical dysplasia causing neonatal drug-resistant epilepsy." Epileptic.Disord. **21**(1): 122-127.

Brant, R. ((web resource)). "Inference for Means: Comparing Two Independent Samples."

Brill, J. and J. R. Huguenard (2010). "Enhanced Infragranular and Supragranular Synaptic Input onto Layer 5 Pyramidal Neurons in a Rat Model of Cortical Dysplasia." Cerebral Cortex **20**(12): 2926-2938.

Buhl, E. H., K. Halasy and P. Somogyi (1994). "Diverse sources of hippocampal unitary inhibitory postsynaptic potentials and the number of synaptic release sites." Nature **368**(6474): 823.

Buhl, E. H., G. Tamas, T. Szilagyi, C. Stricker, O. Paulsen and P. Somogyi (1997). "Effect, number and location of synapses made by single pyramidal cells onto aspiny interneurones of cat visual cortex." Journal of Physiology (Cambridge, Eng.) **500 (Pt 3)**: 689-713.

Bui, A., H. K. Kim, M. Maroso and I. Soltesz (2015). "Microcircuits in Epilepsy: Heterogeneity and Hub Cells in Network Synchronization." <u>Cold Spring Harbor Perspectives in Medicine</u> **5**(11): 13.

Butt, S. J. B., M. Fuccillo, S. Nery, S. Noctor, A. R. Kriegstein, J. G. Corbin and e. al. (2005). "The Temporal and Spatial Origins of Cortical Interneurons Predict Their Physiological Subtype." <u>Neuron</u> **48**(4): 591-604.

Buzsáki, G. and J. Chrobak (1995). "Temporal structure in spatially organized neuronal ensembles: a role for interneuronal networks." <u>Curr Opin Neurobiol</u> **5**(4): 504-510.

Callaway, J. C. and W. N. Ross (1995). "Frequency- dependent propagation of sodium action potentials in dendrites of hippocampal CA1 pyramidal neurons." <u>J Neurophysiol</u> **74**(4): 1395.

Campbell, S. L. and J. J. Hablitz (2008). "Decreased glutamate transport enhances excitability in a rat model of cortical dysplasia." <u>Neurobiol. Dis.</u> **32**(2): 254-261.

Caputi, A., A. Rozov, M. Blatow and H. Monyer (2008). "Two Calretinin- Positive GABAergic Cell Types in Layer 2/ 3 of the Mouse Neocortex Provide Different Forms of Inhibition." <u>Cereb Cortex</u> **19**(6): 1345.

Cardin, J. A., M. Carlen, K. Meletis, U. Knoblich, F. Zhang, K. Deisseroth, L. H. Tsai and C. I. Moore (2009). "Driving fast-spiking cells induces gamma rhythm and controls sensory responses." <u>Nature</u> **459**(7247): 663-667.

Cauli, B., E. Audinat, B. Lambolez, M. C. Angulo, N. Ropert, K. Tsuzuki, S. Hestrin and J. Rossier (1997). "Molecular and physiological diversity of cortical nonpyramidal cells." <u>J Neurosci</u> **17**: 3894-3906.

Cepeda, C., V. M. Andre, M. S. Levine, N. Salamon, H. Miyata, H. V. Vinters and G. W. Mathern (2006). "Epileptogenesis in pediatric cortical dysplasia: the dysmature cerebral developmental hypothesis." <u>Epilepsy Behav.</u> **9**(2): 219-235.

Chapman, C. and J. Lacaille (1999). "Intrinsic theta-frequency membrane potential oscillations in hippocampal CA1 interneurons of stratum lacunosum-moleculare." <u>J Neurophysiol</u> **81**(3): 1296-1307.

Chassoux, F., E. Landre, S. Rodrigo, F. Beuvon, B. Turak, F. Semah and B. Devaux (2008). "Intralesional recordings and epileptogenic zone in focal polymicrogyria." <u>Epilepsia</u> **49**(1): 51-64.

Chen, W., A. Tankovic, P. B. Burger, H. Kusumoto, S. F. Traynelis and H. Yuan (2017). "Functional evaluation of a de novo GRIN2A mutation identified in a patient with profound global developmental delay and refractory epilepsy." <u>Mol. Pharmacol.</u> **91**(4): 317-330.

Chen, Z. F., M. J. Brodie, D. Liew and P. Kwan (2018). "Treatment outcomes in patients with newly diagnosed epilepsy treated with established and new antiepileptic drugs: a 30-year longitudinal cohort study." JAMA Neurol. **75**: 279-286.

Cobb, S. R., E. H. Buhl, K. Halasy, O. Paulsen and P. Somogyi (1995). "Synchronization of neuronal activity in hippocampus by individual GABAergic interneurons." Nature **378**(6552): 75.

Cossart, R., M. Esclapez, J. C. Hirsch, C. Bernard and B. A. Yehezkel (1998). "GluR5 kainate receptor activation in interneurons increases tonic inhibition of pyramidal cells." Nat Neurosci **1**(6): 1243-1256.

Crome, L. (1952). "Microgyria." J Path Bact **64**: 479-495.

Dahlin, M. and S. Prast-Nielsen (2019). "The gut microbiome and epilepsy." EBioMedicine **44**: 741-746.

Dávid, C., A. Schleicher, W. Zuschratter and J. F. Staiger (2007). "The innervation of parvalbumin-containing interneurons by VIP- immunopositive interneurons in the primary somatosensory cortex of the adult rat." Eur J Neurosci **25**(8): 2329-2340.

David, Y., L. P. Cacheaux, S. Ivens, E. Lapilover, U. Heinemann, D. Kaufer and A. Friedman (2009). "Astrocytic Dysfunction in Epileptogenesis: Consequence of Altered Potassium and Glutamate Homeostasis?" Neurobiol. Dis. **29**(34): 10588-10599.

de Leon, G. A. (1972). "Observations on cerebral and cerebellar microgyria." Acta Neuropathol.(Berl) **20**: 278-287.

de Lorente, N. R. (1934). "Studies on the structure of the cerebral cortex – II. Continuation of the study of the ammonic system." Journal of Psychology **46**: 113-177.

Defazio, R. A. and J. J. Hablitz (1999). "Reduction of Zolpidem Sensitivity in a Freeze Lesion Model of Neocortical Dysgenesis." Journal of Neurophysiology **81**(1): 404-407.

Defazio, R. A. and J. J. Hablitz (2000). "Alterations in NMDA receptors in a rat model of cortical dysplasia." J Neurophysiol **83**: 315-321.

Defelipe, J. (1997). "Types of neurons, synaptic connections and chemical characteristics of cells immunoreactive for calbindin- D28K, parvalbumin and calretinin in the neocortex." J Chem Neuroanat **14**(1): 1-19.

Defelipe, J. (1999). "Chandelier cells and epilepsy." Brain **122**(10): 1807.

Defelipe, J., S. H. Hendry, T. Hashikawa, M. Molinari and E. G. Jones (1990). "A Microcolumnar Structure of Monkey Cerebral-Cortex Revealed by Immunocytochemical Studies of Double Bouquet Cell Axons." <u>Neuroscience</u> **37**(3): 655-673.

Defelipe, J., S. H. Hendry and E. G. Jones (1989). "Visualization of Chandelier Cell Axons by Parvalbumin Immunoreactivity in Monkey Cerebral Cortex." <u>Proc Natl Acad Sci U S A</u> **86**(6).

del Río, J. A., L. de Lecea, I. Ferrer and E. Soriano (1994). "The Development of Parvalbumin-Immunoreactivity in the Neocortex of the Mouse." <u>Brain Res Dev Brain Res</u> **81**(2): 247-259.

Deleuze, C., G. S. Bhumbra, A. Pazienti, J. Lourenc, C. Mailhes, A. Aguirre, M. Beato and A. Bacci (2019). "Strong preference for autaptic self-connectivity of neocortical PV interneurons facilitates their tuning to γ-oscillations." <u>PLoS Biol</u> **17**(9).

Demeulemeester, H., F. Vandesande, G. A. Orban, C. W. Heizmann and R. Pochet (1989). "Calbindin D-28K and parvalbumin immunoreactivity is confined to two separate neuronal subpopulations in the cat visual cortex, whereas partial coexistence is shown in the dorsal lateral geniculate nucleus." <u>Neuroscience Letters</u> **99**(6-11).

Devinsky, O., A. Vezzani, S. Najjar, N. C. De Lanerolle and M. A. Rogawski (2013). "Glia and epilepsy: excitability and inflammation." <u>Trends Neurosci.</u> **36**(3): 10.

Di Pasquale, E., K. D. Keegan and J. L. Noebels (1997). "Increased excitability and inward rectification in layer V cortical pyramidal neurons in the epileptic mutant mouse Stargazer." <u>J Neurophysiol</u> **77**(2): 621-631.

Di Rocco, F., S. Giannetti, P. Gaglini, C. Di Rocco and A. Granato (2002). "Dendritic architecture of corticothalamic neurons in a rat model of microgyria." <u>Childs Nerv.Syst.</u> **18**: 690-693.

Donkelaar, H. J. T. (2016). "Polymicrogyria: the common endpoint of many different aetiological processes." <u>Dev Med Child Neurol</u> **58**(1).

Dossi, E., F. Vasile and N. Rouach (2018). "Human astrocytes in the diseased brain." <u>Brain Res Bull</u> **136**: 139-156.

Douglas, R. and K. Martin (1998). "The Synaptic Organization of the Brain." <u>Oxford University Press, New York</u> **4th edition**.

Du, J., L. Zhang, M. Weiser, B. Rudy and C. J. Mcbain (1996). "Developmental expression and functional characterization of the potassium- channel subunit Kv3.1b in parvalbumin-containing interneurons of the rat hippocampus." <u>Journal of Neuroscience</u> **16**(2): 506.

Dvorak, K. and J. Feit (1977). "Migration of neuroblasts through partial necrosis of the cerebral cortex in newborn rats. Contribution to the problems of morphological development and developmental period of cerebral microgyria." Acta Neuropathol **38**: 203-212.

Dvorak, K., J. Feit and Z. Jurankova (1978). "Experimentally induced focal microgyria and status verrucosus deformis in rats. Pathogenesis and interrelation histological and autoradiographical study." Acta Neuropathol **44**: 121-129.

Eadie, M. J. and P. F. Bladin (2001). A Disease Once Sacred, A History of the Medical Understanding of Epilepsy. England, John Libbey and Co., LTD.

Ekanem, N., L. Reed, N. Weston and K. Jacobs (2019). "Enhanced responses to somatostatin interneuron activation in developmentally malformed cortex." Epilepsia Open **4**(2): 4.

El-Gaby, M., Y. Zhang, K. Wolf, C. J. Schwiening, O. Paulsen and O. A. Shipton (2016). "Archaerhodopsin Selectively and Reversibly Silences Synaptic Transmission through Altered pH." Cell Reports **16**: 2259-2268.

Ellender, T. and O. Paulsen (2010). "The many tunes of perisomatic targeting interneurons in the hippocampal network." Front Neural Circuits **4**.

Eriksson, K. J. and M. J. Koivikko (1997). "Prevalence, classification, and severity of epilepsy and epileptic syndromes in children." Epilepsia **38**(12): 1275-1282.

Eriksson, S. H., M. Thom, J. Heffernan, W. R. Lin, B. N. Harding, M. V. Squier and S. M. Sisodiya (2001). "Persistent reelin-expressing Cajal-Retzius cells in polymicrogyria." Brain **124**: 1350-1361.

Falco-Waltera, J. J., I. E. Scheffer and R. S. Fishera (2018). "The new definition and classification of seizures and epilepsy." Epilepsy Research **139**: 73-79.

Fanselow, E. E., K. A. Richardson and B. W. Connors (2008). "Selective, state- dependent activation of somatostatin- expressing inhibitory interneurons in mouse neocortex." J Neurophysiol **100**(5): 2640.

Farghaly, W. M. A., H. N. El-Tallawy, T. A. Rageh, E. M. Mohamed, N. A. Metwally, G. A. Shehata, R. Badry and M. A. Abd-Elhamed (2013). "Epidemiology of uncontrolled epilepsy in the Al-kharga district, new valley, Egypt." Seizure **22**: 611-616.

Fasulo, L., S. Saucedo, L. Caceres, S. Solis and R. Caraballo (2012). "Migrating Focal Seizures During Infancy: A Case Report and Pathologic Study." Pediatric Neurology **46**(3): 182-184.

Feldbauer, K., D. Zimmermann, V. Pintschovius, J. Spitz, C. Bamann and E. Bamberg (2009). "Channelrhodopsin-2 Is a Leaky Proton Pump." Proc Natl Acad Sci U S A **106**(30): 12317-12322.

Fellin, T., O. Pascual, S. Gobbo, T. Pozzan, P. G. Haydon and G. Carmignoto (2004). "Neuronal synchrony mediated by astrocytic glutamate through activation of extrasynaptic NMDA receptors." Neuron **43**(5): 729-743.

Fiest, M. K. S., M.K. , B. S. Wiebe, L. S. Patten, L. C. Kwon, L. J. Dykeman, L. T. Pringsheim, L. Lorenzetti and L. N. Jetté (2017). "Prevalence and incidence of epilepsy: A systematic review and meta-analysis of international studies." Neurology **88**(3): 296-303.

Fishell, G. and B. Rudy (2011). "Mechanisms of Inhibition within the Telencephalon: " Where the Wild Things Are." Annual Review of Neuroscience **34**: 535-567.

Fisher, R. S., C. Acevedo, A. Arzimanoglou, A. Bogacz, J. H. Cross, C. E. Elger, J. Engel, L. Forsgren, J. A. French, M. Glynn, D. C. Hesdorffer, B. I. Lee, G. W. Mathern, S. L. Moshé, E. Perucca, I. E. Scheffer, T. Tomson, M. Watanabe and S. Wiebe (2014). "ILAE Official Report: A practical clinical definition of epilepsy." Epilepsia **55**(4): 475-482.

Fitsiori, A., S. B. Hiremath, J. Boto, V. Garibotto and M. I. Vargas (2019). "Morphological and Advanced Imaging of Epilepsy: Beyond the Basics." Children **6**(43): 24.

Flint, A. C. and A. R. Kriegstein (1997). "Mechanisms underlying neuronal migration disorders and epilepsy." Curr.Opin.Neurol. **10**: 92-97.

Forro, T., O. Valenti, B. Lasztoczi and T. Klausberger (2015). "Temporal organization of GABAergic interneurons in the intermediate CA1 hippocampus during network oscillations." Cerebral Cortex **25**(5): 1228.

Freund, T. F. (2003). "Interneuron Diversity series: Rhythm and mood in perisomatic inhibition." Trends Neurosci. **26**(9): 489-495.

Freund, T. F. and G. Buzsaki (1996). "Interneurons of the hippocampus." Hippocampus **6**(4): 347.

Freund, T. F. and A. I. Gulys (1997). "Inhibitory control of GABAergic interneurons in the hippocampus." Can J Physiol Pharmacol **75**(5): 479-487.

Freund, T. F. and I. Katona (2007). "Perisomatic Inhibition." Neuron **56**(1): 33-42.

Frey, L. C. (2003). "Epidemiology of posttraumatic epilepsy: a critical review." Epilepsia **44 Suppl 10**: 11-17.

Friede, R. L. (1989). "Developmental neuropathology." <u>Berlin: Springer-Verlag</u>: 335p.

Frotscher, M. (1998). "Cajal-Retzius cells, Reelin, and the formation of layers." <u>Curr Opin Neurobiol</u> **8**: 570-575.

Fuentealba, P., R. Begum, M. Capogna, S. Jinno, L. F. Márton, J. Csicsvari and e. al. (2008). "Ivy Cells: A Population of Nitric- Oxide- Producing, Slow- Spiking GABAergic Neurons and Their Involvement in Hippocampal Network Activity." <u>Neuron</u> **57**(6): 917-929.

Fujiwara-Tsukamoto, Y., Y. Isomura, M. Imanishi, T. Ninomiya, M. Tsukada, Y. Yanagawa and e. al. (2010). "Prototypic seizure activity driven by mature hippocampal fast- spiking interneurons." <u>Journal of Neuroscience</u> **30**(41): 13679.

Fukuda, T. and T. Kosaka (2000). "Gap Junctions Linking the Dendritic Network of GABAergic Interneurons in the Hippocampus. ." <u>Journal of Neuroscience</u> **20**(4): 1519-1528.

Galarreta, M. and S. Hestrin (1998). "Frequency-dependent synaptic depression and the balance of excitation and inhibition in the neocortex." <u>Nat Neurosci</u> **1**(7): 587.

Ganter, P., P. Szücs, O. Paulsen and P. Somogyi (2004). "Properties of horizontal axo- axonic cells in stratum oriens of the hippocampal CA1 area of rats in vitro." <u>Hippocampus</u> **14**(2): 232-243.

Gaytant, M. A., G. I. Rours, E. A. Steegers, J. M. Galama and B. A. Semmekrot (2003). "Congenital cytomegalovirus infection after recurrent infection: case reports and review of the literature." <u>Eur J Pediatr</u> **162**: 248-253.

Geiger, J. R., A. Roth, B. Taskin and P. Jonas (1999). "Glutamate-mediated synaptic excitation of cortical interneurons." <u>Handb Exp Pharm</u> **141**: 363-398.

George, A. L. and K. M. Jacobs (2011). "Altered intrinsic properties of neuronal subtypes in malformed epileptogenic cortex." <u>Brain Res</u> **1374**: 116-128.

Giannetti, S., P. Gaglini, F. Di Rocco, C. Di Rocco and A. Granato (2000). "Organization of cortico-cortical associative projections in a rat model of microgyria." <u>Neuroreport</u> **11**(10): 2185-2189.

Giannetti, S., P. Gaglini, A. Granato and C. Di Rocco (1999). "Organization of callosal connections in rats with experimentally induced microgyria." <u>Childs Nerv.Syst.</u> **15**(9): 444-448.

Gibson, J. R., M. Beierlein and B. W. Connors (1999). "Two networks of electrically coupled inhibitory neurons in neocortex." <u>Nature</u> **402**: 75-79.

Gibson, J. R., M. Beierlein and B. W. Connors (2005). "Functional properties of electrical synapses between inhibitory interneurons of neocortical layer 4." J Neurophysiol **93**(1): 467.

Gilioli, I., A. Vignoli, E. Visani, M. Casazza, L. Canafoglia, V. Chiesa, E. Gardella, F. La Briola, F. Panzica, G. Avanzini, M. P. Canevini, S. Franceschetti and S. Binelli (2012). "Focal epilepsies in adult patients attending two epilepsy centers: Classification of drug-resistance, assessment of risk factors, and usefulness of "new" antiepileptic drugs: Parmacoresistance in Focal Epilepsies." Epilepsia **53**(4): 733-740.

Glauser, T., S. Shinnar, D. Gloss, B. Alldredge, R. Arya, J. Bainbridge, M. Bare, T. Bleck, W. E. Dodson, L. Garrity, A. Jagoda, D. Lowenstein, J. Pellock, J. Riviello, E. Sloan and D. M. Treiman (2016). "Evidence-Based Guideline: Treatment of Convulsive Status Epilepticus in Children and Adults: Report of the Guideline Committee of the American Epilepsy Society." Epilepsy Curr. **16**(1): 48-61.

Glen, S. ((web resource)). "Pooled Standard Deviation."

Glock, C., J. Nagpal and A. Gottschalk (2015). "Microbial Rhodopsin Optogenetic Tools: Application for Analyses of Synaptic Transmission and of Neuronal Network Activity in Behavior." Methods Mol Biol **1327**: 87-103.

Gonchar, Y. A., Q. Wang and A. Burkhalter (2007). "Multiple Distinct Subtypes of GABAergic Neurons in Mouse Visual Cortex Identified by Triple Immunostaining." Front Neuroanat **1**(3).

Guerreiro, M. M., L. F. Quesney, V. Salanova and G. J. Snipes (2003). "Continuous Electrocorticogram Epileptiform Discharges Due to Brain Gliosis." Journal of Clinical Neurophysiology **20**(4): 239-242.

Guerrini, R. and R. Carrozzo (2002). "Epileptogenic brain malformations: clinical presentation, malformative patterns and indications for genetic testing." Seizure. **11 Suppl A**: 532-543.

Guerrini, R. and T. Filippi (2005). "Neuronal migration disorders, genetics, and epileptogenesis." J.Child Neurol. **20**(4): 287-299.

Guerrini, R., F. Sicca and L. Parmeggiani (2003). "Epilepsy and malformations of the cerebral cortex." Epileptic.Disord. **5 Suppl 2**: S9-26.

Gulyás, A. I., N. Hájos and T. F. Freund (1996). "Interneurons containing calretinin are specialized to control other interneurons in the rat hippocampus." Journal of Neuroscience **16**(3397).

Gulyás, A. I., N. Hájos, I. Katona and T. F. Freund (2003). "Interneurons are the local targets of hippocampal inhibitory cells which project to the medial septum." Eur J Neurosci **17**(9): 1861-1872.

Gulyás, A. I., M. Megías, Z. Emri and T. F. Freund (1999). "Total number and ratio of excitatory and inhibitory synapses converging onto single interneurons of different types in the CA1 area of the rat hippocampus." Journal of Neuroscience **19**(22): 10082.

Gulyás, A. I. M., M., Z. Emri and T. F. Freund (1999). "Total number and ratio of excitatory and inhibitory synapses converging onto single interneurons of different types in the CA1 area of the rat hippocampus." Journal of Neuroscience **19**(22): 10082.

Gupta, A., Y. Wang and H. Markram (2000). "Organizing Principles for a Diversity of GABAergic Interneurons and Synapses in the Neocortex." Science **287**(5451): 273-278.

Hájos, N., L. Acsády and T. F. Freund (1996). "Target Selectivity and Neurochemical Characteristics of VIP- immunoreactive Interneurons in the Rat Dentate Gyrus." Eur J Neurosci **8**(7): 1415-1431.

Hájos, N. and I. Mody (1997). "Synaptic communication among hippocampal interneurons: properties of spontaneous IPSCs in morphologically identified cells. ." Journal of Neuroscience **17**(21): 8427.

Hanson, E., N. C. Danbolt and C. G. Dulla (2016). "Astrocyte membrane properties are altered in a rat model of developmental cortical malformation but single-cell astrocytic glutamate uptake is robust." Neurobiol. Dis. **89**: 157-168.

Hauser, W. A. and D. C. Hersdorffer (1990). "Epilepsy : frequency, causes, and consequences."

Hayashi, N., Y. Tsutsumi and A. J. Barkovich (2002). "Polymicrogyria without porencephaly/schizencephaly. MRI analysis of the spectrum and the prevalence of macroscopic findings in the clinical population." Neuroradiology **44**(8): 647-655.

Herman, A. M., L. Huang, D. K. Murphey, I. Garcia and B. R. Arenkiel (2014). "Cell type-specific and time-dependent light exposure contribute to silencing in neurons expressing Channelrhodopsin-2." eLife **3**.

Higo, S., K. Akashi, K. Sakimura and N. Tamamaki (2009). "Subtypes of GABAergic Neurons Project Axons in the Neocortex." Front Neuroanat **3**.

Hoffman, D. A., J. C. Magee, C. M. Colbert and D. Johnston (1997). "K+ channel regulation of signal propagation in dendrites of hippocampal pyramidal neurons." Nature **387**(6636): 869.

Holmgren, C., T. Harkany, B. Svennenfors and Y. Zilberter (2003). "Pyramidal cell communication within local networks in layer 2/ 3 of rat neocortex." J Physiol **551**(1): 139-153.

Hou, Z.-H. and X. Yu (2013). "Activity-regulated somatostatin expression reduces dendritic spine density and lowers excitatory synaptic transmission via postsynaptic somatostatin receptor 4." J Biol Chem **288**: 2501-2509.

Hu, H., J. Z. Cavendish and A. Agmon (2013). "Not all that glitters is gold: off-target recombination in the somatostatin-IRES-Cre mouse line labels a subset of fast-spiking interneurons." Front Neural Circuits **7**: 195.

Hull, C., H. Adesnik and M. Scanziani (2009). "Neocortical disynaptic inhibition requires somatodendritic integration in interneurons. ." Journal of Neuroscience **29**(28): 8991.

Humphreys, P., G. D. Rosen, D. M. Press, G. F. Sherman and A. M. Galaburda (1991). "Freezing lesions of the developing rat brain: A model for cerebrocortical microgyria." J.Neuropathol.Exp.Neurol. **50**: 145-160.

Hussain, S. and R. Sankar (2011). "Pharmacologic Treatment of Intractable Epilepsy in Children: A Syndrome-Based Approach." Seminars in Pediatric Neurology **18**(3): 7.

Inan, Blázquez-Lorca, Merchán-Pérez, Anderson, DeFelipe and Yuste. (2013). "Dense and Overlapping Innervation of Pyramidal Neurons by Chandelier Cells." J Neurosci **33**(5): 1907-1914.

Jacobs, K. M., M. J. Gutnick and D. A. Prince (1996). "Hyperexcitability in a model of cortical maldevelopment." Cereb Cortex **6**(3): 514-523.

Jacobs, K. M., B. J. Hwang and D. A. Prince (1999a). "Focal epileptogenesis in a rat model of polymicrogyria." Journal of Neurophysiology **81**: 159-173.

Jacobs, K. M., V. N. Kharazia and D. A. Prince (1999b). "Mechanisms underlying epileptogenesis in cortical malformations." Epilepsy Research **36**: 165-188.

Jacobs, K. M., M. Mogensen, L. Warren and D. A. Prince (1999c). "Experimental microgyri disrupt the barrel field pattern in rat somatosensory cortex." Cerebral Cortex **9**(7): 733-744.

Jacobs, K. M. and D. A. Prince (2005). "Excitatory and inhibitory postsynaptic currents in a rat model of epileptogenic microgyria." J Neurophysiol. **93**(2): 687-696.

Janmohamed, M., M. J. Brodie and P. Kwan (2019). "Pharmacoresistance–Epidemiology, mechanisms, and impact on epilepsy treatment." Neuropharmacology **107790**.

Jin, X., K. Jiang and D. A. Prince (2014). "Excitatory and inhibitory synaptic connectivity to layer V fast-spiking interneurons in the freeze lesion model of cortical microgyria." <u>J Neurophysiol</u> **112**(7): 1703-1713.

Jinno, S. (2009). "Structural Organization of Long- Range GABAergic Projection System of the Hippocampus." <u>Front Neuroanat</u> **3**.

Jiruska, P., M. de Curtis, J. G. R. Jefferys, C. A. Schevon, S. J. Schiff and K. Schindler (2012). "Synchronization and desynchronization in epilepsy: controversies and hypotheses." <u>Journal of Physiology</u> **591**(4): 787-797.

Jonas, P., J. Bischofberger, D. Fricker and R. Miles (2004). "Interneuron Diversity series: Fast in, fast out – temporal and spatial signal processing in hippocampal interneurons." <u>Trends Neurosci.</u> **27**(1): 30-40.

Jones, E. G. and A. Peters (1984). <u>Cerebral Cortex: Cellular Components of the Cerebral Cortex; Vol 1</u>. New York, Plenum Publishing Corp.

Judkins, A. R., D. Martinez, P. Ferreira, W. B. Dobyns and J. A. Golden (2011). "Polymicrogyria includes fusion of the molecular layer and decreased neuronal populations but normal cortical laminar organization." <u>Journal of Neuropathology and Experimental Neurology</u> **70**(6): 438-443.

Kalilani, L., X. Sun, B. Pelgrims, M. Noack-Rink and V. Villanueva (2018). "The epidemiology of drug-resistant epilepsy: a systematic review and meta analysis." <u>Epilepsia</u> **59**: 2179-2193.

Kamada, T., W. Sun, K.-i. Takase, H. Shigeto, S. O. Suzuki, Y. Ohyagi and J.-i. Kira (2013). "Spontaneous seizures in a rat model of multiple prenatal freeze lesioning." <u>Epilepsy Research</u> **105**: 280-291.

Kapfer, C., L. G. Lindsey, V. A. Bassam and M. Scanziani (2007). "Supralinear increase of recurrent inhibition during sparse activity in the somatosensory cortex." <u>Nat Neurosci</u> **10**(6): 743.

Katona, I., L. Acsády and T. F. Freund (1999). "Postsynaptic targets of somatostatin- immunoreactive interneurons in the rat hippocampus." <u>Neuroscience</u> **88**(1): 37-55.

Katona, L., D. Lapray, T. Viney, A. Oulhaj, Z. Borhegyi, B. Micklem and e. al. (2014). "Sleep and Movement Differentiates Actions of Two Types of Somatostatin- Expressing GABAergic Interneuron in Rat Hippocampus." <u>Neuron</u> **82**(4): 872-886.

Kawaguchi, Y. (1993). "Groupings of nonpyramidal and pyramidal cells with specific physiological and morphological characteristics in rat frontal cortex." <u>Journal of Neurophysiology</u> **69**: 416-431.

Kawaguchi, Y. and K. Hama (1987). "Fast-spiking non-pyramidal cells in the hippocampal CA3 region, dentate gyrus and subiculum of rats." Brain Res **425**: 351-355.

Kawaguchi, Y. and K. Hama (1988). "Physiological heterogeneity of nonpyramidal cells in rat hippocampal CA1 region." Exp Brain Res **72**(3): 494-502.

Kawaguchi, Y., F. Karube and Y. Kubota (2006). "Dendritic branch typing and spine expression patterns in cortical nonpyramidal cells." Cereb Cortex **16**(5): 696-711.

Kawaguchi, Y. and Y. Kubota (1984). "The distribution and morphological characteristics of the intracortical VIP-positive cell: an immunohistochemical analysis. ." Brain Res **292**(292): 269-282.

Kawaguchi, Y. and Y. Kubota (1993). "Correlation of physiological subgroupings of nonpyramidal cells with parvalbumin- and calbindinD28k-immunoreactive neurons in layer V of rat frontal cortex." Journal of Neurophysiology **70**: 387-396.

Kawaguchi, Y. and Y. Kubota (1996). "Physiological and morphological identification of somatostatin- or vasoactive intestinal polypeptide- containing cells among GABAergic cell subtypes in rat frontal cortex." Journal of Neuroscience **16**(8): 2701.

Kawaguchi, Y. and Y. Kubota (1997). "GABAergic cell subtypes and their synaptic connections in rat frontal cortex." Cereb.Cortex **7**(6): 476-486.

Kellinghaus, C., G. Moddel, H. Shigeto, Z. Ying, B. Jacobsson, J. Gonzalez-Martinez, C. Burrier, D. Janigro and I. M. Najm (2007). "Dissociation between in vitro and in vivo epileptogenicity in a rat model of cortical dysplasia." Epileptic.Disord. **9**(1): 11-19.

Khoshkhoo, S., D. Vogt and V. S. Sohal (2017). "Dynamic, Cell-Type-Specific Roles for GABAergic Interneurons in a Mouse Model of Optogenetically Inducible Seizures." Neuron **93**: 291-298.

Kisvárday, Z. F., K. A. C. Martin, D. Whitteridge and P. Somogyi (1985). "Synaptic connections of intracellularly filled clutch cells: A type of small basket cell in the visual cortex of the cat." J Comp Neurol **241**(2): 111-137.

Kits, K. S. and H. D. Mansvelder (2000). "Regulation of exocytosis in neuroendocrine cells: spatial organization of channels and vesicles, stimulus-secretion coupling, calcium buffers and modulation." Brain Res Rev **33**(1): 78-94.

Klaassen, A., J. Glykys, J. Maguire, C. Labarca, I. Mody and J. Boulter (2006). "Seizures and enhanced cortical GABAergic inhibition in two mouse models of human autosomal dominant nocturnal frontal lobe epilepsy." Proc.Natl.Acad.Sci.U.S.A **103**(50): 19152-19157.

Klausberger, T. (2009). "GABAergic interneurons targeting dendrites of pyramidal cells in the CA1 area of the hippocampus." Eur J Neurosci **30**(6): 947-957.

Klausberger, T., F. M. László, A. Baude, J. B. R. David, J. M. Peter and P. Somogyi (2003). "Spike timing of dendrite- targeting bistratified cells during hippocampal network oscillations in vivo." Nature Neuroscience **7**(1): 41.

Klausberger, T. and P. Somogyi (2008). "Neuronal diversity and temporal dynamics: the unity of hippocampal circuit operations." Science **321**(5885): 53.

Krook-Magnuson, E., C. Varga, S. Lee and I. Soltesz (2012). "New dimensions of interneuronal specialization unmasked by principal cell heterogeneit." Trends Neurosci. **35**(3): 175-184.

Kubota, Y. and Y. Kawaguchi (1993). "Two distinct subgroups of cholecystokinin- immunoreactive cortical interneurons." Brain Res **752**(1): 175-183.

Kubota, Y., N. Shigematsu, F. Karube, A. Sekigawa, S. Kato, N. Yamaguchi, Y. Hirai, M. Morishima and Y. Kawaguchi (2011). "Selective Coexpression of Multiple Chemical Markers Defines Discrete Populations of Neocortical GABAergic Neurons." Cereb Cortex **21**(8): 1803-1817.

Kuhlman, S. J. and Z. J. Huang (2008). "High-Resolution Labeling and Functional Manipulation of Specific Neuron Types in Mouse Brain by Cre-Activated Viral Gene Expression." Plos One **3**(4).

Kun, L. N., L. W. Ling, Y. W. Wah and T. T. Lian (1999). "Epidemiologic study of epilepsy in young Singaporean men." Epilepsia **40**: 1384-1387.

Kuzniecky, R., F. Andermann and R. Guerrini (1993). "Congenital bilateral perisylvian syndrome: Study of 31 patients. The CBPS Multicenter Collaborative Study." Lancet Neurol. **341**: 608-612.

Kwag, J. and O. Paulsen (2009). "The timing of external input controls the sign of plasticity at local synapses." Nature Neuroscience **12**(10): 1219.

Kwan, P., A. Arzimanoglou, A. T. Berg, M. J. Brodie, W. A. Hauser, G. Mathern, S. L. Moshé, E. Perucca, S. Wiebe and J. French (2010). "Definition of drug resistant epilepsy: consensus proposal by the ad hoc task force of the ILAE commission on therapeutic strategies." Epilepsia **51**(6): 1069-1077.

Kwan, P. and M. J. Brodie (2002). "Refractory Epilepsy: A Progressive, Intractable but Preventable Condition?" Seizure **11**(2): 77-84.

Kwan, P. and M. J. Brodie (2006). "Combination therapy in epilepsy - When and what to use." Drugs **66**(14): 1817-1829.

Lacaille, J. C., A. L. Mueller, D. D. Kunkel and P. A. Schwartzkroin (1987). "Local circuit interactions between oriens/ alveus interneurons and CA1 pyramidal cells in hippocampal slices: electrophysiology and morphology." Journal of Neuroscience **7**(7): 1979.

Lacaille, J. C. and P. Schwartzkroin (1988). "Stratum lacunosum-moleculare interneurons of hippocampal CA1 region. I. Intracellular response characteristics, synaptic responses, and morphology." Journal of Neuroscience **8**(4): 1400-1410.

Lapray, D., B. Lasztoczi, M. Lagler, J. V. Tim, L. Katona, O. Valenti and e. al. (2012). "Behavior-dependent specialization of identified hippocampal interneurons." Nat Neurosci **15**(9): 1265.

Laurie, D. J., W. Wisden and P. H. Seeburg (1992). "The distribution of thirteen GABAA receptor subunit mRNAs in the rat brain. III. Embryonic and postnatal development." J.Neurosci. **12**: 4151-4172.

Le Magueresse, C. and H. Monyer (2013). "GABAergic Interneurons Shape the Functional Maturation of the Cortex." Neuron **77**(3): 388-405.

Ledri, M., M. G. Madsen, L. Nikitidou, D. Kirik and M. Kokaia (2014). "Global Optogenetic Activation of Inhibitory Interneurons during Epileptiform Activity." Journal of Neuroscience **34**(9): 3364-3377.

Lee, K. H., Y. J. Lee, J. H. Seo, J. E. Baumgartner and M. Westerveld (2019). "Epilepsy surgery in Children versus Adults." J Korean Neurosurg Soc. **62**(3): 328-335.

Lee, K. S., F. Schottler, J. L. Collins, G. Lanzino, D. Couture, A. Rao, K. Hiramatsu, Y. Goto, S. C. Hong, H. Caner, H. Yamamoto, Z. F. Chen, E. Bertram, S. Berr, R. Omary, H. Scrable, T. Jackson, J. Goble and L. Eisenman (1997). "A genetic animal model of human neocortical heterotopia associated with seizures." J.Neurosci. **17**: 6236-6242.

Lee, S., J. Hjerling-Leffler, E. Zagha, G. Fishell and B. Rudy (2010). "The largest group of superficial neocortical GABAergic interneurons expresses ionotropic serotonin receptors." Journal of Neuroscience **30**(50): 16796.

Leresche, N., E. Asprodini, Z. Emri, D. W. Cope and V. Crunelli (2000). "Somatostatin inhibits GABAergic transmission in the sensory thalamus via presynaptic receptors." Neuroscience **98**: 513-522.

Letinic, K., R. Zoncu and P. Rakic (2002). "Origin of GABAergic neurons in the human neocortex." Nature **417**(6889): 645.

Leventer, R. J., R. Guerrini and W. B. Dobyns (2008). "Malformations of cortical development and epilepsy." Dialogues.Clin.Neurosci. **10**(1): 47-62.

Leventer, R. J., A. Jansen, D. T. Pilz, N. Stoodley, C. Marini, F. Dubeau, J. Malone, L. A. Mitchell, S. Mandelstam, I. E. Scheffer, S. F. Berkovic, F. Andermann, E. Andermann, R. Guerrini and W. B. Dobyns (2010). "Clinical and Imaging Heterogeneity of Polymicrogyria: A Study of 328 Patients." Brain **133**(Pt 1): 1415-1427.

Li, D., P. Li, Z. He, D. Cen, Z. Meng, L. Liang and X. Luo (2012). "Human Intravenous Immunoglobulins Suppress Seizure Activities and Inhibit the Activation of GFAP-Positive Astrocytes in the Hippocampus of Picrotoxin-Kindled Rats." International Journal of Neuroscience **122**(4): 200-208.

Löscher, W. (2005b). "How to Explain Multidrug Resistance in Epilepsy?" Epilepsy Curr. **5**(3): 107-112.

Löscher, W. and A. Friedman (2020). "Structural, Molecular, and Functional Alterations of the Blood-Brain Barrier during Epileptogenesis and Epilepsy: A Cause, Consequence, or Both?" Int J Mol Sci **21**(2).

Löscher, W. and H. Potschka (2005a). "Drug resistance in brain diseases and the role of drug efflux transporters." Nat.Rev.Neurosci. **6**: 591-602.

Losonczy, A., L. Zhang, R. Shigemoto, P. Somogyi and Z. Nusser (2002). "Cell type dependence and variability in the short- term plasticity of EPSCs in identified mouse hippocampal interneurones." J Physiol **542**(1): 193-210.

Ludwig, M. and Q. J. Pittman (2003). "Talking back: dendritic neurotransmitter release." Trends Neurosci. **26**: 255-261.

Luhmann, H. J., N. Karpuk, M. Qü and K. Zilles (1998). "Characterization of neuronal migration disorders in neocortical structures. II. Intracellular in vitro recordings." Journal of Neurophysiology **80**(1): 92-102.

Maccaferri, G. and R. Dingledine (2002). "Control of feedforward dendritic inhibition by NMDA receptor-dependent spike timing in hippocampal interneurons." Journal of Neuroscience **22**(13): 5462.

Maccaferri, G. and J. C. Lacaille (2003). "Interneuron Diversity series: Hippocampal interneuron classifications--making things as simple as possible, not simpler." Trends Neurosci. **26**(10): 564-571.

Maccaferri, G., J. D. Roberts, P. Szucs, C. A. Cottingham and P. Somogyi (2000). "Cell surface domain specific postsynaptic currents evoked by identified GABAergic neurones in rat hippocampus in vitro." J Physiol **524**(1): 193-210.

Magee, J. C. and D. Johnston (1997). "A Synaptically Controlled, Associative Signal for Hebbian Plasticity in Hippocampal Neurons." Science **275**(5297): 209-213.

Magnotti, L. M., D. A. Goodenough and D. L. Paul (2011). "Functional heterotypic interactions between astrocyte and oligodendrocyte connexins." Glia **59**: 26-34.

Maillard, L. and G. Ramantani (2018). "Epilepsy surgery for polymicrogyria: a challenge to be undertaken." Epileptic.Disord. **20**(5): 319-338.

Mann, E. O. and I. Mody (2008). "The multifaceted role of inhibition in epilepsy: seizure-genesis through excessive GABAergic inhibition in autosomal dominant nocturnal frontal lobe epilepsy." Curr.Opin.Neurol. **21**(2): 155-160.

Marchi, A., D. Pennaroli, S. Lagarde, A. McGonigal, F. Bonini, R. Carron, A. Lépine, N. Villeneuve, A. Trebuchon, F. Pizzo, D. Scavarda and F. Bartolomei (2019). "Epileptogenicity and surgical outcome in post stroke drug resistant epilepsy in children and adults." Epilepsy Res. **155**.

Markram, H., M. Toledo-Rodriguez, Y. Wang, A. Gupta, G. Silberberg and C. Wu (2004). "Interneurons of the neocortical inhibitory system." Nat.Rev.Neurosci. **5**(10): 793-807.

Markram, H., Y. Wang and M. Tsodyks (1998). "Differential signaling via the same axon of neocortical pyramidal neurons." Proc.Natl.Acad.Sci.U.S.A **95**(9): 5323-5328.

Martina, M., J. H. Schultz, H. Ehmke, H. Monyer and P. Jonas (1998). "Functional and molecular differences between voltage- gated K+ channels of fast- spiking interneurons and pyramidal neurons of rat hippocampus." Journal of Neuroscience **18**(20): 8111.

Masuda, K., T. Toda, Y. Shinmyo, H. Ebisu, Y. Hoshiba, M. Wakimoto, Y. Ichikawa and H. Kawasaki (2015). "Pathophysiological analyses of cortical malformation using gyrencephalic mammals." Sci Rep **5**.

Mátyás, F., T. F. Freund and A. I. Gulyás (2004). "Convergence of excitatory and inhibitory inputs onto CCK- containing basket cells in the CA1 area of the rat hippocampus." Eur J Neurosci **19**(5): 1243-1256.

Mcbain, C. J., T. J. Dichiara and J. A. Kauer (1994). "Activation of metabotropic glutamate receptors differentially affects two classes of hippocampal interneurons and potentiates excitatory synaptic transmission." Journal of Neuroscience **14**(7): 4433.

Mcbain, C. J. and R. Dingledine (1993). "Heterogeneity of synaptic glutamate receptors on CA3 stratum radiatum interneurones of rat hippocampus." J Physiol **462**: 373.

McBain, C. J. and A. Fisahn (2001). "Interneurons unbound." Nat.Rev.Neurosci. **2**: 11-23.

McClure, M., S. Threlkeld and R. Fitch (2006). "Auditory processing and learning/memory following erythropoietin administration in neonatally hypoxic-ischemic injured rats." Brain Res. **132**(1): 7.

McGarry, L. M., A. M. Packer, E. Fino, V. Nikolenko, T. Sippy and R. Yuste (2010). "Quantitative classification of somatostatin-positive neocortical interneurons identifies three interneuron subtypes." Front Neural Circuits **4**(12): 19.

Mckhann, G. M., J. Schoenfeld-Mcneill, D. Born, M. M. Haglund and G. A. Ojemann (2000). "Intraoperative hippocampal electrocorticography to predict the extent of hippocampal resection in temporal lobe epilepsy surgery." Journal of Neurosurgery **93**(1): 44-52.

Miles, R., K. Tóth, A. I. Gulyás, N. Hájos and T. F. Freund (1996). "Differences between Somatic and Dendritic Inhibition in the Hippocampus." Neuron **16**(4): 815-823.

Mittmann, W., P. Chadderton and M. Häusser (2004). "Neuronal Microcircuits: Frequency-Dependent Flow of Inhibition." Current Biology **14**(19): R837-839.

Miyoshi, G., S. J. B. Butt, H. Takebayashi and G. Fishell (2007). "Physiologically distinct temporal cohorts of cortical interneurons arise from telencephalic Olig2- expressing precursors." Journal of Neuroscience **27**(29): 7786.

Miyoshi, G., J. Hjerling-Leffler, T. Karayannis, V. H. Sousa, S. J. B. Butt, J. Battiste and e. al. (2010). "Genetic fate mapping reveals that the caudal ganglionic eminence produces a large and diverse population of superficial cortical interneurons." Journal of Neuroscience **30**(5): 1582.

Montenegro, M. A., M. M. Guerreiro, I. Lopes-Cendes, C. A. Guerreiro and F. Cendes (2002). "Interrelationship of genetics and prenatal injury in the genesis of malformations of cortical development." Arch.Neurol. **59**(7): 1147-1153.

Naimo, G. D., M. Guarnaccia, T. Sprovieri, C. Ungaro, F. L. Conforti, S. Andò and S. Cavallaro (2019). "A Systems Biology Approach for Personalized Medicine in Refractory Epilepsy." International Journal of Molecular Sciences **20**(15).

Nyíri, G., F. A. Stephenson, T. F. Freund and P. Somogyi (2003). "Large variability in synaptic n--methyl- d- aspartate receptor density on interneurons and a comparison with pyramidal- cell spines in the rat hippocampus." Neuroscience **119**(2): 347-363.

O'Neill, K., B. Akum, S. Dhawan, M. Kwon, C. Langhammer and B. Firestein (2015). "Assessing effects on dendritic arborization using novel Sholl analyses." Frontiers in Cellular Neuroscience **9**(285).

Oberheim, N. A., G. F. Tian, X. Han, W. Peng, T. Takano, B. Ransom and M. Nedergaard (2008). "Loss of astrocytic domain organization in the epileptic brain." The Journal of Neuroscience **28**(13): 3264-3276.

Oláh, S., M. Füle, G. Komlósi, C. Varga, R. Báldi, P. Barzó and G. Tamás (2009). "Regulation of cortical microcircuits by unitary GABA-mediated volume transmission." Nature **461**: 1278-1281.

Osawa, S., M. Iwasaki, R. Hosaka, Y. Matsuzaka, H. Tomita, T. Ishizuka, E. Sugano, E. Okumura, H. Yawo, N. Nakasato, T. Tominaga and H. Mushiake (2013). "Optogenetically Induced Seizure and the Longitudinal Hippocampal Network Dynamics." Plos One **8**(4).

Oskoui, M., R. I. Webster, X. Zhang and M. I. Shevell (2005). "Factors predictive of outcome in childhood epilepsy." J. Child Neurol. **20**: 898-904.

Otsuka, T. and Y. Kawaguchi (2009). "Cortical inhibitory cell types differentially form intralaminar and interlaminar subnetworks with excitatory neurons." Journal of Neuroscience **29**(34): 10533.

Oviedo, H. and A. D. Reyes (2002). "Boosting of neuronal firing evoked with asynchronous and synchronous inputs to the dendrite." Nat Neurosci **5**(3): 261.

Packer, A. M. and R. Yuste (2011). "Dense, unspecific connectivity of neocortical parvalbumin- positive interneurons: a canonical microcircuit for inhibition? ." Journal of Neuroscience **31**(37): 13260.

Panatier, A. and R. Robitaille (2016). "Astrocytic mGluR5 and the tripartite synapse." Neuroscience **323**: 29-34.

Paolicelli, R. C., G. Bolasco, F. Pagani, L. Maggi, M. Scianni, P. Panzanelli, M. Giustetto, T. A. Ferreira, E. Guiducci, L. Dumas, D. Ragozzino and C. T. Gross (2011). "Synaptic Pruning by Microglia Is Necessary for Normal Brain Development." Science **333**(6048): 1456-1458.

Pascual-Castroviejo, I., S. I. Pascual-Pascual, J. Viaño, V. Martinez and R. Palencia (2001). "Unilateral polymicrogyria: a common cause of hemiplegia of prenatal origin." Brain and Development **23**(4): 216-222.

Pasti, L., A. Volterra, T. Pozzan and G. Carmignoto (1997). "Intracellular calcium oscillations in astrocytes: A highly plastic, bidirectional form of communication between neurons and astrocytes in situ." Journal of Neuroscience **17**(20): 7817-7830.

Patrick, S. L., B. W. Connors and C. E. Landisman (2006). "Developmental changes in somatostatin-positive interneurons in a freeze-lesion model of epilepsy." Epilepsy Res. **70**(2-3): 161-171.

Pawelzik, H., A. P. Bannister, J. Deuchars, M. Ilia and A. M. Thomson (1999). "Modulation of bistratified cell IPSPs and basket cell IPSPs by pentobarbitone sodium, diazepam and Zn 2+: dual recordings in slices of adult rat hippocampus." Eur J Neurosci **11**(10): 3552-3564.

Pawelzik, H., D. I. Hughes and A. M. Thomson (2002). "Physiological and morphological diversity of immunocytochemically defined parvalbumin- and cholecystokinin- positive interneurones in CA1 of the adult rat hippocampus." J Comp Neurol **443**(4): 346-367.

Perrenoud, Q., J. Rossier, H. Geoffroy, T. Vitalis and T. Gallopin (2013). "Diversity of GABAergic Interneurons in Layer VIa and VIb of Mouse Barrel Cortex." Cerebral Cortex **23**: 423-441.

Peters, A. (1990). "The largest group of superficial neocortical GABAergic interneurons expresses ionotropic serotonin receptors." J Neurocytol. **19**(5): 672-685.

Peters, A. (1991). "The fine structure of the nervous system : neurons and their supporting cells. ." Oxford University Press, New York **3rd edition**.

Peters, A. and K. M. Harriman (1988). "Enigmatic bipolar cell of rat visual cortex." J Comp Neurol **267**(3): 409-432.

Pi, H. J., B. Hangya, D. Kvitsiani, J. I. Sanders, Z. J. Huang and A. Kepecs (2013). "Cortical interneurons that specialize in disinhibitory control." Nature **503**(7477): 521-+.

Picot, M.-C., M. Baldy-Moulinier, J.-P. Daurès, P. Dujols and A. Crespel (2008). "The prevalence of epilepsy and pharmacoresistant epilepsy in adults: a population-based study in a Western European country." Epilepsia **49**: 1230-1238.

Porter, J. T., B. Cauli, J. F. Staiger, B. Lambolez, J. Rossier and E. Audinat (1998). "Properties of bipolar VIPergic interneurons and their excitation by pyramidal neurons in the rat neocortex." Eur J Neurosci **1998**(10): 12.

Porter, J. T., C. K. Johnson and A. Agmon (2001). "Diverse types of interneurons generate thalamus-evoked feedforward inhibition in the mouse barrel cortex." J Neurosci **21**(8): 2699-2710.

Prince, D. A. (1985). "Physiological Mechanisms of Focal Epileptogenesis." Epilepsia **26**(Suppl 1): S3-S14.

Prince, D. A. and K. Jacobs (1998). "Inhibitory function in two models of chronic epileptogenesis." Epilepsy Research **32**(1-2): 83-92.

Ragsdale, D. S. and M. Avoli (1998). "Sodium channels as molecular targets for antiepileptic drugs." Brain Res Rev **26**: 16-28.

Ramantani, G., L. Koessler and S. Colnat-Coulbois (2013). "Intracranial evaluation of the epileptogenic zone in regional infrasylvian polymicrogyria." Epilepsia **54**(2): 296-304.

Ramón y Cajal, S. (1893). "Estructura del asta de Ammon y fascia dentate." Ann. Sociedad Española de Historia Natural.

Rao, V. R. and D. H. Lowenstein (2015). "Epilepsy." Current Biology **25**: R733-R752.

Ray, S., E. Niebur, S. S. Hsiao, A. Sinai and N. E. Crone (2008). "High-frequency gamma activity (80-150 Hz) is increased in human cortex during selective attention." Clin Neurophysiol **119**(1): 116-133.

Redecker, C., H. J. Luhmann, G. Hagemann, J. M. Fritschy and O. W. Witte (2000). "Differential downregulation of GABAA receptor subunits in widespread brain regions in the freeze-lesion model of focal cortical malformations." J Neurosci **20**: 5045-5053.

Regehr, W. G. (2012). "Short-Term Presynaptic Plasticity." Cold Spring Harbor Perspectives in Biology **4**(7).

Remy, S. and H. Beck (2006). "Molecular and cellular mechanisms of pharmacoresistance in epilepsy." Brain **129**(1): 18-35.

Remy, S., S. Gabriel, B. W. Urban, D. Dietrich, T. N. Lehmann, C. E. Elger, U. Heinemann and H. Beck (2003). "A novel mechanism underlying drug resistance in chronic epilepsy." Annals of Neurology **53**(4): 469-479.

Reyes, A., R. Lujan, A. Rozov, N. Burnashev, P. Somogyi and B. Sakmann (1998). "Target-cell-specific facilitation and depression in neocortical circuits." Nat Neurosci **1**(4): 279-285.

Ribak, C. (1978). "Aspinous and sparsely- spinous stellate neurons in the visual cortex of rats contain glutamic acid decarboxylase." J Neurocytol. **7**(4): 461-478.

Richter, L., C. d. Graaf, W. Sieghart, Z. Varagic, M. Mörzinger, I. J. P. d. Esch, G. F. Ecker and M. Ernst (2012). "Diazepam-bound GABAA receptor models identify new benzodiazepine binding-site ligands." Nature Chemical Biology **8**: 455-464.

Robel, S. and H. Sontheimer (2015). "Glia as drivers of abnormal neuronal activity." Nature Neuroscience **19**: 28-33.

Rogawski, M. A. (2013). "The intrinsic severity hypothesis of pharmacoresistance to antiepileptic drugs." Epilepsia **54**: 33-40.

Rogers, J. H. and A. Resibois (1992). "Calretinin and calbindin-D28k in rat brain: patterns of partial co-localization." Neuroscience **51**: 843-865.

Rosen, G. D., D. Burstein and A. M. Galaburda (2000). "Changes in efferent and afferent connectivity in rats with induced cerebrocortical microgyria." J Comp Neurol **418**: 423-440.

Rosen, G. D., K. M. Jacobs and D. A. Prince (1998). "Effects of neonatal freeze lesions on expression of parvalbumin in rat neocortex." Cereb.Cortex **8**(8): 753-761.

Rosen, G. D., B. Mesples, M. Hendriks and A. M. Galaburda (2006). "Histometric changes and cell death in the thalamus after neonatal neocortical injury in the rat." Neuroscience **Epub ahead of print**.

Rosen, G. D., D. M. Press, G. F. Sherman and A. M. Galaburda (1992). "The development of induced cerebrocortical microgyria in the rat." J.Neuropathol.Exp.Neurol. **51**: 601-611.

Rosen, G. D., G. F. Sherman and A. M. Galaburda (1996). "Birthdates of neurons in induced microgyria." Brain Res. **727**: 71-78.

Rowan, M. J. M., G. DelCanto, J. J. Yu, N. Kamasawa and J. M. Christie (2016). "Synapse-Level Determination of Action Potential Duration by K+ Channel Clustering in Axons." Neuron **91**(2): 370-383.

Royer, S., B. V. Zemelman, A. Losonczy, J. Kim, F. Chance, J. C. Magee and G. Buzsaki (2012). "Control of timing, rate and bursts of hippocampal place cells by dendritic and somatic inhibition." Nature Neuroscience **15**(5): 769-775.

Rudy, B., G. Fishell, S. Lee and J. Hjerling-Leffler (2011). "Three groups of interneurons account for nearly 100% of neocortical GABAergic neurons." Developmental Neurobiology **71**(1): 45.

Rudy, B. and C. J. McBain (2001). "Kv3 channels: voltage-gated K+ channels designed for high-frequency repetitive firing." Trends Neurosci. **24**(9): 517-526.

Scantlebury, M. H., P. L. Ouellet, C. Psarropoulou and L. Carmant (2004). "Freeze lesion-induced focal cortical dysplasia predisposes to atypical hyperthermic seizures in the immature rat." Epilepsia **45**(6): 592-600.

Scheffer, I. E., S. Berkovic, G. Capovilla, M. B. Connolly, J. French, L. Guilhoto, E. Hirsch, S. Jain, G. W. Mathern, S. L. Moshé, D. R. Nordli, E. Perucca, T. Tomson, S. Wiebe, Y. H. Zhang and S. M. Zuberi (2017). "ILAE classification of the epilepsies: Position paper of the ILAE Commission for Classification and Terminology." Epilepsia **58**(4): 512-521.

Schuele, S. U. and H. O. Luders (2008). "Intractable epilepsy: management and therapeutic alternatives." Lancet Neurol. **7**(6): 514-524.

Schwartzkroin, P. A. and L. H. Mathers (1978). "Physiological and morphological identification of a nonpyramidal cell type." Brain Res **157**: 1-10.

Schweitzer, P., S. G. Madamba and G. R. Siggins (1998). "Somatostatin increases a voltage-insensitive K+ conductance in rat CA1 hippocampal neurons." Journal of Neurophysiology **79**(3): 1230-1238.

Scott, J. C., J. L. Timothy and W. C. Barry (2007). "Synaptic basis for intense thalamocortical activation of feedforward inhibitory cells in neocortex." Nat Neurosci **10**(4): 462.

Sedel, F., I. Gourfinkel-An, O. Lyon-Caen, M. Baulac, J. M. Saudubray and V. Navarro (2007). "Epilepsy and inborn errors of metabolism in adults: a diagnostic approach." J.Inherit.Metab Dis. **30**(6): 846-854.

Segev, I. and M. London (1999). "Dendrites." Oxford University Press, New York.

Sengupta, P. (2013). "The Laboratory Rat: Relating Its Age With Human's." Int J Prev Med **4**(6): 624-630.

Shain, C., S. Ramgopal, Z. Fallil, I. Parulkar, R. Alongi, R. Knowlton and A. Poduri (2013). "Polymicrogyria-associated epilepsy: a multicenter phenotypic study from the Epilepsy Phenome/Genome Project." Epilepsia **54**(8): 1368-1375.

Sik, A., M. Penttonen, A. Ylinen and G. Buzsaki (1995). "Hippocampal CA1 Interneurons- an in vivo Intracellular Labeling Study." J Neurosci **15**(10): 6651-6665.

Sik, A., A. Ylinen, M. Penttonen and G. Buzsáki (1994). "Inhibitory CA1- CA3- Hilar Region Feedback in the Hippocampus." Science **265**(5179): 1722-1724.

Silberberg, G. and H. Markram (2007). "Disynaptic inhibition between neocortical pyramidal cells mediated by martinotti cells." Neuron **53**: 735-746.

Sisodiya, S. M. (2000). "Surgery for malformations of cortical development causing epilepsy." Brain **123 (Pt 6)**: 1075-1091.

Sisodiya, S. M. (2004). "Malformations of cortical development: burdens and insights from important causes of human epilepsy." <u>Lancet Neurol.</u> **3**(1): 29-38.

Sisodiya, S. M., W. R. Lin, B. N. Harding, M. V. Squier and M. Thom (2002). "Drug resistance in epilepsy: expression of drug resistance proteins in common causes of refractory epilepsy." <u>Brain</u> **125**: 22-31.

Skjei, K. L. and D. J. Dlugos (2011). "The Evaluation of Treatment-Resistant Epilepsy." <u>Seminars in Pediatric Neurology</u> **18**(3): 20.

Somogyi, J., A. Baude, Y. Omori, H. Shimizu, S. E. Mestikawy, M. Fukaya and e. al. (2004). "GABAergic basket cells expressing cholecystokinin contain vesicular glutamate transporter type 3 (VGLUT3) in their synaptic terminals in hippocampus and isocortex of the rat." <u>Eur J Neurosci</u> **19**(3): 552-569.

Somogyi, P. and A. Cowey (1981). "Combined golgi and electron microscopic study on the synapses formed by double bouquet cells in the visual cortex of the cat and monkey." <u>J Comp Neurol</u> **195**(547-66).

Somogyi, P., T. F. Freund and A. Cowey (1982). "The Axo-Axonic Interneuron in the Cerebral-Cortex of the Rat, Cat and Monkey." <u>Neuroscience</u> **7**(11): 2577-2607.

Somogyi, P. and T. Klausberger (2005). "Defined types of cortical interneurone structure space and spike timing in the hippocampus." <u>Journal of Physiology</u> **562**(1): 9-26.

Somogyi, P., G. Tamas, R. Lujan and E. H. Buhl (1998). "Salient features of synaptic organisation in the cerebral cortex." <u>Brain Res.Brain Res.Rev.</u> **26**(2-3): 113-135.

Squier, W. and A. Jansen (2014). "Polymicrogyria: pathology, fetal origins and mechanisms." <u>acta neuropathol commun</u> **2**.

Stafstrom, C. E. and L. Carmant (2015). "Seizures and Epilepsy: An Overview for Neuroscientists." <u>Cold Spring Harbor Perspectives in Medicine</u> **5**(a022426): 18.

Staiger, J. F., C. Masanneck, A. Schleicher and W. Zuschratter (2004). "Calbindin- containing interneurons are a target for VIP- immunoreactive synapses in rat primary somatosensory cortex." <u>J Comp Neurol</u> **468**(2): 179.

Steinhäuser, C., G. Seifert and P. Bedner (2012). "Astrocyte dysfunction in temporal lobe epilepsy: K+ channels and gap junction coupling." <u>Glia</u> **60**(8).

Steriade, M. (2000). "Corticothalamic resonance, states of vigilance and mentation." Neuroscience **101**(2): 243-276.

Storm-Mathisen, J., K. L. Alfhild, A. T. Bore, L. V. Jorunn, P. Edminson, Š. H. Finn-Mogens and e. al. (1983). "First visualization of glutamate and GABA in neurones by immunocytochemistry." Nature **301**(5900): 517.

Stutterd, C. A. and R. J. Leventer (2014). "Polymicrogyria: A Common and Heterogeneous Malformation of Cortical Development." Am J Med Genet Part C Semin Med Genet **166**(C): 227-239.

Sukhotinsky, I., A. M. Chan, O. J. Ahmed, V. R. Rao, V. Gradinaru, C. Ramakrishnan, K. Deisseroth, A. K. Majewska and S. S. Cash (2013). "Optogenetic Delay of Status Epilepticus Onset in an In Vivo Rodent Epilepsy Model." Plos One **8**(4).

Sullivan, L. ((web resource)). "Power and Sample Size Determination."

Sultan, Liu, Li, Shen, Li, Zhang, Dean, Ma and Shi (2018). "Progressive divisions of multipotent neural progenitors generate late-born chandelier cells in the neocortex." Nature Communications **9**(1).

Sun, Q. Q., J. R. Huguenard and D. A. Prince (2005). "Reorganization of barrel circuits leads to thalamically-evoked cortical epileptiform activity." Thalamus Relat Syst **3**(4): 261-273.

Sun, Q. Q., J. R. Huguenard and D. A. Prince (2006). "Barrel cortex microcircuits: thalamocortical feedforward inhibition in spiny stellate cells is mediated by a small number of fast-spiking interneurons." J Neurosci **26**(4): 1219-1230.

Sun, Q. Q., C. Zhou, W. Yang and D. Petrus (2016). "Continuous spike-waves during slow-wave sleep (CSWS) in a mouse model of focal cortical dysplasia (FCD)." Epilepsia **57**(10): 1581-1593.

Super, H., S. P. Perez and E. Soriano (1997). "Survival of Cajal-Retzius cells after cortical lesions in newborn mice: a possible role for Cajal-Retzius cells in brain repair." Brain Res.Dev.Brain Res. **98**: 9-14.

Sweeney, M. D., Z. Zhao, A. Montagne, A. R. Nelson and B. V. Zlokovic (2019). "Blood-Brain Barrier: From Physiology to Disease and Back." Physiol Rev **99**(1): 21-78.

Szabadics, Varga, Molnár, Oláh, Barzó and Tamás (2006). "Excitatory Effect of GABAergic Axo-Axonic Cells in Cortical Microcircuits." Science **311**(5758): 233-235.

Szabadics, J. and I. Soltesz (2009). "Functional specificity of mossy fiber innervation of GABAergic cells in the hippocampus." Journal of Neuroscience **29**(13): 4239.

Szydlowski, S. N., I. P. Dorocic, H. Planert, M. Carlen, K. Meletis and G. Silberberg (2013). "Target Selectivity of Feedforward Inhibition by Striatal Fast-Spiking Interneurons." Journal of Neuroscience **33**(4): 1678-1683.

Takano, T. (2012). "Altered distribution of inhibitory interneurons in polymicrogyria." Epilepsy Res. **102**(1-2): 113-116.

Takano, T. and K. Matsui (2015). "Increased expression of GAP43 in interneurons in a rat model of experimental polymicrogyria." J Child Neurol **30**(6): 716-728.

Tallent, M. K. and G. R. Siggins (1997). "Somatostatin depresses excitatory but not inhibitory neurotransmission in rat CA1 hippocampus." J Neurophysiol **78**(6): 3008-3018.

Tanaka, K. F., K. Watase, T. Manabe, K. Yamada, M. Watanabe, K. Takahashi, H. Iwama, T. Nishikawa, N. Ichihara, T. Kikuchi, S. Okuyama, N. Kawashima, S. Hori, M. Takimoto and K. Wada (1997). "Epilepsy and exacerbation of brain injury in mice lacking the glutamate transporter GLT-1." Science **276**(5319): 699-702.

Tang, F., A. M. S. Hartz and B. Bauer (2017). "Drug-resistant epilepsy: multiple hypotheses, few answers." Front Neurol **8**.

Taube, J. S. and P. A. Schwartzkroin (1988). "Mechanisms of long- term potentiation: EPSP/ spike dissociation, intradendritic recordings, and glutamate sensitivity." Journal of Neuroscience **8**(5): 1632.

Temkin, O. (1933). "The doctrine of epilepsy in the Hippocratic writings." Bulletin of the History of Medicine **8**: 55.

Thomson, A. M. and J. Deuchars (1997). "Synaptic interactions in neocortical local circuits: dual intracellular recordings in vitro." Cerebral Cortex **7**(6): 510-522.

Tian, G. F., H. Azmi, T. Takano, Q. Xu, W. Peng, J. Lin, N. A. Oberheim, N. Lou, X. Wang, H. R. Zielke, J. Kang and M. Nedergaard (2005). "An astrocytic basis of epilepsy." Nat Med **11**(9): 973-981.

Tishler, D. M., K. I. Weinberg, D. R. Hinton, N. Barbaro, G. M. Annett and C. Raffel (1995). "MDR1 gene expression in brain of patients with medically intractable epilepsy." Epilepsia **36**: 1-6.

Toledo-Rodriguez, M., B. Blumenfeld, C. Wu, J. Luo, B. Attali, P. Goodman and e. al. (2004). "Local circuit interactions between oriens/ alveus interneurons and CA1 pyramidal cells in hippocampal slices: electrophysiology and morphology." Cerebral Cortex **14**(12): 1310-1327.

Tomioka, R., K. Okamoto, T. Furuta, F. Fujiyama, T. Iwasato, Y. Yanagawa, K. Obata, T. Kaneko and N. Tamamaki (2005). "Demonstration of long-range GABAergic connections distributed throughout the mouse neocortex." European Journal of Neuroscience **21**(6).

Traub, R. D., I. Pais, A. Bibbig, E. H. Buhl, S. G. Hormuzdi, H. Monyer and e. al. (2003). "Contrasting Roles of Axonal (Pyramidal Cell) and Dendritic (Interneuron) Electrical Coupling in the Generation of Neuronal Network Oscillations." Proc Natl Acad Sci U S A **100**(3): 1370-1374.

Tricoire, L., K. A. Pelkey, M. I. Daw, V. H. Sousa, G. Miyoshi, B. Jeffries and e. al. (2010). "Common origins of hippocampal Ivy and nitric oxide synthase expressing neurogliaform cells." Journal of Neuroscience **30**(6): 2165.

van der Knaap, M. S. and J. Valk (1991). "The MR spectrum of peroxisomal disorders." Neuroradiology **33**(1): 30-37.

Vermeiren, C., M. Najimi, N. Vanhoutte, S. Tilleux, I. D. Hemptinne, J. M. Maloteaux and E. Hermans (2005). "Acute up-regulation of glutamate uptake mediated by mGluR5a in reactive astrocytes." Journal of Neurochemistry **94**(2).

Viana, F. and B. Hille (1996). "Modulation of high voltage-activated calcium channels by somatostatin in acutely isolated rat amygdaloid neurons." J Neurosci **16**: 6000-6011.

Vida, I., K. Halasy, C. Szinyei, P. Somogyi and E. H. Buhl (1998). "Unitary IPSPs evoked by interneurons at the stratum radiatum- stratum lacunosum- moleculare border in the CA1 area of the rat hippocampus in vitro." J Physiol **506**(3): 755.

Vucurovic, K., T. Gallopin, I. Ferezou, A. Rancillac, P. Chameau, J. A. van Hooft and e. al. (2010). "Serotonin 3A Receptor Subtype as an Early and Protracted Marker of Cortical Interneuron Subpopulations." Cereb Cortex **20**(10): 2333-2347.

Wahle, P. (1993). "Differential regulation of substance P and somatostatin in Martinotti cells of the developing cat visual cortex." J Comp Neurol **329**(4): 519.

Wang, T., T. Kumada, T. Morishima, S. Iwata, T. Kaneko, Y. Yanagawa, S. Yoshida and A. Fukuda (2014). "Accumulation of GABAergic neurons, causing a focal ambient GABA gradient, and downregulation of KCC2 are induced during microgyrus formation in a mouse model of polymicrogyria." Cereb Cortex **24**(4): 1088-1101.

Wang, Y., A. Gupta and H. Markram (1999). "Anatomical and functional differentiation of glutamatergic synaptic innervation in the neocortex." Journal of Physiology **93**(4): 305-317.

Wang, Y., A. Gupta, M. Toledo-Rodriguez, C. Z. Wu and H. Markram (2002). "Anatomical, physiological, molecular and circuit properties of nest basket cells in the developing somatosensory cortex." Cereb Cortex **12**(4): 395-410.

Wang, Y., M. Toledo-Rodriguez, A. Gupta, C. Wu, G. Silberberg, J. Luo and H. Markram (2004). "Anatomical, physiological and molecular properties of Martinotti cells in the somatosensory cortex of the juvenile rat." J Physiol **561**(Pt 1): 65-90.

Weiss, N. and G. W. Zamponi (2019). "T-type Calcium Channels: From Molecule to Therapeutic Opportunities." Int J Biochem Cell Biol **108**: 34-39.

Wetherington, J., G. Serrano and R. Dingledine (2008). "Astrocytes in the Epileptic Brain." Neuron **58**(2): 168-178.

Whittington, M. A., R. D. Traub and G. R. J. John (1995). "Synchronized oscillations in interneuron networks driven by metabotropic glutamate receptor activation." Nature **373**(6515): 612.

Wilson, J. V. K. and E. H. Reynolds (1990). "Translation and analysis of a cuneiform text forming part of a Babylonian treatise on epilepsy." Medical History **34**(02): 13.

Wilson, N. R., C. A. Runyan, F. L. Wang and M. Sur (2012). "Division and subtraction by distinct cortical inhibitory networks in vivo." Nature **488**(7411): 343-348.

Wlodarczyk, A. I., C. Xu, I. Song, M. Doronin, Y. W. Wu, M. C. Walker and A. Semyanov (2013). "Tonic GABAA conductance decreases membrane time constant and increases EPSP-spike precision in hippocampal pyramidal neurons." Front Neural Circuits **25**(7).

Woodruff, Xu, Anderson and Yuste (2009). "Depolarizing effect of neocortical chandelier neurons." Front Neural Circuits **3**.

Wu, X.-B., B. Liang and Y.-J. Gao (2016). "The increase of intrinsic excitability of layer V pyramidal cells in the prelimbic medial prefrontal cortex of adult mice after peripheral inflammation." Neuroscience Letters **611**: 40-45.

Wyllie, E. (2000). "Surgical treatment of epilepsy in pediatric patients." Can.J Neurol.Sci. **27**(2): 106-110.

Xiang, Z., J. R. Huguenard and D. A. Prince (2002). "Synaptic inhibition of pyramidal cells evoked by different interneuronal subtypes in layer v of rat visual cortex." J Neurophysiol. **88**(2): 740-750.

Xu, H., H. Y. Jeong, R. Tremblay and B. Rudy (2013). "Neocortical Somatostatin-Expressing GABAergic Interneurons Disinhibit the Thalamorecipient Layer 4." Neuron **77**(1): 155-167.

Xu, Q., L. Guo, H. Moore, R. R. Waclaw, K. Campbell and S. A. Anderson (2010). "Sonic Hedgehog Signaling Confers Ventral Telencephalic Progenitors with Distinct Cortical Interneuron Fates." Neuron **65**(3): 328-340.

Xu, X. and E. M. Callaway (2009). "Laminar specificity of functional input to distinct types of inhibitory cortical neurons." Journal of Neuroscience **29**(1): 70.

Xu, X., K. D. Roby and E. M. Callaway (2006). "Mouse cortical inhibitory neuron type that coexpresses somatostatin and calretinin." J Comp Neurol **499**(1): 144-160.

Xue, M., B. V. Atallah and M. Scanziani (2014). "Equalizing Excitation-Inhibition Ratios Across Visual Cortical Neurons." Nature **511**(7511): 569-600.

Yavorska, I. and M. Wehr (2016). "Somatostatin-expressing inhibitory interneurons in cortical circuits." Front Neural Circuits **10**(76).

Yoshimura, Y. and M. C. Edward (2005). "Fine-scale specificity of cortical networks depends on inhibitory cell type and connectivity." Nat Neurosci **8**(11): 1552.

Yuan, H., K. B. Hansen, J. P. Zhang, T. M., T. C. Markello, K. V. F. H. Fajardo, C. M., G. Golas, D. R. Adams and C. F. Boerkoel (2014). "Functional analysis of a de novo GRIN2A missense mutation associated with early-onset epileptic encephalopathy." Nature Communications **5**.

Zhang, C. and P. Kwan (2019). "The concept of drug-resistant epileptogenic zone." Front. Neurol. **10**.

Zilberter, Y., K. M. M. Kaiser and B. Sakmann (1999). "Dendritic GABA Release Depresses Excitatory Transmission between Layer 2/ 3 Pyramidal and Bitufted Neurons in Rat Neocortex." Neuron **24**(4): 979-988.

Zilles, K., M. Qu, A. Schleicher and H. J. Luhmann (1998). "Characterization of neuronal migration disorders in neocortical structures: quantitative receptor autoradiography of ionotropic glutamate, GABA(A) and GABA(B) receptors." European Journal of Neuroscience **10**: 3095-3106.

Zsombok, A. and K. M. Jacobs (2005). "Postsynaptic currents in layer iv neurons of epileptogenic malformed ferret cortex." Society for Neuroscience Abstracts **31**: 668.

Zsombok, A. and K. M. Jacobs (2007). "Postsynaptic Currents Prior to Onset of Epileptiform Activity in Rat Microgyria." J Neurophysiol **98**(1): 178-186.

Vita

"Shake your head it's empty"
Emily Haines, Metric

안드 뚜 김버리 재이컵스, 퍽유.

Black Lives Matter.